UNIVERSITA' DEGLI STUDI DI MILANO

Scuola di Dottorato di Ricerca in Scienze Biochimiche, Nutrizionali e Metaboliche

Direttore: Prof. Sandro Sonnino

Dottorato di Ricerca in Scienze Biochimiche – XXVIII Ciclo

SIALIDASE NEU3 EXPRESSION IN A HUMAN MODEL OF CARDIAC ISCHEMIA AND ITS INTERPLAY WITH THE HYPOXIA-INDUCIBLE FACTOR (HIF-1α) SIGNALING PATHWAY.

Relatore: Prof. Luigi Anastasia

Coordinatore: Prof. Francesco Bonomi

Tesi di Dottorato di ANDREA GARATTI

Matricola: R10321

ANNO ACCADEMICO 2014/2015

Sommario

CHAPTER 1: Introduction

1.1 Epidemiology of Heart Failure

Heart failure (HF) is a major public health problem, with a prevalence of more than 5.8 million in the United States and more than 23 million worldwide. In 1997, HF was singled out as an "*emerging epidemic*"[1].

In the American Heart Association (AHA)/American College of Cardiology guidelines[2], HF is defined as "a complex clinical syndrome that can result from any structural or functional cardiac disorder that impairs the ability of the ventricle to fill or eject blood." The guidelines underscore that "it is largely a clinical diagnosis that is based on a careful history and physical examination." As HF is a syndrome and not a disease, its diagnosis relies on a clinical examination and can be challenging. To assess the burden of HF in populations and study its epidemiology, standardized criteria that can be used on a large scale for its ascertainment from medical records are needed.

Several criteria have been proposed to diagnose HF, including the Framingham criteria[3], the Boston criteria[4], the Gothenburg criteria[5], and the European Society of Cardiology criteria[6].

Using standardized criteria, the incidence of HF in an earlier study from Framingham was between 1.4 and 2.3 per 1000/y among persons aged 29 to 79 years. However, the size of the cohort inherently limits the power to analyze secular trends in this report.

Croft et al[7], comparing the rates of initial hospitalization for HF using Medicare hospital claims in 1986 and 1993, reported an increase in the initial hospitalization for HF, while acknowledging limitations related to the lack of validation and possible incomplete ascertainment of incidence. Data from the Henry Ford Health system[8], a managed care organization, indicated that the prevalence of HF was increasing over time but did not detect any secular change in incidence or mortality. In the Framingham Heart Study[9] and the Olmsted County Study[10] which include outpatient HF, the incidence of HF remained stable

over time or even declined in women. It should be noted that, although the interpretation and informal comparison of trends across studies is appropriate, as adjustment approaches differ, the absolute numbers couldn't be compared. Importantly, the trends noted among the elderly are different and data from the Kaiser Permanente system comparing the incidence of HF in 1970–1974 and 1990–1994 among persons aged ≥65 years indicated that the age-adjusted incidence increased by 14% over time and was greater for older persons and for men[11]. The Framingham and Olmsted County studies also reported trends toward increasing HF incidence among older persons, which are concerning given the aging of the population. In the Rotterdam Heart Study, the lifetime risk of HF at the age of 55 years was 33% for men and 29% for women[12]. These numbers are commensurate with the data from the United States.

In summary, the overall prevalence of HF ranges from 1% to 12% based on available data from the United States and Europe. The incidence of HF varies across studies largely reflecting differences in ascertainment and adjustment approaches. These methodological differences, however, do not affect the interpretation of secular trends in incidence where the focus is on the evolution over time. Temporal trends are congruent across studies and quite informative for the investigation of the HF epidemic because they indicate that the incidence of HF is stable or perhaps even decreasing over time. Available data indicate that lifetime risks are high regardless of sex, race, and geography, underscoring the importance of population-wide efforts to contain the burden of HF.

1.2 Mortality of HF

After the diagnosis of HF, survival estimates are 50% and 10% at 5 and 10 years, respectively[13], and left ventricular dysfunction is associated with an increase in the risk of sudden death[14].

In the Henry Ford Health system, which includes outpatient encounters, the median survival was 4.2 years without any discernible improvement over time. Similarly, among >2 million elderly Medicare beneficiaries, early- and long-term mortality remained quite high (115% at 30 days and 37% at 1 year)[15]. Data from Framingham and Olmsted County underscored the persistently high mortality of HF in these populations, despite improvements over time; indeed, after age adjustment, estimated 5-year mortality rates were 59% in men and 45% in women during the time period 1990–1999 in Framingham and 50% in men and 46% in women during the time period 1996–2000 in Olmsted County. Improvements in survival were noted more specifically within an elderly population as shown by data from the Kaiser Permanente system. Indeed, during the two decades between the mid-1970s and mid-1990s after adjustment for age and comorbidities, survival after the diagnosis of HF improved by 33% in men and 24% in women. Importantly, in the Kaiser Permanente study, improvement in survival was primarily associated with β-blocker treatment. Data from Ontario[16] and Scotland[17] also support the observation that although survival after HF diagnosis remains quite poor, improvements have been detected since the late 1990s. Altogether, these trends in mortality coincide temporally with major changes in the treatment of HF and thus suggest that HF treatment is effective in the community but that much progress remains to be accomplished. The causes of death in HF can be challenging to ascertain. In the community, cardiovascular deaths are less frequent among subjects with preserved EF. Indeed, in Olmsted County, MN, among 1063 persons with HF, the leading cause of death in subjects with preserved EF was non-cardiovascular (49%) versus coronary disease (43%) for subjects with reduced EF. The proportion of cardiovascular deaths decreased from 69% in 1979–1984 to 40% in 1997–2002 (P=0.007) among subjects with preserved EF contrasting with a modest change among those with reduced EF (77%–64%, P=0.08)[18]. The shift in the distribution of the causes of death toward less cardiovascular causes is congruent with the

major burden of comorbid conditions in HF and is of crucial importance for the management of HF and the interpretation of its outcomes.

In summary, survival after the diagnosis of HF remains quite poor but has improved substantially over time. The results are consistent across studies and, combined with the aforementioned trends in incidence, indicated that the epidemic of HF is an epidemic of hospitalizations among survivors who now live longer with the disease.

1.3 Hospitalizations in HF

HF is characterized by periodic exacerbations that require treatment intensification most often in the hospital and is the single most frequent cause of hospitalization in persons aged ≥65 years. Nearly one million hospitalizations for HF occur each year with rates of hospitalization continuing to rise. This trend, coupled with the forecasting of a major increase in the prevalence of HF by the AHA[19], underscores the persisting severity of the burden that HF creates on healthcare systems and the need for continued surveillance of HF trends to delineate strategies for management. A subsequent analysis of CMS data indicates that after an initial hospitalization, 25% of HF patients are readmitted within 30 days with 35% of readmissions also attributed to HF[20]. Data from the Veteran's Affairs Health Care System also support the notion that as mortality was decreasing, readmission rates have in fact increased over time[21]. Taken collectively, these important reports suggest that that threshold for admitting patients with HF to the hospital might be evolving. However, once patients have been hospitalized with HF, their risk of readmission is not decreasing over time but they will be readmitted rather infrequently because of HF. National Hospital Discharge Survey data from 1979 to 2004 indicate that although HF was the first-listed diagnosis for 30% to 35% of these hospitalizations, the proportion with respiratory diseases and non-cardiovascular, non-respiratory diseases as the first-listed diagnoses increased over time[22]. In the community of Olmsted County, among incident HF cases diagnosed between

1987 and 2006, hospitalizations were common after HF diagnosis, with 83% of the patients hospitalized at least once but the reason for hospitalization was HF in only 17% of hospitalizations, whereas 62% were attributed to non-cardiovascular causes[23]. Using the Nationwide Inpatient Sample, Blecker et al reported on trends in HF hospitalizations between 2001 and 2009. Primary HF hospitalizations declined, but hospitalizations with a secondary diagnosis of HF remained stable[24].

In summary, these data underscore the major role of comorbidity in HF[25] and that, to reduce the burden of hospitalizations in HF, strategies must consider both cardiac disease and noncardiac conditions. While initial hospitalizations are seemingly decreasing, readmissions after an initial hospitalization are not declining such that, with the increased survival of patients living with HF, the overall burden of hospitalizations in HF remains large.

1.4 Treatment of HF

Heart Transplantation

Heart transplantation is an accepted treatment for end-stage HF[26]. Although controlled trials have never been conducted, there is consensus that transplantation—provided that proper selection criteria are applied—significantly increases survival, exercise capacity, quality of life, and return to work compared with conventional treatment. Apart from the shortage of donor hearts, the main challenges in transplantation are the consequences of the limited effectiveness and complications of immunosuppressive therapy in the long term (i.e. antibody-mediated rejection, infection, hypertension, renal failure, malignancy, and coronary artery vasculopathy).

Mechanical Circulatory Support

For selected patients with end-stage HF, transplantation remains the gold-standard treatment, with good long-term survival. However, because of the increasing numbers of

patients with end-stage HF, limited organ donation, and technological advances, MCS with an LV assist device (LVAD) or bi-ventricular assist device (BiVAD) is increasingly seen as an alternative for some of these individuals. Initially MCS was used as a short-term BTT treatment but is now being used long-term, as so-called 'destination therapy (DT)', in patients not eligible for transplantation. Ventricular assist devices may ultimately become a more general alternative to transplantation, as current 2- to 3-year survival rates in carefully selected patients receiving the latest continuous flow devices are much better than with medical therapy only[27]. Patients receiving these devices also have a post-transplant survival rate similar to those not requiring bridging. However, despite technological improvements, bleeding, thromboembolism (both of which can cause stroke), infection, and device failure remain significant problems; these issues, plus the high cost of devices and implantation, have limited their wider use. It is recommended that such devices are only implanted and managed at tertiary heart failure centers with appropriately trained, specialist HF physicians and surgeons. Ideally these centers should also undertake transplantation.

Coronary Revascularization in HF

Surgical (and percutaneous) coronary revascularization is indicated for the relief of angina pectoris in patients with HF, and surgical coronary revascularization is indicated for 'prognostic' reasons in other patients with severe CAD, particularly those with three-vessel disease or left-main stenosis.

The benefit–risk balance for CABG in patients without angina/ischemia or without viable myocardium remains uncertain. Patients with >10% of dysfunctional but viable LV myocardium may be more likely to benefit from myocardial revascularization (and those with ≤10% less likely to benefit) although this approach to patient selection for revascularization is unproven. Several non-invasive techniques can be used to assess myocardial viability. Nuclear imaging has a high sensitivity, whereas techniques evaluating

contractile reserve have lower sensitivity but higher specificity. CMR is excellent for assessing the transmural extent of scar, but is not better at detecting viability or predicting recovery of wall motion.

The choice between percutaneous coronary intervention and CABG should be made by the Heart Team, including a HF specialist, and be based on the extent of CAD, expected completeness of revascularization, associated valvular disease, and the presence of co-morbidities.

Surgical Ventricular Reconstruction

LV remodeling is a complex process that may occur in several clinical conditions, including MI, leading to chamber dilatation, altered configuration and increased wall stress. LV remodeling usually begins within the first few hours after an MI and results from the fibrotic repair of the necrotic area with scar formation, elongation and thinning of the infarcted zone. LV volumes increase, a response that is sometimes considered adaptive, associated with stroke volume augmentation, in an effort to maintain a normal cardiac output as the ejection fraction declines[28]. However, beyond this early stage, the remodeling process is driven predominantly by eccentric hypertrophy of the non-infarcted remote regions, resulting in increased wall mass, chamber enlargement and geometric distortion[29].

Surgical LV reconstruction (LVR) has been introduced as an optional therapeutic strategy aimed at reducing LV volumes through the exclusion of the scar tissue, thereby reducing the ventricle to a more physiological volume, reshaping the distorted chamber and improving cardiac function through a reduction of LV wall stress in accordance with the principle of Laplace's law. Since LV wall stress is directly proportional to LV internal radius and pressure and inversely proportional to wall thickness, any intervention to optimize this relationship would be beneficial either in terms of improving wall compliance and reducing filling pressure or, as wall stress is a crucial determinant of afterload, in terms of enhancing

contractile performance of the LV by increasing the extent and velocity of systolic fiber shortening[30].

Furthermore, LVR of failing ventricles is usually combined with myocardial revascularization with the aim of treating the underlying coronary artery disease. Finally, although the matter of functional chronic ischemic mitral regurgitation (MR), in terms of whether, when and how it should be corrected, is still considerably controversial, it should be pointed out that LVR offers either the possibility of repairing the mitral valve through the LV opening or the potential of improving mitral functioning by reducing LV volumes, papillary muscles distance and hence rebuilding a more normal geometry[31]. Although a large amount of reports drawn on various data sets from registries and mainly observational studies have shown that LVR is effective and relatively safe with a favorable 5-year outcome[32], the results from the STICH trial have called into question the additional benefit of the surgical LVR. Beyond the debate that will probably continue for a long time, the Task Force on Myocardial Revascularization of the European Society of Cardiology (ESC) and the European Association for Cardio-Thoracic Surgery (EACTS) recognized the merit of LVR, which has been included as a surgical option combined with CABG in selected HF patients with a scar in the LAD territory and a baseline LVESVI ≥60 ml/ m2 (Class of Recommendation IIb; level of evidence B)[33].

1.5 Rationale for a translational approach for HF therapy

Ischemic heart disease continues to be the single most frequent cause of death worldwide. Although acute and long-term mortality following acute myocardial infarction (AMI) has declined thanks to therapeutic advances, 12% of patients still die within 6 months of AMI.

Overall medical, surgical and transplantation therapy are largely ineffective to effectively cure the growing number of patients affected by HF. In the last decade HF cardiologists and physicians were more and more involved in developing a translational approach to HF, in

order to better understand the cellular and molecular basis of the disease to finally develop new therapeutic strategy.

The discovery in 2001 that stem cells have the potential to regenerate the heart in infarcted mice was rapidly translated into the clinic[34]. Cell-based products (CBPs) have been evaluated in patients with AMI, refractory angina and chronic heart failure (CHF) to assess whether these therapies are safe and efficacious in improving heart function and preventing the development of end-stage heart failure.

However meta-analyses of clinical data show contradictory results; furthermore the clinical development of cell-based therapies in patients with CHF is more challenging than in AMI. Indeed patients with CHF have a different pathophysiology and clinical presentation with extensive remodeling, collagen accumulation, and profound ultra-structural changes.

One interesting approach, developed in our laboratory was to investigate the role of the Hypoxia Inducible Factor (HIF) in protecting skeletal muscle cells and cardiomyocytes from hypoxia or ischemia. Indeed there are several mechanisms that activate and regulate HIF expression. In this view, one possible therapeutic approach could be the activation of HIF in order to increase the cardiac response to hypoxic stress.

1.6 Molecular Mechanisms in response to cellular hypoxia: the Hypoxia Inducible Factor (HIF)

Hypoxia determines important consequences at a functional level that can ultimately lead to cellular death and tissue irreversible damage. Under hypoxic condition, cells activate a complex of protective genetic pathways, that are yet to be completely understood, aiming to enhance cellular survival despite oxygen deprivation. The key factor of cellular response to hypoxia is the *Hypoxia Inducible Factor 1α* (HIF-1α), a transcriptional factor that regulates the cellular response to reduced oxygen availability[35]. In fact, it has been demonstrated that

HIF-1 is expressed ubiquitously in almost all mammalian cells. This basic helix-loop-helix (bHLH)-Per-AHR-ARNT-Sim (PAS) transcription factor is a key element in sensing changes of cellular oxygen tension. HIF-1 is a heterodimer composed of an oxygen-sensitive α subunit and constitutively expressed β subunit (ie arylhydrocarbon receptor nuclear translocator -ARNT)[36]. More explicitly, oxygen levels can affect the protein stability, subcellular localization and transcriptional activity of the HIF α subunits (HIF-1α, HIF-2α and HIF-3α), whereas the ARNT subunit is constitutively expressed in the nucleus and its activity is not affected by hypoxia[37]. As illustrated in Figure 1, under normoxic condition, the α subunit of HIF-1 is rapidly ubiquitinated and degraded proteosomally by hydroxylation of prolyl residues. This process is primarily controlled by a family of oxygen-dependent prolyl hydroxylases (PHDs; including PHD1, PHD2, and PHD3), whose enzymatic activity is regulated by oxygen availability. In fact, they use molecular oxygen, 2-oxo-glutarate and iron to hydroxylate these residues within the oxygen-dependent degradation domain (ODD) of HIF-1α (***Figure 1.1***). The product of the von Hippel-Lindau tumor suppressor gene (pVHL) then binds to these hydroxyproline residues[38]. Additionally, acetylation of lysine in the same domain by an acetyl transferase (ARD1) favors the interaction of HIF-1α with pVHL[39]. pVHL binding to a region of ODD of HIF α subunits initiates HIF-α proteolysis by acting as the recognition component of a ubiquitin ligase complex. Multiple ubiquitin molecules attach covalently to the targeted protein and this ubiquitin- tagged substrate is degraded by the 26S proteasome[40].

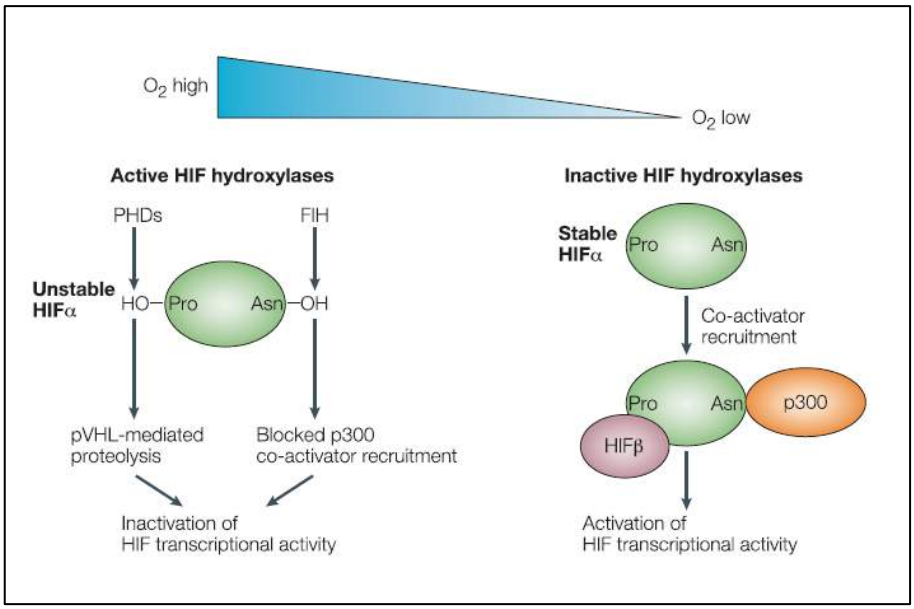

Figure 1.1: HIF-1α activating mechanism through prolyl hydroxylases family.

In addition to proteolytic degradation, another oxygen-dependent regulatory mechanism is the inhibition of transcriptional activity of HIF-1. In normoxic conditions, the factor inhibiting HIF-1 (FIH-1), β-hydroxylates the asparaginyl-803 residue of C terminal activation domain of HIF-1α, which is the interaction site for the transcriptional co-activator p300 therefore prevents the interaction of HIF-1α with co-activators[41]. Under hypoxic condition, HIF-1α becomes stabilized, translocates from the cytoplasm to the nucleus, and it heterodimerizes with HIF-1β[42]. This hypoxia-induced nuclear translocation of HIF-1α protects HIF-1α from VHL-mediated proteasomal degradation. In addition, a distinct hypoxia-dependent signal is required for stabilization of HIF-1α[43]. The heterodimerization forms a transcriptionally active HIF complex, which in turn associates with hypoxia responsive elements (HRE) in the regulatory regions of target genes and binds to transcriptional co-activators to induce gene expression (***Figure 1.2***). Among three HIF α isoforms, HIF-1α and HIF-2α are closely related and their transcriptional activities are both through interaction with hypoxia responsive elements of target genes[44].

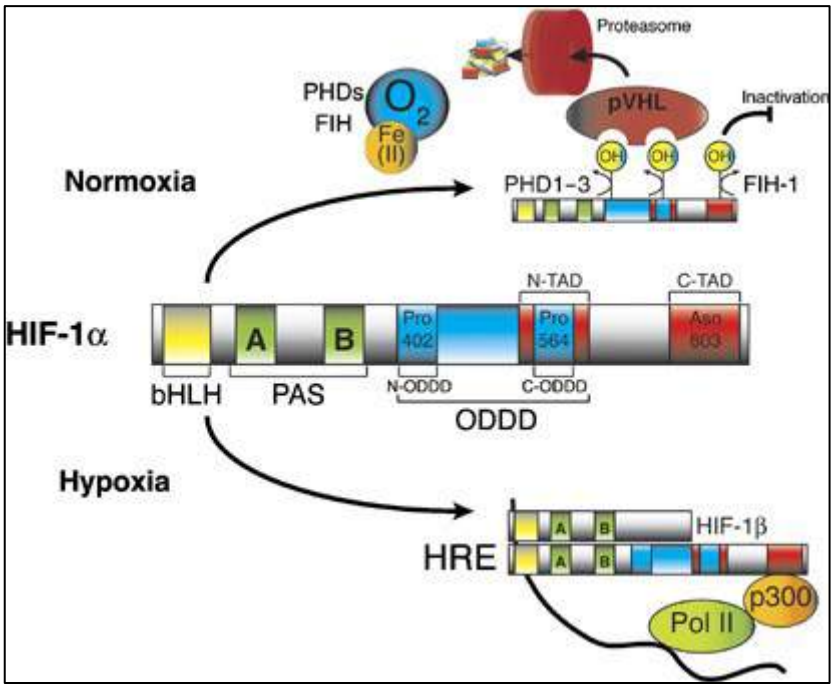

Figure 1.2: Molecular mechanisms of HIF-1α activation; Weidermann A et Al[45].

One of the mediators of hypoxic stress is p53; after oxygen deprivation p53 is stabilized via several post translational modifications[46]. Increased p53 levels lead to increased expression of genes involved in cell cycle arrest, such as p21 and ultimately to the expression of genes involved in apoptosis[47]. Counteracting p53 action is another mediator of the hypoxic response, Hypoxia Inducible Factor 1 (HIF-1) that promotes the transcription of genes involved in adaptation to low oxygen levels through one or more Hypoxia Resposive Element (HRE) in their promoters. Recent studies, including ours, proved that p53 and HIF-1 compete for the co-activator p300 and by doing so they antagonize each other until the integration of different signals reaches its balance and the fate of the cell is determined[48] (***Figure 1.3***).

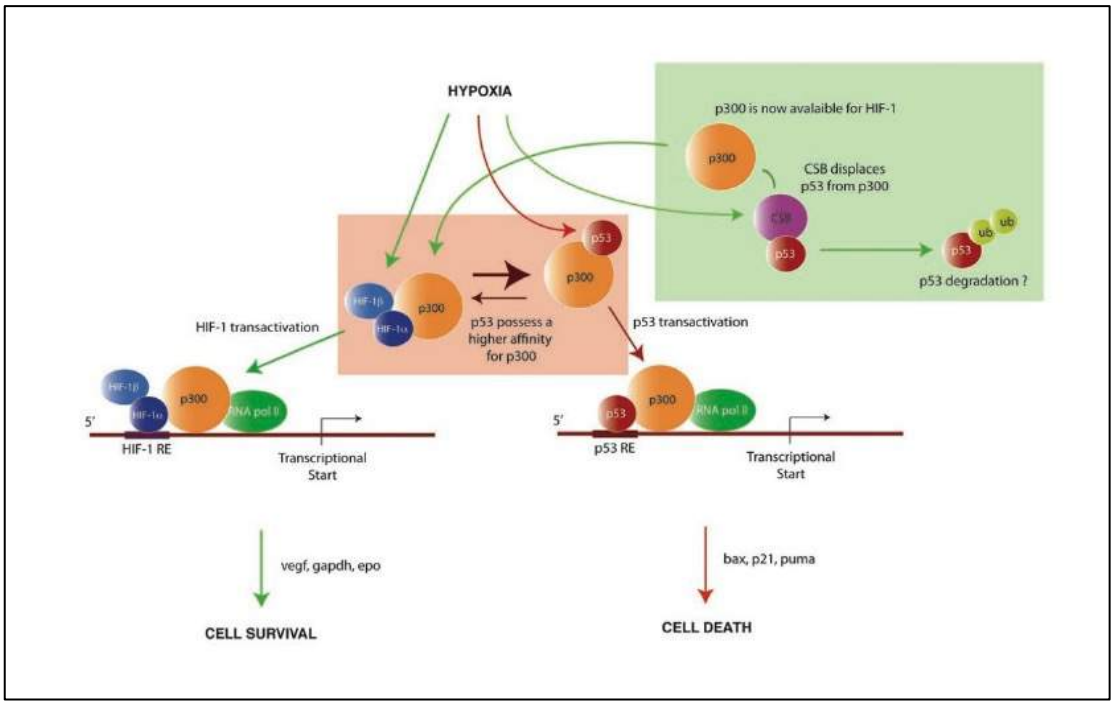

Figure 1.3: Mechanisms of HIF-1α and p53 activation under hypoxia. Frontini M et Al[49].

1.7 HIF-1 targeted genes

Transfer of hydrogen atoms and electrons to molecular oxygen is the final stage of oxidative phosphorylation, which is the most important mechanism of energy (ATP) production in mammalian cells. Consequently, intracellular O2 concentrations are precisely regulated in order to maintain cellular and systemic function. HIF-1 transcriptional complex plays an essential role in cellular and systemic oxygen homeostasis by inducing transcription of more than a hundred hypoxia responsive genes (***Figure 1.4***). For instance, a previous study demonstrated that more than 2% of all human genes are directly or indirectly regulated by HIF-1 in arterial endothelial cells[50]. The genes regulated at the transcription level by HIF-1 are involved in a wide-spectrum of cellular functional events, including angiogenesis, vascular reactivity and remodeling, vasomotor control, glucose and energy metabolism, erythropoiesis, iron homeostasis, pH regulation, cell proliferation and viability, nucleotide metabolism, matrix metabolism, and metal transport[51]. Many of these functional processes

are related to homeostatic responses to low oxygen tension. Moreover, hypoxia is not the only inducer for the transcriptional activity of HIF-1 in living cells. This is because PHDs are dependent on iron as well as molecular oxygen. The displacement of iron by cobaltous ions or iron chelators inhibits the catalytic activity of the enzymes, which results in the hypoxia-independent activation of HIF[52]. In addition, several other non-hypoxic factors such as growth factors, interleukin 1, prostaglandin E2, thrombin, angiotensin II, serotonin, acetylcholine, thrombin, platelet-derived growth factor and nitric oxide donors may also induce HIF-1 activation[53].

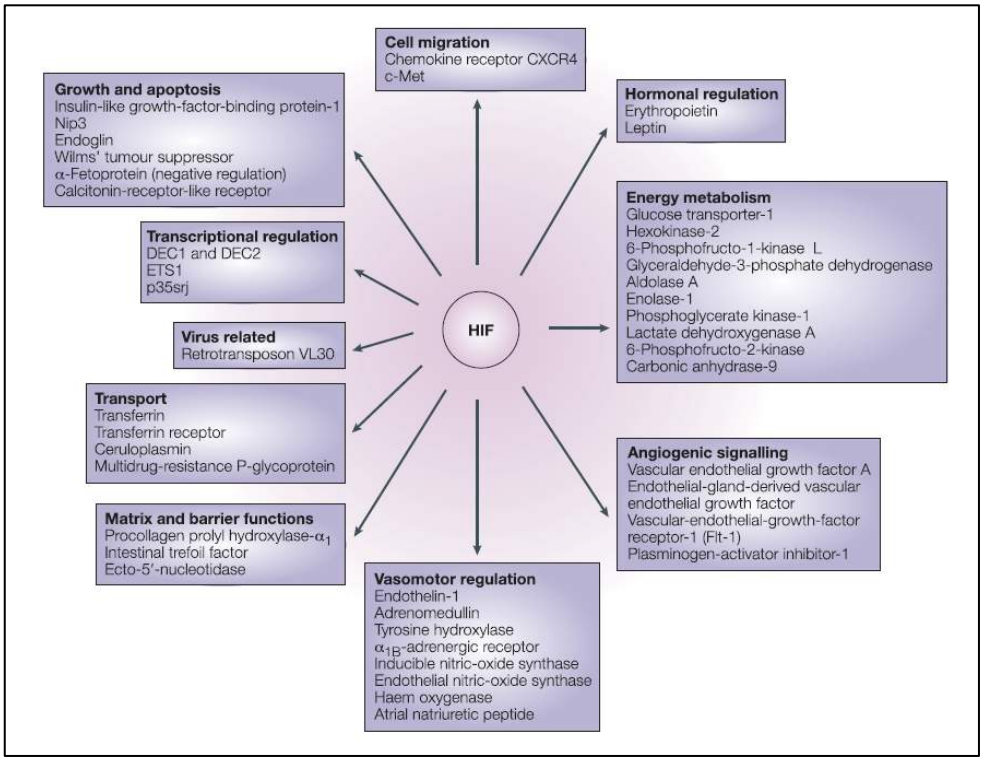

Figure 1.4: Different pathways by which HIF activation regulates the cell response to hypoxia and ischemia.

1.8 HIF-1 and cardioprotection

The role of HIF-1 in mediating cardioprotection was first demonstrated by Cai et al in 2003[54]. Intermittent systemic hypoxia occurs in many common physiological and pathophysiological conditions in human life, which could be caused by environmental

factors (e.g. high altitude) or by various cardiopulmonary disorders (e.g. heart failure, chronic obstructive pulmonary disease, and sleep apnea) and hematological diseases (e.g. anemia)[55]. In fact, the intermittent exposures to hypoxia are much more frequently than chronic exposure to hypoxia. Interestingly, a few well-controlled protocols of intermittent hypoxia can induce protective effects against myocardial infarction in rodents via a signaling mechanism that depends upon inducible nitric oxide synthase (iNOS)[56]. Since iNOS gene has the HRE in its promoter region and HIF-1 is essential for the hypoxic regulation of iNOS gene expression in cardiomyocytes, it is logical to speculate a role for HIF-1 in intermittent hypoxia-induced cardioprotection. This concept was experimentally proved first by Cai and colleagues who demonstrated that the cardioprotective effect of intermittent hypoxia is dependent on HIF-1α gene dosage in wild-type mice, indicated by better left ventricular contractile function and significantly smaller infarct size following ischemia-reperfusion in the animals pretreated with intermittent hypoxia. Moreover they found that in the heterozygous HIF-1α knockout mice, exposure to intermittent hypoxia 24 h before lethal ischemia had no protective effect on functional recovery or infarct size. More recently, Belaidi et al showed in a rat model that intermittent hypoxia induced delayed cardioprotection against ventricular post-ischemic contractile dysfunction and myocyte necrosis was mediated by upregulation of iNOS via HIF-1[57]. Interestingly HIF-1α is also proposed as involved in the mechanism of intermittent hypoxia induced right ventricular protection against ischemia-reperfusion injury of right ventricle[58].

1.9 Angiogenesis and other factors in anti-ischemic cardioprotection mediated by HIF-1

The substrate preference of ischemic heart shifts from fatty acid to glucose utilization. The role of HIF-1α is important in the early phase of stress response where a transition from

aerobic to anaerobic metabolism occurs. HIF-1α controls the factors in glucose metabolism which allows cells to shift from aerobic metabolism to anaerobic glycolysis. HIF-1α also affects mitochondrial metabolism by inducing pyruvate dehydrogenase kinase, which prevents entry of pyruvate into mitochondria, thus reduces mitochondrial respiration, and by altering composition of the cytochrome oxidase complex[59]. In addition, a previous study suggested that the adenovirus mediated expression of constitutively stable, hybrid HIF-1α protects cultured neonatal cardiomyocytes against simulated ischemia-reperfusion injury by inducing multiple protective genes[60]. Furthermore, the levels of HIF-1α and VEGF increase in the myocardium when patients develop acute coronary artery occlusion. The increased VEGF expression by HIF-1α could induce coronary angiogenesis in myocardium, which in turn provides an enhanced capacity for coronary blood flow and oxygen supply to cardiac muscle during myocardial ischemic/hypoxic events[61].

1.10 Cardioprotection by pharmacological activators of HIF-1

Cobalt chloride

Xi and colleagues were the first to discover the cardioprotective effects induced by $CoCl_2$[62]. They found that a single low dose of $CoCl_2$ induced delayed cardioprotection through selective activation of HIF-1α, AP-1, and iNOS, without affecting another key transcription factor — nuclear factor kappa B in mice. These findings were conceptually confirmed by others in a translational model of myocardial ischemia-reperfusion injury following deep hypothermic circulatory arrest in neonatal piglets. $CoCl_2$ pretreatment significantly attenuated myocardial apoptosis and the cardioprotective effects were associated with enhanced cardiac expression of phosphorylated Akt and anti-apoptotic protein Bcl-2 and decreased expression of pro-apoptotic protein Bax[63].

Prolyl hydroxylase inhibitors

Another therapeutic method is increasing endogenous HIF-1 level or activity by blocking HIF-1 inhibitors during normoxia or by increasing the HIF-1 stabilizing agents, which is partially discussed above under pharmacological preconditioning. Inhibition of HIF hydroxylases by 2-oxoglutarate analogs stabilizes HIF and thus hypoxia responsive genes are activated[64]. Inhibition of EGLN1/PHD prolyl hydroxylase led to tissue preservation in the rats undergoing myocardial infarction. Furthermore, HIF-1 activation through PHD inhibition by dimethyloxalylglycine (DMOG) before I/R attenuates tissue injury in rabbit hearts[65]. Cardioprotection by iron chelator deferoxamine is also associated with inhibition of PHDs[66]. These investigators also showed that upregulation of HIF-1α was upregulated with deferoxamine (150 mg/kg/day for 2 days), which led to better reserved contractile functional and calcium transient in the cardiomyocytes exposed to simulated ischemia-reoxygenation in response to positive inotropic agents. Most recently, chronic post-myocardial infarction treatment with a novel orally active potent PHD inhibitor - GSK360A (30 mg/kg/day for 28 days, po) led to a long-term improvement in left ventricular contractile function, remodeling, and vascularity in a rat model of ischemia-induced heart failure. These protective effects were associated with a significant increase of the HIF-1α regulated cardioprotective molecules such as HO-1 and EPO[67].

CHAPTER 2: Aim of the Study

Medical, surgical and transplantation therapies are largely ineffective to successfully cure the growing number of patients affected by HF. Therefore, novel translational approaches have been developed in the past decade in order to better understand the cellular and molecular basis of the disease, with the ultimate goal of developing new therapeutic strategies.

One of the key issues to be solved is that the ischemic/hypoxic condition in HF determines several functional consequences that ultimately lead to cellular death and irreversible damage to cardiac myocytes.

Based on these premises, the main aim of this Ph.D. work was to develop a new approach for the activation and the exploitation of the physiological cellular response to hypoxic stress. In fact, under hypoxic conditions, cells activate several protective (pro-survival and anti-apoptotic) pathways mainly regulated by the transcription factor HIF-1α. In particular, based on some preliminary results preceding the beginning of this Ph.D. work, we decided to investigate the role of sialidase NEU3 in the regulation of the cellular response to hypoxia, through a novel mechanism of activation of HIF-1α. In fact, as described in the following chapter, sialidase NEU3 is a glycohydrolytic enzyme that is bound to the outer leaflet of the plasma membrane, and it has been shown to play a crucial role in many cellular processes, including cell proliferation and differentiation. In particular, it has been reported an activation of the enzyme in cancer, which eventually leads to the activation of pro-survival pathways, with concomitant suppression of apoptosis.

To this purpose, the first step of this Ph.D. work was to develop an in-vitro model of ischemia to test this hypothesis. Thus, murine skeletal myoblasts were engineered by overexpressing or silencing NEU3, subjected to hypoxic conditions in vitro, and then the effects compared to wild-type myoblasts under the same experimental conditions.

In a second phase of this Ph.D. work we sought to test the scope of the newly discovered model to other cell types, and in particular to human cardiomyocytes, as they are mainly affected during heart failure.

Unfortunately, culturing human adult cardiomyocytes in vitro is practically unfeasible, thus we had to develop a new strategy. In fact, as described in the following chapters, we evaluated NEU3 activation using two different models:

- A model of acute cardiac ischemia, that we achieved by analyzing heart specimens obtained during aortic cross-clamp time and extracorporeal circulation in adult patient submitted to cardiac surgical procedures.
- A model of chronic hypoxia, that we could achieve by analyzing heart specimens of neonates and young patients operated for cyanogen congenital cardiac defects.

Both models could be developed in the Cardiac Surgery Unit of IRCCS Policlinico San Donato, where both type of surgeries were performed directly by myself and other surgeons, under the supervision of Dr. L. Menicanti and Dr. A. Frigiola.

CHAPTER 3: In-Vitro model of Skeletal Muscle Cells Ischemia

3.1 Introduction: Role of the Sialidases

Sialidases, also known as neuraminidases, belong to a group of glycohydrolytic enzymes, which remove sialic acid residues from a variety of sialoglycoconjugates. They are widely distributed among the different classes of organisms such as viruses, bacteria, protozoa and vertebrates[68]. Sialidases are thought to be involved in various biological processes like infection, proliferation, differentiation, catabolism, signal transduction, antigenic properties and inter–intra cell interactions[69]. Several mammalian sialidases have been cloned and characterized at the molecular level. In humans, four types of sialidases are known and have been classified based on their subcellular localization as intra lysosomal (NEU1)[70], cytosolic (NEU2)[71], plasma membrane (NEU3)[72] and lysosomal or mitochondrial membrane (NEU4)[73] (***Figure 3.1***)

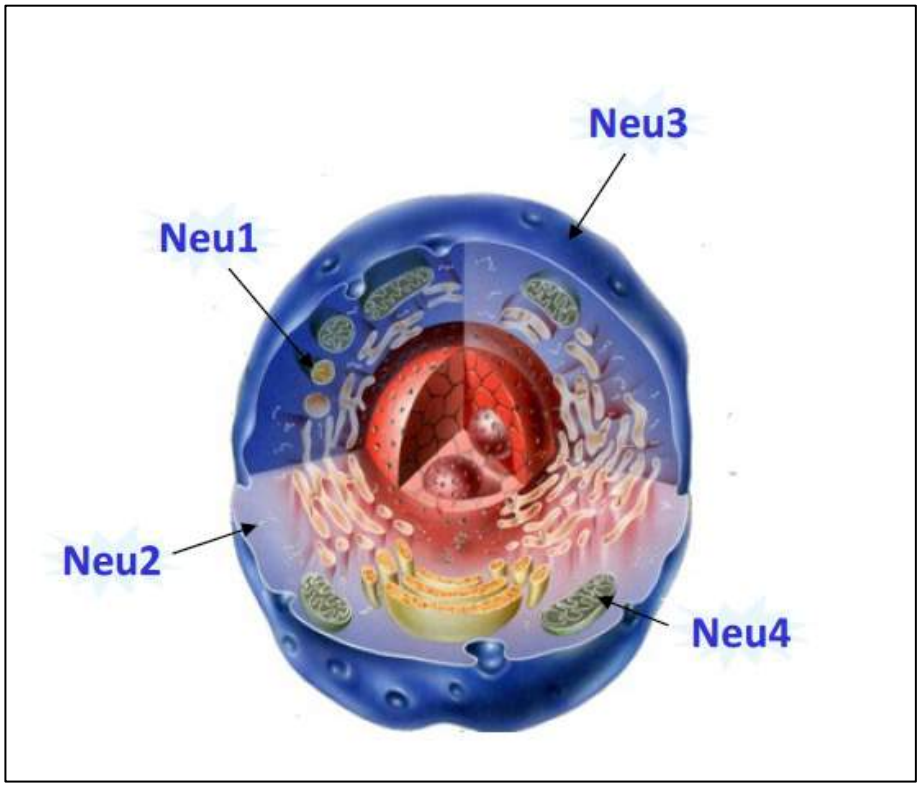

Figure 3.1**:** Cellular localization of mammalian sialidases

Lysosomal sialidase (NEU1) possesses narrow substrate specificity for oligosaccharides, glycopeptides and a synthetic substrate 4MU-Neu5Ac (4-methylumbelliferyl-N-acetylneuraminic acid) and is involved in lysosomal catabolism of sialoglycoconjugates by collaborating with lysosomal proteases or endoglycosidases[74]. Lysosomal storage diseases like sialidosis and galactosialidosis caused by NEU1 deficiency, interferes with the pathways for degradation of sialylated glycoconjugates[75]. In addition to this NEU1 has been proposed to be involved in cellular signaling during immune responses as well as monocytes differentiation[76].

Cytosolic sialidase (NEU2) is active against oligosaccharides, glycopeptides and perhaps gangliosides. In mammals, it has been implicated in myotube formation[77]. The exact mechanism of myoblast differentiation through its natural substrate remains obscure but it is claimed to decrease the GM3 ganglioside content, associated with the cytoskeleton.

Plasma membrane sialidase (NEU3) hydrolyzes gangliosides specifically (except GM1 and GM2) in presence of non-ionic surfactant (Triton X-100)[78]. Since gangliosides are abundant on the plasma membrane and are known modulators of several surface events like cell differentiation, cell proliferation and signal transduction, NEU3 has been shown to be involved in cell surface functions mainly by modulating ganglioside relative content in the lipid rafts. The enzyme is linked to the plasma membrane and has been shown to possess trans-activity because it can also work on the gangliosides present on the plasma membrane of adjacent cells. These key features are likely instrumental for a crucial role played by the enzyme in many cellular processes, including cell proliferation and differentiation. In particular, the increase of sialidase expression and activity during skeletal muscle differentiation has been shown to drive the process, protecting myoblasts from apoptosis[79]. Moreover, an induced overexpression of NEU3 renders murine myoblasts more resistant to cell cycle withdrawing and accelerates the differentiation process, ultimately increasing cell fusion. Finally, NEU3 has been also shown to positively participate to the differentiation

process leading to neurite formation in mice[80] and to the regulation and regeneration of rat hippocampus neurons[81].

Lysosomal or mitochondrial membrane sialidase (NEU4) has broad specificity, active against all major sialoglycoconjugates and has been implicated in the catabolism of glycolipids[82]. A recent report reveals the possibility of NEU4 being involved in apoptosis pathway at the mitochondrial level by regulating ganglioside GD3. Further functions of NEU4 are yet to be explored.

3.2 Development of an in-vitro model

We have previously described that NEU3 sialidase plays a key role in many cellular processes, including cell proliferation and differentiation[83]. However, it should be noted that activation of pro-survival pathways induced by NEU3, with concomitant suppression of apoptosis, has been mostly reported in pathological conditions[84]. For instance, NEU3 aberrant overexpression has been observed to occur in several neoplasms (including colon, ovarian, renal, and prostate cancer) and is considered to be one of the key triggers of tumor growth and invasiveness. In this PhD project we wanted to investigate the physiologic role of NEU3 on cellular homeostasis, with particular emphasis on the possible involvement of NEU3 in cell response to hypoxic stress and in cell machinery opposing cell death. To this purpose, the first step was to develop an in-vitro model of murine skeletal myoblast ischemia in order to investigate NEU3 expression and activity under hypoxic stress. Secondly, the enzyme was stably overexpressed or silenced in murine skeletal myoblasts C2C12, which were then cultured under hypoxic conditions (1% Oxygen), and the results compared with those of wild-type C2C12.

3.3 Materials and Methods

Cell culture

C2C12 mouse myoblasts were obtained from the American Type Culture Collection (ATCC) and cultured in Dulbecco's modified Eagle's medium with high glucose (DMEM) supplemented with 10% (v/v) fetal bovine serum (FBS), 4 mM L-glutamine, 100 U/ml penicillin, and 100 μg/ml streptomycin at 37°C in 5% CO_2, 95% air-humidified atmosphere.

Stable overexpression or silencing of sialidase NEU3 in C2C12 myoblasts

Silencing of NEU3 in C2C12 cells was achieved by designing a short hairpin targeting the mouse NEU3 gene sequence 894-914 (5-GCACCATGGCAAGTTCATTGA-3), (GenBankTM accession no. NM_016720) with the Block-iT RNA iDesigner Software (Invitrogen). Overexpression of NEU3 in C2C12 cells was obtained by cloning the entire NEU3 gene into the plasmid vector pLenti6.3/V5-TOPO® (Thermo Fisher Scientific). Viral particles were formed by transfecting 3 μg of pLenti4/BLOCK-iT-shNEU3 vector or pLenti6.3/V5-TOPO® NEU3 vector and 9 μg of packaging vector mix (Virapower, Thermo Fisher Scientific) in 293FT cells by Lipofectamine® 2000 reagent (Thermo Fisher Scientific). After 48 hours, the culture medium was collected and used to infect proliferating C2C12 cells (multiplicity of infection of 5) according to the manufacturer's procedure. Infected clones were isolated after selection with Blasticidin (3 mg/ml). NEU3-silenced cells were named "iNEU3" cells, whereas overexpressing cells were named "L-NEU3".

Chemical or physical hypoxic treatment

For the 1% O_2 hypoxia experiments, cells were cultured at 37°C in 5% CO_2, 1% O_2 incubator with nitrogen inlet. For chemical hypoxia, 100 μM deferoxamine (DFO, Sigma) was dissolved in the culture medium at the cells were treated for 6 – 24 – 48 – 72 hours.

Cell growth analysis

2 x10^5 C2C12, L-NEU3 or iNEU3 cells were seeded in 100 mm culture dishes and viable cells were counted with the Countess Automated Cell Counter (Thermo Fisher Scientific) every 24 hours up to 3 days using the vital stain Trypan Blue.

RNA extraction and retro-transcription in cDNA

Total RNA was isolated with RNeasy Mini Kit® (QIAGEN), following the protocol suggested by the manufacturer. mRNA quantity and purity were assessed by reading absorbance at 260 nm wavelength with a spectrophotometer Nanodrop (EuroClone). We considered suitable the samples with the following ratio:

- A260/A280 greater than 1,9 that means no contamination by proteins
- A260/A230 greater than 1,9 that means no contamination by carbs or phenol, which could affect retro-transcription efficacy.

All the samples satisfied both the aforementioned conditions. After isolation and purification, 1 µg of RNA was reverse-transcribed to cDNA using the iScript cDNA Synthesis Kit (Bio-Rad Laboratories) according to the manufacturer's instruction.

Briefly, for every sample the reaction mix was prepared as follow:

Reaction Mix	4 µL
Reverse transcriptase	1 µL
RNA	µL equivalent to 1 µg
H_2O	µL to fill the volume
Final Volume	20 µL

The samples were reverse transcribed in a thermocycler using the following protocol:

5 minutes at 25°C; 30 minutes at 42°C; 5 minutes at 85°C and resting at 4°C

Gene expression analysis by Real Time PCR

The quantitative expression of the genes of interest was assessed by Real Time PCR.

Initially, the specific primers to evaluate the expression of the genes of interest have been designed with the "Primer3" software and then checked with the "Blastn" program to control their correct annealing with the identified target genes.

For the analysis the following primers have been used:

PRIMER	**MELTING T (°C)**	**SEQUENCE**
β-actin	57	Fw- AGAGGGAAATCGTGCGTGAC Rev- CTCGTTGCCAATAGTGATGACC
NEU3	57	Fw- TGCGTGTTCAGTCAAGCC Rev- GCAGTAGAGCACAGGGTTAC
HIF-1α	57	Fw- CGCTATCCACATCAAAGCAA Rev- GCACTAGACAAAGTTCACCTGAGA
SP1	57	Fw- ATGCCCCTATTGCAAAGACA Rev- TGGATGTGACAAATGTGCTG
SP3	57	Fw- TGGTAAAAGATTTACACGAAGTGATG Rev- GGACAAACAAACTTCTTCTCACC

The single Real-Time PCR reactions were performed in a 96 well plate, mixing in a final volume of 20 μL the following reagents:

- cDNA; 10 ng
- Primers mix; 0,2 μM
- 1X iQ SYBR Green Supermix (Bio-Rad Laboratories) containing: Sybr Green, Taq polymerase (0.6 U), $MgCl_2$ (3 mM), Buffer (Tris/HCl 20 mM, KCl 50 mM, pH 8.4), dNTPs (200 μM).

The PCR reaction was performed under the following conditions:

- Initial denaturation: 95°C for 2 minutes (1 cycle)
- Denaturation: 95°C for 30 seconds
- Annealing: 57°C for 30 seconds
- Elongation, fluorescence detection: 72°C for 30 seconds
- Final Elongation: 72°C for 2 minutes

The three steps (denaturation, annealing and elongation) were repeated for 40 cycles.

The fold-change in expression of the different genes in L-NEU3 and i-NEU3 cells compared to control C2C12 was normalized to the expression of β-actin mRNA and was calculated by the equation $2^{-\Delta\Delta Ct}$ with iQ5 Software Version 2.0 (Bio-Rad Laboratories). All reactions were performed in triplicate and the accuracy was monitored by analysis of the PCR-product's melting curve.

Sialidase activity assay

Wild-type C2C12 cells, L-NEU3 and i-NEU3 cells were harvested by centrifugation at 2000 rpm for 10 minutes at 4°C and resuspended in PBS containing 1 mM EDTA, 1 μg/ml pepstatin A, 10 μg/ml aprotinin and 10 μg/ml leupeptin. Total cells suspensions were lysed by sonication (2 cycles of 10 burst each) and then centrifuged at 800 rcf for 10 minutes to eliminate unbroken cells and nuclear components. The obtained supernatants were subsequently centrifuged at 200000 rcf at 4°C for 20 minutes on a TL100 Ultracentrifuge (Beckman) to obtain cytosolic and particulate (or membranes) fractions.

The sialidase activity present in the particulate fraction was assayed by a fluorimetric assay using 4-MU-NeuAc (4-methylumbelliferyl N-acetylneuraminic acid). The activity was expressed as U/mg protein: 1U equals to 1μmole of substrate released in 1 minute.

The reaction mixture for each sample was prepared as follow:

- 50 mM Citrate phosphate buffer, pH 3.8
- 0,1 mM MU-NeuAc

- 600 μg BSA
- 30 μg of membrane proteins containing the enzyme

The mixture was brought to a final volume 100 μl with H_2O.

The samples were incubated at 37°C, with shaking, for 1 hour. At the end of the incubation, the reaction was sopped by the addiction of 1,5 ml of 0,2 M glycine pH 10.8 for each sample. The amount of 4-methylumberilliferyl released by the enzyme was determined by measuring the fluorescence emitted. The fluorescence was determined using a Nanodrop fluorometer (excitation: 365λ emission: 448λ).

Protein expression analysis by Western Blot

Western blot is often used in research to separate and identify specific proteins. In this technique a mixture of proteins is separated by gel electrophoresis in the presence of Sodium Dodecyl Sulphate (SDS) and transferred to a membrane that, at a later stage, will be incubated with antibodies specific for the proteins of interest. This technique allows to identify not only the presence/absence of a specific protein but also to determine its molecular weight and relative quantitative expression.

Cells were lysed in ice-cold lysis buffer, containing 1% of nonylphenoxypolyethoxylethanol (NP40, Sigma) in 50 mM Tris-HCl at pH 7.5; 150 NaCl; 0.1% sodium deoxycholate; 1X protease inhibitor cocktail and 1X phosphatase inhibitor cocktail (Sigma). Lysates were incubated for 30 minutes on ice and centrifuged at 14000 rcf for 10 minutes at 4°C.

Before separating proteins by SDS-electrophoresis, their concentrations were measured by the Pierce™ BCA Protein Assay Kit (Thermo Fisher Scientific) following the manufacturer's protocol. 30 μg of proteins were denatured by boiling for 5 minutes in sample buffer (62,5 mM Tris-HCl pH 6.8, 2% SDS (w/v), 10% glycerol (v/v), 5% 2-mercaptoethanol (w/v), 0,01% bromophenol blue (w/v)) and separated on a 10%

polyacrylamide gel in denaturing conditions. A discontinuous gel has been prepared composed by the stacking and the running gels.

Stacking Gel Composition

- Deionized water
- Tris-HCl 1.5 M, pH 6.8
- SDS 0.1% w/v
- Acrylamide 4%
- APS 10% w/v
- TEMED

10% Running Gel composition

- Deionized water
- Tris-HCl 1.5 M, pH 8.8
- SDS 0.1% w/v
- Acrylamide 10-12%
- APS 10% w/v
- TEMED

Proteins were subsequently transferred onto nitrocellulose membranes by electroblotting using 100 Volt for 2 hours. Then, the membranes were incubated overnight in Tris-buffered saline (TBS: 10 mM Tris-HCl, pH 7.4, 150 mM NaCl), 0.1% (v/v) Tween 20 (TBS-Tween) containing 5% (w/v) dried milk or 5% (w/v) bovine serum albumin (BSA; Sigma) for the blocking buffer. Blots were incubated with a primary antibody in the appropriate blocking solution for 3 hours at room temperature.

The primary antibodies used for the analysis were the following:

PRIMARY ANTIBODY	DILUTION	MANUFACTURER
EGFR	1:1000	Cell Signaling ®
p-EGFR	1:1000	Cell Signaling ®
AKT	1:100	Santa Cruz ®
p-AKT	1:100	Santa Cruz ®
HIF-1α	1:1000	Novus Biologicals ®
p70S6K	1:1000	Cell Signaling ®
p-p70S6K	1:1000	Cell Signaling ®
β-actin	1:5000	Abcam ®

The membrane were washed 4 times for 10 minutes with TBS-Tween and then incubated with the appropriate secondary antibody conjugated with horseradish peroxidase (HRP) for 1 hour at room temperature. After 4 washes in TBS-Tween, the protein bands were detected using an ECL detection kit (Thermo Fisher Scientific) as described by the manufacturer.

Treatment of cell cultures with [3-^{3}H]-Sphingosine

The determination of the ganglioside pattern of wild-type C2C12, L-NEU3 and i-NEU3 cells was accomplished by radioactive metabolic labeling with [3-^{3}H]-Sphingosine (Perkin Elmer).

[3-^{3}H]-Sphingosine is a natural precursor of sphingolipids. When cells are placed in culture medium supplemented with radiolabeled sphingosine, it is absorbed and used into the biosynthetic pathways of sphingolipids. The metabolic products are radioactive, and after extraction and separation by HPTLC, it is possible to evaluate the cellular sphingolipid

content in terms of both quality and quantity.

[3-^{3}H]-Sphingosine was dissolved in methanol, transferred into a sterile glass tube, and then dried under a nitrogen stream. The residue was dissolved in an appropriate volume of pre-warmed (37°C) 10% fetal bovine serum DMEM medium to obtain a final sphingosine concentration of 3 x 10^{-8} M (corresponding to 0.4 μCi/100 mm dish). The solution was sonicated for 2 minutes and vortexed for 1 minute. This procedure was repeated 3 times. The degree of solubilization (> 70%) was verified by counting theradioactivity by β-counter (Perkin Elmer).

A total of 1 x 10^{6} cells were incubated in this medium for a 2 hours pulse followed by a 24 hours chase, a condition warranting a steady-state metabolic condition. At the end of the 24 hours chase, cells were harvested and lyophilized for the lipids extraction and analysis.

Lipid extraction and analysis

The lyophilized cells were resuspended in 25 μl of water, sonicated in ultrasonic bath and vortexed. In order to obtain a good solubilization, two lipid extractions were made.

- **First extraction**

10 volumes of methanol were added to the aqueous solution of cells. The resulting mixture was sonicated in ultrasonic bath for 2 minutes and vortexed for 1 minute. Then, 20 volumes of chloroform were added. Sonication in ultrasonic bath for 2 minutes and agitation were repeated. The samples were shaken on an Eppendorf shaker for 10 minutes and centrifuged at 10000 rcf for 10 minutes at room temperature. The supernatant containing the lipids was transferred to a new eppendorf.

- **Second extraction**

10 volumes of a mixture of chloroform/methanol 2:1were added to pellet. The samples were sonicated in ultrasonic bath, vortexed and shaken for 10 minutes; then, samples were centrifuged at 10000 rcf for 10 minutes at room temperature. The lipid supernatant was

collected and combined with that collected after the first extraction. The protein pellets, after the evaporation of solvent, were digested overnight at room temperature in 50 µl of 1N NaOH and subsequently, brought to 1 ml with water. Protein concentration was then measured by the Lowry method. The lipid radioactivity was evaluated to determine the percentage yield of the lipid extraction.

- **Partition of lipids**

This procedure allows to divide the extracted lipid in an aqueous phase (FA), containing gangliosides, and an organic phase (FO), containing neutral glycolipids.

The partition was divided into two phases:

- **First partition**

In order to separate the aqueous from the organic phase, a volume of water equal to 20% of the total solution was added to lipid extracts. Samples were vortexed and mixed on a Eppendorf mixer for 15 minutes and centrifuged at 3500 rcf for 5 minutes. The aqueous phase was collected and transferred to a new eppendorf.

- **Second partition**

A mixture of methanol/water 1:1, equal to 40% of the initial volume, was added to the organic phase. The separation of the aqueous phase from the organic phase was obtained by vortexing and agitation on an Eppendorf shaker for 15 minutes and, finally, centrifugation at 3500 rcf for 5 minutes. The aqueous phase was collected and added to the one obtained in the first separation. The two separated phases were dried under nitrogen stream and suspended in a mixture of chloroform/methanol 2:1. The aqueous phase was resuspended in 100 µl of solvent, while the organic phase was resuspended in 200 µl. Radioactivity assays of the two phases were performed to determine the percentage yield of the partition. Neutral glycolipids of the organic phase were then separated by HPTLC using a chloroform/methanol/water (110:40:6 (v/v/v)) solvent system whereas gangliosides were separated by a chloroform/methanol/0.2% aqueous $CaCl_2$ (60:40:9 (v/v/v)) solvent system.

[3-^{3}H]-Sphingolipids were identified by referring to radiolabeled standards and quantified by radiochromatoimaging (Beta-Imager 2000, Biospace). The content of the component detected was expressed as dpm/mg of total proteins.

Silencing of GM3 Synthase by siRNA Transfection

Specific siRNA duplexes targeting GM3 synthase, siRNA transfection reagents, and reduced-serum transfection medium were purchased from Santa Cruz Biotechnology. The day before transfection, $2x10^{5}$ C2C12 myoblasts were seeded in each well of a 6-well cell culture plate in DMEM containing 10% FBS without antibiotics and incubated for 24 hours at 37°C and 5% CO_2. The next day, transfection complexes were prepared using GM3 synthase siRNA, siRNA transfection reagent, and transfection medium according to the manufacturer's protocol and were added to each well. The final concentration of GM3 synthase siRNA duplexes used was 3μg .A scrambled siRNA (Santa Cruz Biotechnology) was used as negative control. GM3 synthase primers: forward, 5'-TTCTGGGGCCATGATAAGAA-3' and reverse 5'-TGACTGAGGTCGTAGCCAAA-3'.

3.4 Results

Effects of Hypoxia on Wild-type C2C12 Proliferation and NEU3 Expression and Activity

Wild-type C2C12 cells were cultured for 72 h in 1% oxygen or DFO, which is widely used at this concentration to chemically mimic hypoxia by chelating iron. The final concentration of 100 μM was chosen because it was more toxic than 1% oxygen, but not completely lethal, and could allow us to test NEU3 effects under severe hypoxic stress. Exposure to 1% oxygen caused a marked reduction of proliferation compared with untreated C2C12. DFO treatment caused massive cell death, as only few cells were alive after a 72 h treatment, and widespread cell debris could be observed in the culture plates. NEU3 expression, measured by qPCR, underwent a progressive and remarkable increase during 1% O_2 or DFO treatment. NEU3 activity increased markedly over time during exposure to 1%O_2 and, to a minor extent, upon DFO treatment. NEU3 activity with DFO could not be determined at 72 h due to the massive extent of cell death (***Figure 3.2***).

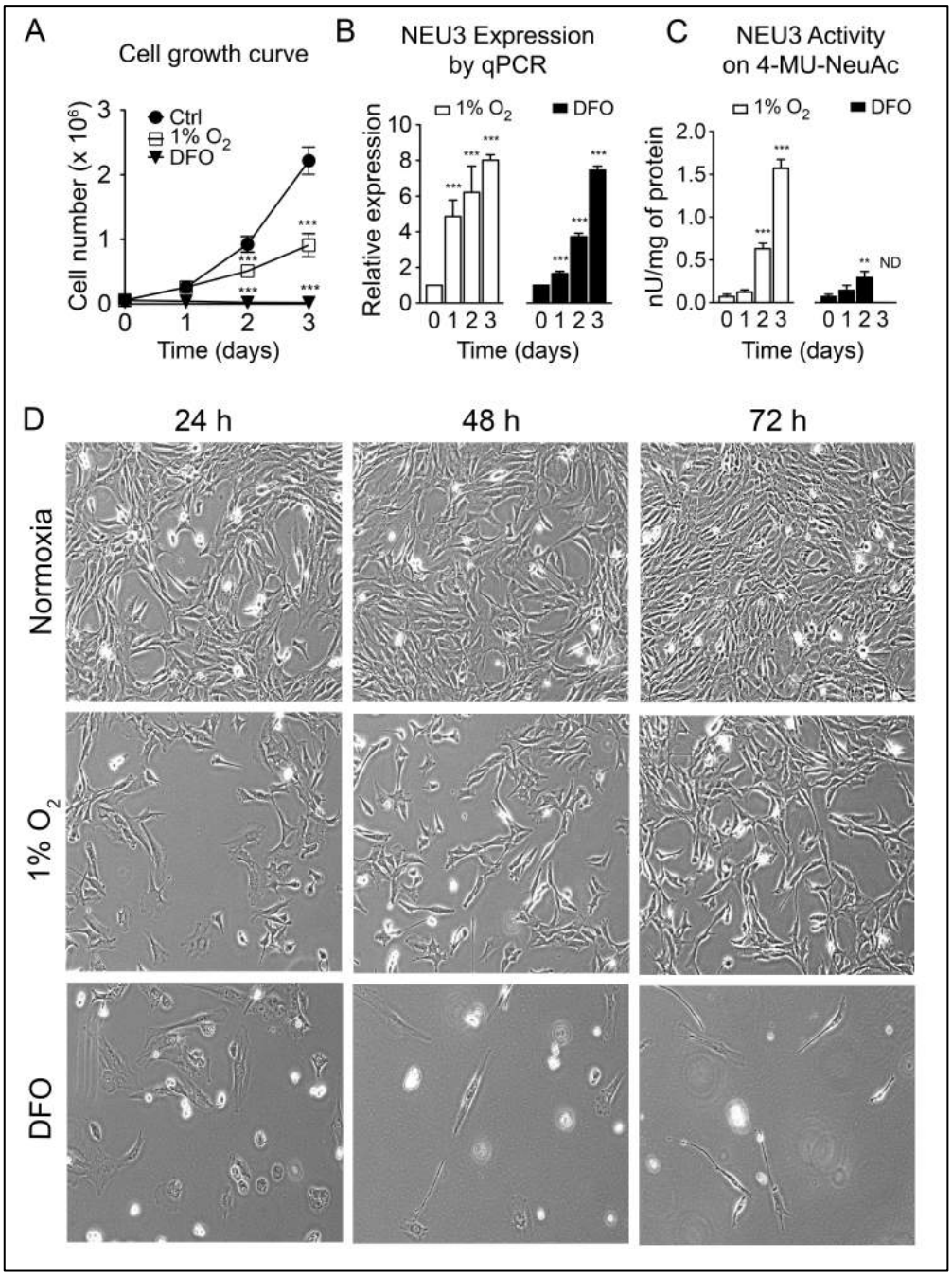

Figure 3.2. Effects of hypoxia on C2C12 cell proliferation and NEU3 expression and activity. Proliferating C2C12 cells were cultured for 24, 48, and 72 h in normoxia or in 1% O2 and 100 μM DFO hypoxic conditions. A, cell growth curves. B, NEU3 expression by qPCR. C, NEU3 activity on 4-MU-NeuAc. All data are means±S.D. of three different experiments. Statistical differences were determined by one-way ANOVA. **, $p<0.001$; ***, $p<0.0001$ compared with initial values. D, phase-contrast microscopic images at 10x magnification.

Effects of NEU3 Sialidase Overexpression and Silencing on C2C12 Proliferation under Hypoxia

C2C12 cells were transduced with a lentiviral vector containing the murine NEU3 sialidase gene. Among five clone tested, clone 2 (hereafter named L-NEU3) showed the highest sialidase expression, which was 19-fold higher than in C2C12, whereas sialidase activity was approximately 3-fold higher. C2C12 cells were also transduced with a lentiviral vector engineered to silence NEU3 with a shRNA targeting the coding region of the enzyme. The selected clone, hereafter named i-NEU3, showed the lowest sialidase expression levels, quantified as a 2.5-fold reduction compared with wild-type C2C12, whereas sialidase activity displayed a 3-fold decrease. C2C12, L-NEU3, and i-NEU3 cells were then cultured for 3 days in normoxia, or 1% oxygen, or 100 μM DFO and analyzed for cell growth. As shown in ***Figure 3.3***, under normoxic conditions cell growth was slightly higher (approximately 15% after 3 days) in L-NEU3 compared with C2C12 cells, whereas in i-NEU3 cells it was much lower (approximately 40% less). In 1% O2 conditions, L-NEU3 cells had a proliferation reduction after 3 days in culture which was much lower than control C2C12 cells (33% versus 58%), whereas i-NEU3 cells underwent a drop in proliferation close to 90%. Upon DFO treatment, proliferation appears to be blocked in all cell types, with a cell survival after 3 days of 80% for L-NEU3 cells, 30% for C2C12 cells, and 27% for i-NEU3 cells. Panels D in ***Figure 3.3*** show that L-NEU3 cells reached confluence after 3 days culture in normoxic conditions, as well as at 1% O2, but little proliferation occurred in DFO. By contrast, i-NEU3 cells exhibited clear signs of massive cell death in both 1%O2 and DFO because many dead cells could be found floating in the culture dish.

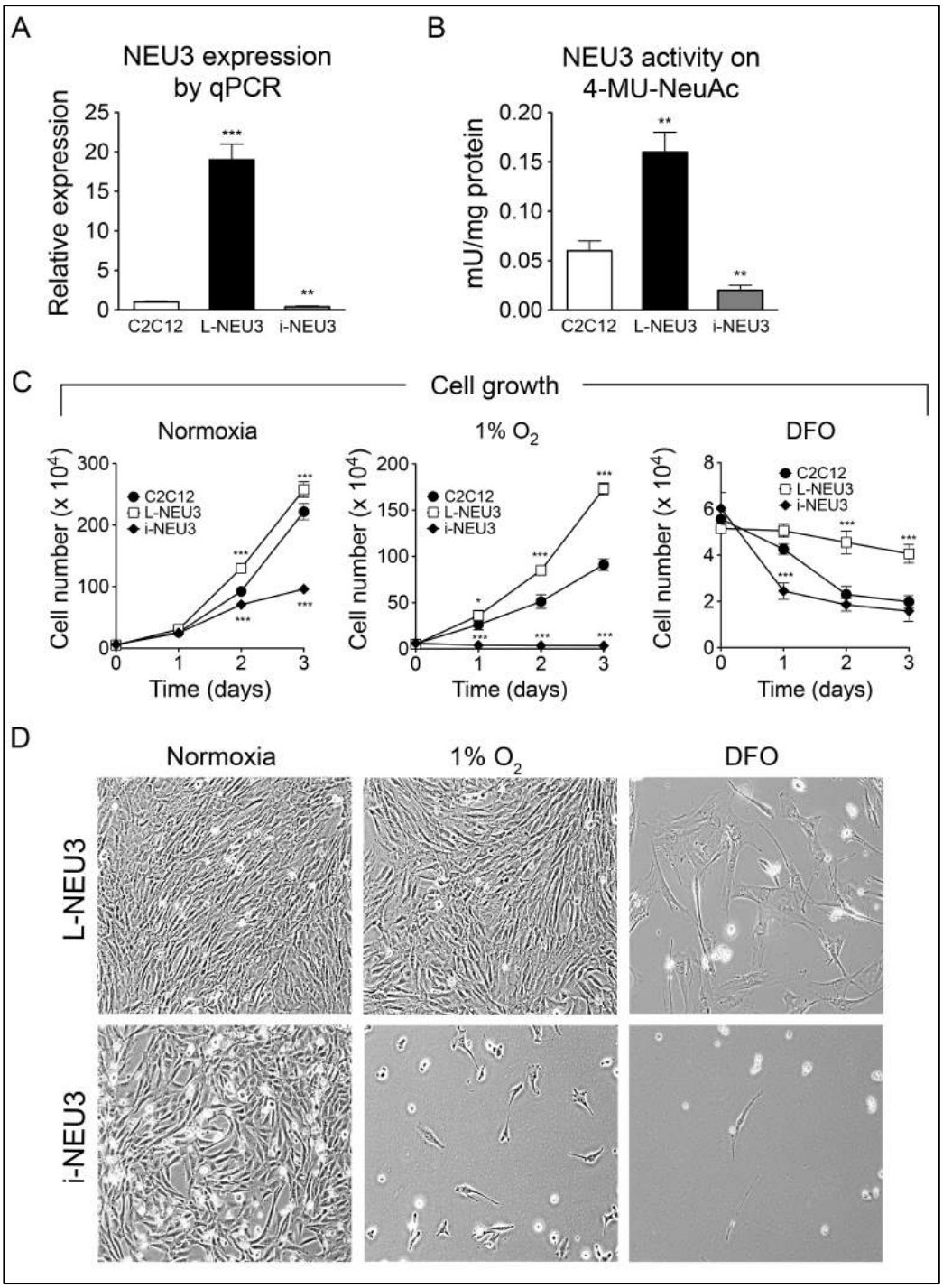

Figure 3.3: Effects of NEU3 overexpression or silencing on C2C12 resistance to hypoxic conditions. A, qPCR analysis of NEU3 mRNA expression levels. B, NEU3 activity on 4-MU-NeuAc. Data are means±S.D. of three different experiments, significance according to two-way ANOVA. **, $p<0.001$; ***, $p<0.0001$ compared with wild-type C2C12 cells. C, growth curves of cells cultured in normoxia, 1% oxygen and 100 μM DFO. D, phase-contrast microscopy (10x magnification) of L-NEU3 and i-NEU3 cells cultured in normoxia, 1% O2, and 100 μM DFO for 72 h.

Sphingolipid Pattern Analysis

The glycosphingolipid profile of control C2C12, L-NEU3, and i-NEU3 cells was determined by administration of [3-^{3}H]sphingosine, which led to an extensive and stable 3-^{3}H-labeling of cell sphingolipids, namely gangliosides, neutral glycosphingolipids, sphingomyelin, and ceramide, at steady-state conditions. Analysis of the ganglioside pattern revealed a 35% reduction ofGM3in L-NEU3 cells, whereas a 2-fold increase of the same ganglioside could be observed in i-NEU3 cells, making GM3 approximately 97% of the total ganglioside content. (***Figure 3.4***, A and B). However, no significant variation could be detected for the other major gangliosides in L-NEU3 cells, whereas i-NEU3 showed a significant reduction in GM2 (-89%) and GD1a (-96%). Conversely the radioactive patterns of the sphingolipids contained in the organic phase did not exhibit significant differences upon overexpression or silencing of NEU3, with only a minor increase of GlcCer, LacCer, and SM in L-NEU3 cells (***Figure 3.4***, C and D).

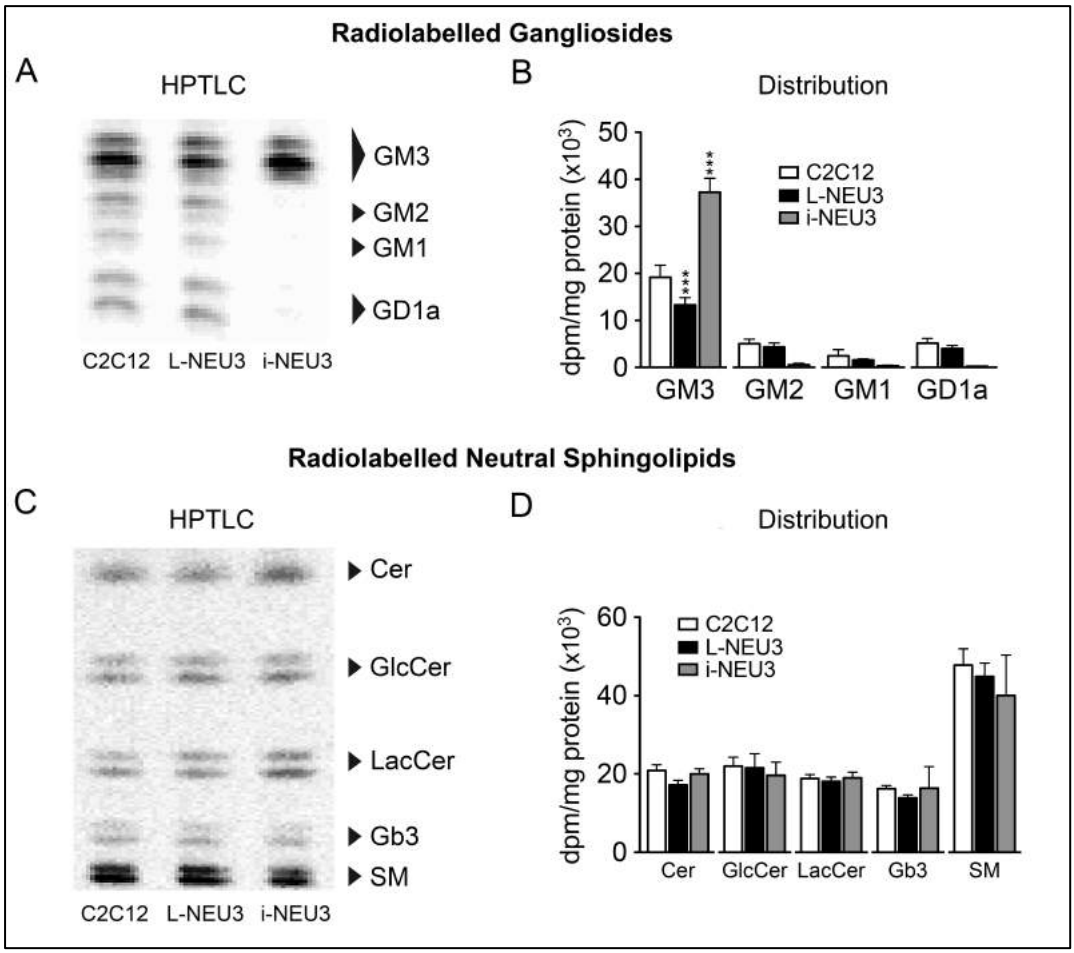

Figure 3.4: **Effects of NEU3 activity on the sphingolipid pattern.** Proliferating C2C12, L-NEU3, and i-NEU3 cells were metabolically labeled with [3-^{3}H]sphingosine. *A*) radiochromatoscanning images of HPTLC separation of gangliosides contained in the aqueous phase. *B*) ganglioside distribution expressed as dpm/mg of protein. *C*) radiochromatoscanning images of HPTLC separation of sphingolipids contained in the organic phase. *D*) sphingolipid distribution expressed as dpm/mg of protein. Data of *B* and *D* represent means±S.D. (*error bars*) of five different experiments (significance according to two-wayANOVA:**, $p<0.001$ and ***, $p<0.0001$ compared with wild-type C2C12 cells).

NEU3 activation of HIF-1α through the EGFR-mediated signaling pathway

Analysis of the ganglioside pattern revealed a 35% reduction of GM3 in L-NEU3 cells, whereas a 2-fold increase of the same ganglioside could be observed in i-NEU3 cells, making GM3 approximately 97% of the total ganglioside content. Because ganglioside GM3 is known to inhibit EGFR autophosphorylation, we tested whether NEU3-induced reduction of GM3 would affect the activity of key proteins of the EGFR-mediated signaling cascade, in their inactive and/or active (phosphorylated) forms, thus leading to regulation of HIF-1α expression. Therefore, the levels of these proteins in all three cell-lines (control C2C12, L-NEU3, and i-NEU3) under normoxic and hypoxic conditions (1% O2 at 3, 6, and 24 h) were analyzed by Western blotting. Results revealed that HIF-1α, could not be detected in control C2C12 cells grown for 3, 6, and 24 h in normoxia as expected, because HIF-1α is degraded under normoxic conditions by the ubiquitin-proteasome system. Analogous results were observed in i-NEU3 cells. Conversely, L-NEU3 cells exhibited substantial levels of HIF-1α even under normoxia. Upon cell culturing in 1% oxygen, HIF-1α protein level increased over time in all cells, although in L-NEU3 it reached the highest levels. In particular, in L-NEU3 cells, high levels were reached already within 3 h under hypoxia, whereas comparable levels were reached by control C2C12 only at 6 h, and by i-NEU3 at 24 h. Western blot analysis of the EGFR-mediated signaling cascade, leading to HIF-1α activation, revealed similar trends, because EGFR, phospho-EGFR, AKT, phospho-AKT, p70S6K, and phospho-p70S6K were all activated earlier in L-NEU3 cells and exhibited higher levels compared with control C2C12. The increments of all measured proteins were delayed and exhibited anyhow lower levels in i-NEU3 cells (***Figure 3.5***).

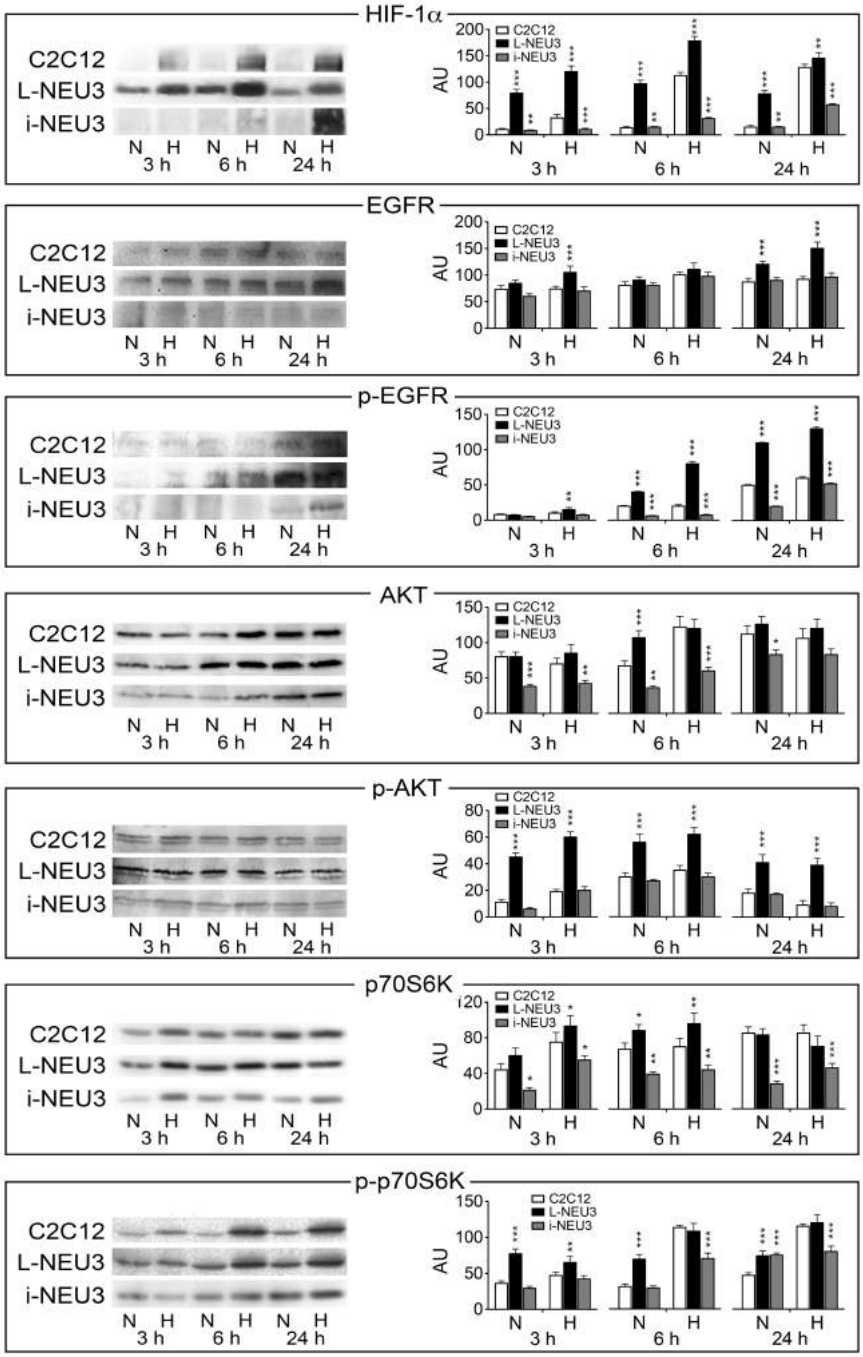

Figure 3.5: **Analysis of EGFR-mediated signaling pathway by Western blotting**. Total proteins from C2C12, L-NEU3, and i-NEU3 cells cultured for 3, 6, and 24 h in 1% O2 anoxic conditions were stained with anti-HIF-1α (A), anti-EGFR antibody (B), anti-phospho-EGFR antibody (C), anti-AKT antibody (D), antiphospho-AKT antibody (E), anti-p70S6K (F), and anti-phospho-p70S6K (G). Changes in protein content were quantified by densitometry and are represented in columns. N, normoxic; H, hypoxic. All data are the means±S.D. (error bars) of three different experiments. Statistical differences were determined by two-way ANOVA. *, $p < 0.05$; **, $p < 0.001$; and ***, $p < 0.0001$ compared with C2C12 cells.

Silencing of GM3 Synthase

To test whether the observed effects go through NEU3-induced GM3 depletion and consequent EGFR activation, we tested whether we could mimic NEU3 effects by silencing GM3 synthase, thus reducing GM3 cell content. To this purpose, wild-type C2C12 were transfected with specific siRNA duplexes targeting GM3 synthase. Analysis by qPCR revealed a 50% reduction in GM3 synthase expression compared with controls (***Figure 3.6-A***). Analysis of the sphingolipid pattern by administration of [3-^{3}H]sphingosine (***Figure 3.6 B and C***), revealed a significant decrease of ganglioside GM3, which was approximately 35% less than controls, whereas both lactosylceramide and globotriaosyl ceramide were markedly increased. Analysis of cell growth under normoxia revealed a significant, although minimal, increase in cell proliferation in GM3 synthase-down-regulated C2C12 (***Figure 3.6-D***). Cells were then subjected to 1%O2 and monitored for 48 h. Cell growth analysis showed a significant cell number reduction after 48 h in hypoxia in control C2C12, as expected. However, down-regulation of GM3 synthase rendered myoblasts more resistant to hypoxia, as we could detect a 25% increase of alive cells after 48 h in hypoxia, compared with control cells (***Figure 3.6-E***).

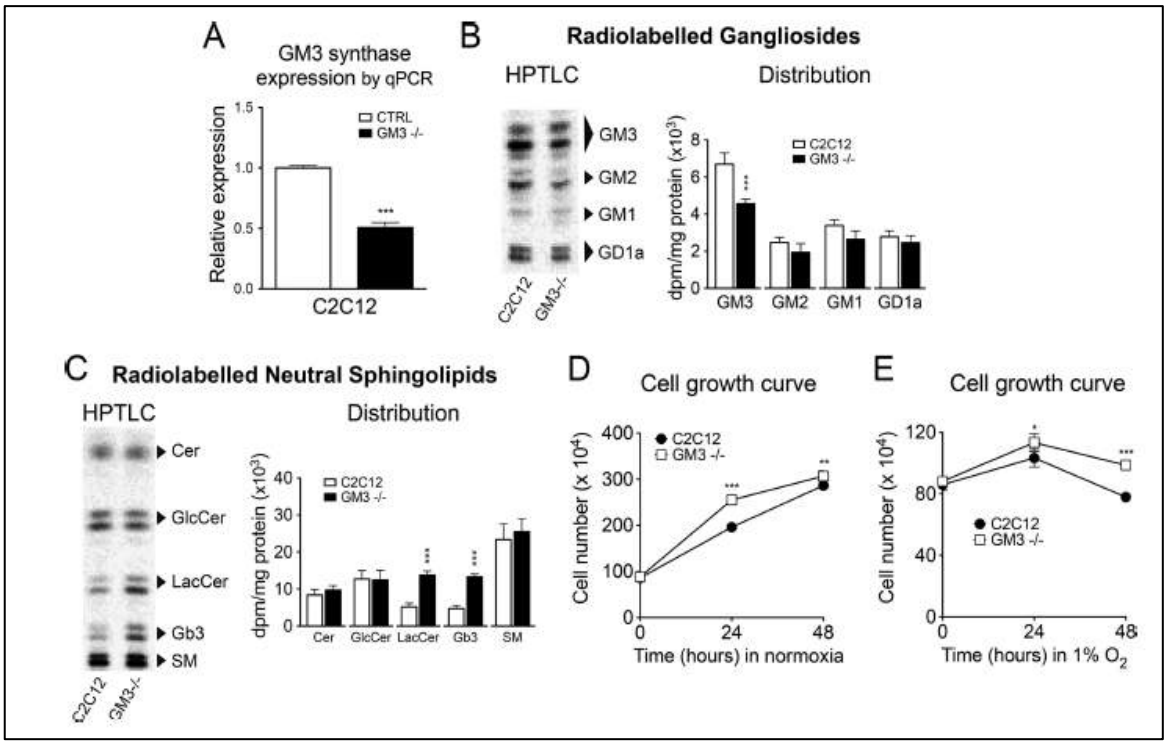

Figure 3.6: **Silencing of GM3synthase increases C2C12 resistance to hypoxia**. A, qPCR analysis of GM3 synthase mRNA expression levels in control and GM3 synthase-silenced C2C12 cells. B, radiochromatoscanning images of HPTLC separation of gangliosides contained in the aqueous phase. C, radiochromatoscanning images of HPTLC separation of sphingolipids contained in the organic phase. Sphingolipid distribution is expressed as dpm/mg of protein. Data of B and C represent means±S.D. (error bars) of three different experiments. Significance was determined according to two-way ANOVA. ***, $p<0.0001$ compared with wild-type C2C12 cells. D and E, growth curves of cells cultured in normoxia (D) and in 1% oxygen (E). Data of D and E are means±S.D. of three different experiments. Significance was determined according to two-way ANOVA. *, $p<0.005$; **, $p<0.001$; and ***, $p<0.0001$ compared with wild-type C2C12 cells.

Activation of SP1/SP3 under Hypoxia

Wild-type C2C12cells were subjected to 1% O2 for 48 h to test the activation of transcription factors SP1 and SP3, which have been recently found to bind to NEU3 promoter region. Analysis of SP1 and SP3 expression by qPCR revealed a significant increase of both factors under hypoxia (***Figure 3.7, A and B***), supporting a possible mechanism of endogenous activation of NEU3 under hypoxia (***Figure 3.7-C***).

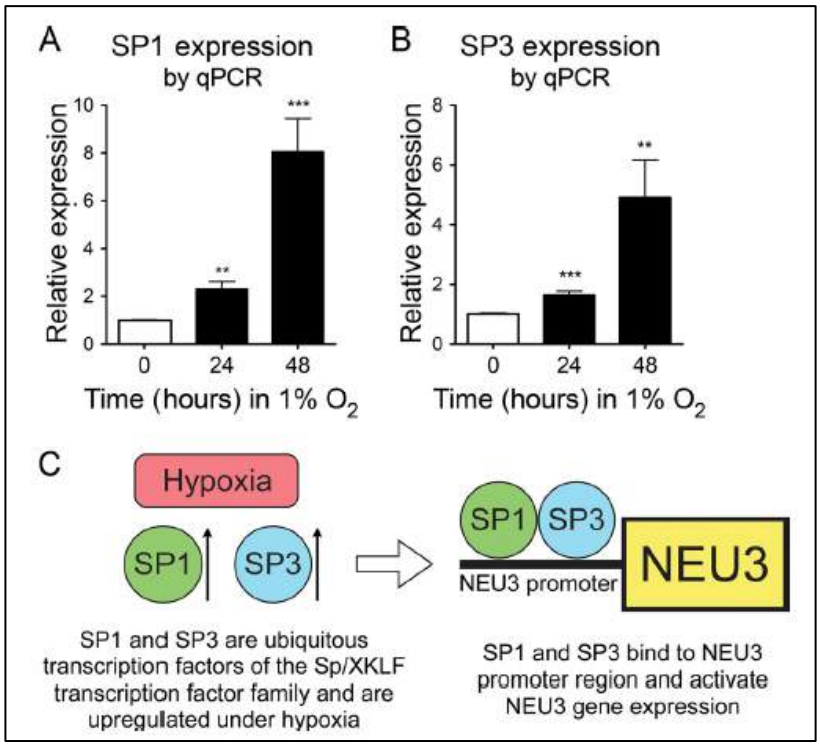

Figure 3.7: Activation of SP1 and SP3 under hypoxia could lead to NEU3 up-regulation. A and B) qPCR analysis of SP1 and SP3mRNAexpression levels in C2C12 cells cultured in 1% O2 up to 48 h. C) schematic representation of SP1/SP3-mediated activation of NEU3 sialidase under hypoxia.

3.5 Discussion

The experiments performed in this in-vitro model allowed us to draw the following conclusions:

1) Endogenous NEU3 sialidase expression and activity are up-regulated in murine skeletal muscle cells (C2C12) upon oxygen starvation, leading to a signaling cascade resulting in the activation of HIF-1α.
2) Moreover, induced overexpression of NEU3 significantly increases HIF-1α expression and cell resistance to hypoxic stress, whereas NEU3 silencing causes the opposite effects and renders myoblasts more susceptible to apoptosis.

These data substantiate the hypothesis that NEU3 sialidase, which was found to be activated under hypoxic conditions, can activate the EGFR pro-survival signaling pathway by controlling the content of ganglioside GM3. To test this hypothesis, the effects of NEU3 overexpression and silencing were studied on the EGFR signaling pathway. As anticipated, NEU3 overexpression causes a reduction of ganglioside GM3, which is known to block EGFR autophosphorylation. Therefore, upon NEU3 up-regulation, the net effect is that EGFR signaling cascade is activated, as demonstrated by the activation of pro-survival and anti-apoptotic signaling molecules down-stream of EGFR, including AKT, p70S6K, and ultimately HIF-1α. This causes an increased resistance of myoblasts to hypoxia, ultimately opposing apoptotic cell death. Notably, upon NEU3 overexpression, HIF-1α mRNA and protein levels were also up-regulated. Analysis of NEU3-activated EGFR signaling revealed the activation of p70, which is known to promote HIF-1α transcription (***Figure 3.8***).

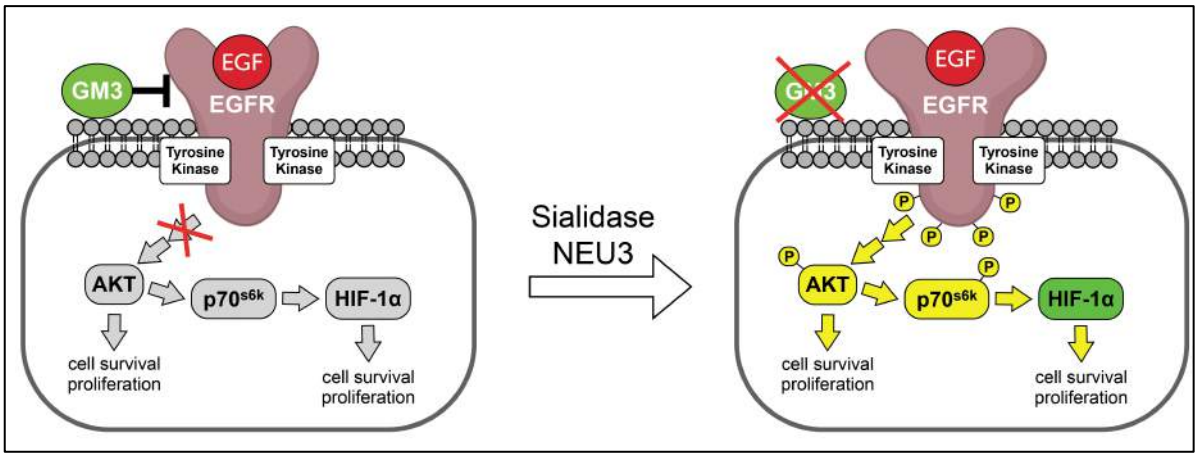

Figure 3.8: Scheme of EGFR signaling pathway activated by NEU3-induced GM3 reduction. A) NEU3 removing sialic acid from gangliosides exposed on the outer membrane of adjacent cells B) mechanism of NEU3 activation of pro-survival signaling cascades, ultimately up-regulating HIF-1α

These findings could also be useful for a better understanding of the NEU3 role in cancer, where sustained levels of HIF-1α are observed[85] and are necessary for malignant progression under hypoxic conditions, which is the most suitable environment for tumor proliferation and growth. To further support the hypothesis of a key role played by ganglioside GM3 in activating the EGFR signaling cascade, we tried to mimic NEU3 overexpression effects on reducing GM3 content by silencing GM3 synthase. Remarkably, GM3 synthase down-regulation, although only partial, caused a reduction in GM3 content in C2C12 cells which caused an increased cell survival upon subjection to hypoxia in 1% O2. Noticeably, although GM3 is approximately 97% of the total ganglioside content in i-NEU3 cells, a significant reduction of gangliosides GD1a and GM2 could be observed upon NEU3 silencing. Therefore, at this stage, we cannot exclude an involvement of these sphingolipids in NEU3 activity. Finally, whereas NEU3effects and mechanism of action seem to be clarified, little is known about how and whether the enzyme is physiologically up-regulated under hypoxia. Interestingly, it has been recently reported the binding of transcription factor SP1 and SP3 to the NEU3 promoter region[86]. These factors are ubiquitous transcription

factors (of the Sp/XKLF transcription factor family) that are involved in basal transcription and housekeeping gene expression, and they are known to be activated under hypoxic conditions[87]. Therefore, it is tempting to speculate that NEU3 response upon oxygen starvation might be regulated through SP1/SP3 activation. Interestingly, upon subjecting C2C12 cells to 1% O2, both SP1 and SP3 mRNA levels were found up-regulated, thus supporting their involvement in activating NEU3 gene transcription under hypoxic stress. Further investigations to test this hypothesis are ongoing in our laboratories. In a translational perspective, it would be very interesting to test whether NEU3 effects can be recognized also in other cells, in particular in those critically affected under hypoxic conditions in many pathologies, like cardiomyocytes and neural cells.

As cardiac surgery offers the unique opportunity of in-vivo model of cardiac ischemia-reperfusion, the second step of my PhD project was to investigate NEU3/HIF1α expression and activity in human cardiomyocytes from sample obtained during routine adult cardiac procedures.

CHAPTER 4: Acute Model of Cardiac Ischemia in Humans

4.1 Introduction: Extracorporeal Perfusion

Extracorporeal circulation (ECC) is a powerful technology that makes open-heart surgery, temporary circulatory or respiratory assistance, and long-term life support possible. Extracorporeal perfusion systems circulate blood and, depending on the application, ventilate, cool, rewarm or process blood. Because tubing transverses the skin barrier, all extracorporeal perfusion systems are designed for temporary application. Of necessity, blood comes into contact with the various biomaterials of the perfusion circuit, and unfortunately, this contact activates blood proteins and cells of the body's defense system. Consequences of this activation cause most of the morbidity associated with the technology.

Open-heart surgery required the development of a means to both pump and ventilate blood. The actual development of this technology has a long history spanning over 100 years and was enabled by the discovery of heparin in 1916 and protamine in 1937. Before John and Mary Gibbon developed the "heart-lung machine", others had experimented with blood pumps and extracorporeal oxygenation of venous blood[88]. On May 6, 1953, Dr. Gibbon successfully closed an atrial septal defect in Cecelia Bovalak using cardiopulmonary bypass (CPB) provided by a machine made to the Gibbon design by the International Business Machines Corporation. The first successful series of patients with open-heart surgery using CPB was reported by Kirklin and DuShane in 1955. Since that time, multiple technical advances in equipment and practice have decreased the morbidity and mortality of extracorporeal circulation, reduced the need for massive blood transfusions and widened applications of the technology.

4.2 Conduction of Open Heart Surgery using ECC

The heart-lung machine is the most “option-laden” model of extracorporeal perfusion systems. The basic components are one or more venous cannula, a venous reservoir, an oxygenator/heat exchanger, a pump, an arterial line filter and an arterial cannula. The machine is built from biocompatible materials that, by definition, are nontoxic, nonimmunogenic, nonallergic and nonmutagenic.

Through one or more venous cannulas, deoxygenated blood drains by gravity into the extracorporeal circuit or pump-oxigenator system. The number of venous cannulas depends on the type of cardiac surgical procedure and, to some extent, on the surgeon’s preference. When one cannula is used, it is usually placed in the right atrium through the right atrial appendage. When two cannulas are used, they are placed in the superior and inferior venae cavae. Many surgeons for operations involving the aortic valve, the ascending aorta and coronary bypass procedures, use a single cavoatrial cannula. Two venous cannulas are necessary to work on the mitral valve, on the right atrium or ventricle.

The arterial cannula is usually placed in the ascending aorta just proximal to the innominate artery, but it can be placed anywhere in the arterial system that is large enough to accommodate the necessary flow. Alternative cannulation sites include the femoral, iliac and axillary arteries.

When ECC is started, an aortic cross-clamp is applied on the ascending aorta just proximally to the arterial line, in order to exclude the aortic root (and the coronary arteries) from the systemic circulation. This allowed the surgeon to operate on an empty, bloodless heart. On the other hand during aortic cross-clamp time, the heart is not perfused, so it is globally ischemic. To minimize the potential myocardial damage during this phase, several strategies to implement myocardial protection (cardioplegia, systemic cooling and topical cooling) have been developed during cardiac surgery history, and will be described in the next paragraph.

When surgery is finished, aortic cross-clamp is removed and the heart is allowed to reperfuse in an empty beating condition, in order to recover from the ischemic phase. Finally the heart is weaned from ECC and the chest is closed in a standard fashion.

4.3 Cardioplegia and Myocardial Protection.

The first open-heart surgery operation in 1952, used whole-body systemic hypothermia (~28 °C) and brief (~6 min) circulatory arrest. At that time, it was known that hypothermia was a protective mechanism that reduced organ oxygen requirement, particularly to the brain. The subsequent development of cardiopulmonary bypass prevented injury to the brain and other systemic organs, but the extended periods of global ischemia required to repair complex cardiac pathologies leading to increased mortality (often as high as 65%). A common phenomenon was the ‘stone-heart’, the result of maintained and irreversible contracture precipitated by ATP utilization during ischemia[89]. In an attempt to ameliorate this problem, Melrose et al.[90] introduced the concept of ‘elective reversible cardiac arrest’ using an intracoronary artery infusion of a high concentration of potassium citrate (77 mmol/L) added to blood. This ‘pharmacological arrest’ (now termed cardioplegia) induced a cell membrane depolarization, preventing conduction of the action potential and resulted in diastolic cardiac arrest. Reversibility of arrest was easily achieved by washout of the solution. However, this elevated potassium (hyperkalemia) citrate solution was subsequently found to induce focal myocardial necrosis and caused the death of many patients, resulting in the use of hyperkalemic solutions being abandoned for almost 20 years. Over this time period, surgeons used various techniques to protect the heart during ischemia, including continuous or intermittent normothermic perfusion, electrically induced ventricular fibrillation or topical (and profound) hypothermia; surgical results were generally good, but mortality rates were high (around 10–20%). Interestingly, the concept of pharmacological

arrest had been maintained throughout this period by surgeons in Germany, using cardioplegia developed by Bretschneider[91] and now known as HTK solution. This solution was sodium-poor, calcium-free and contained procaine, a sodium channel blocker; it induced arrest by maintaining a polarized cell membrane and was used routinely with considerable success. Unfortunately, however, these advances were not widely known until much later due to original publications in the German literature. In the mid-1970s, to address the continued influence of ischemic injury during cardiac surgery, cardioplegic solutions were reintroduced into surgical practice. These solutions (developed in both the USA and in the UK) were based on a 'extracellular-type' ionic formulation and had moderately elevated potassium chloride concentrations[92]. Although earlier experimental studies had suggested that the focal necrosis seen in patients resulted from the high citrate concentrations, rather than the high potassium, this was not subsequently confirmed. At St. Thomas' Hospital in London, David Hearse (a biochemist) in collaboration with Mark Braimbridge (a cardiac surgeon) developed the St. Thomas' Hospital cardioplegic solutions. These solutions were characterized and optimized for each component (based on plasma concentrations) and had potassium concentrations of either 20 or 16 mmol/L (in St. Thomas' Hospital cardioplegic solution No. 1 or 2, respectively), elevated magnesium concentrations of 16 mmol/L, and normal ionized calcium concentrations. St. Thomas' Hospital cardioplegia was first used surgically in 1975[93]; within 2–3 years, the use of crystalloid buffer-based cardioplegia became the predominant cardioprotective technique throughout the world, with the St. Thomas' solution being the most widely used crystalloid solution. Further development of cardioplegic solutions (from Buckberg's group)[94] used blood as the vehicle for the arresting and protective agents. Blood cardioplegia is now the most commonly used form of hyperkalemic cardioplegia. Elective induction of ischemic cardiac arrest forms the cornerstone of myocardial protection for the majority of cardiac procedures (coronary artery bypass surgery and valve surgery) during cardiac operations.

Cardioprotection during this ischemia involves the application of a cardioplegic solution to induce rapid myocardial arrest and induce a flaccid diastolic state that allows the surgeon a relaxed non-beating operating field—the induction of 'cardioplegia', defined as 'an elective, rapid and reversible paralysis of the heart during cardiac surgery'. The institution of cardioplegic arrest ensures that myocardial oxygen consumption (MVO2) is significantly reduced[95], as is the ATP depletion characteristic of severe ischemia. Cardiac arrest can be induced in a number of ways, by targeting specific processes within excitation–contraction coupling (***Figure 4.1***).

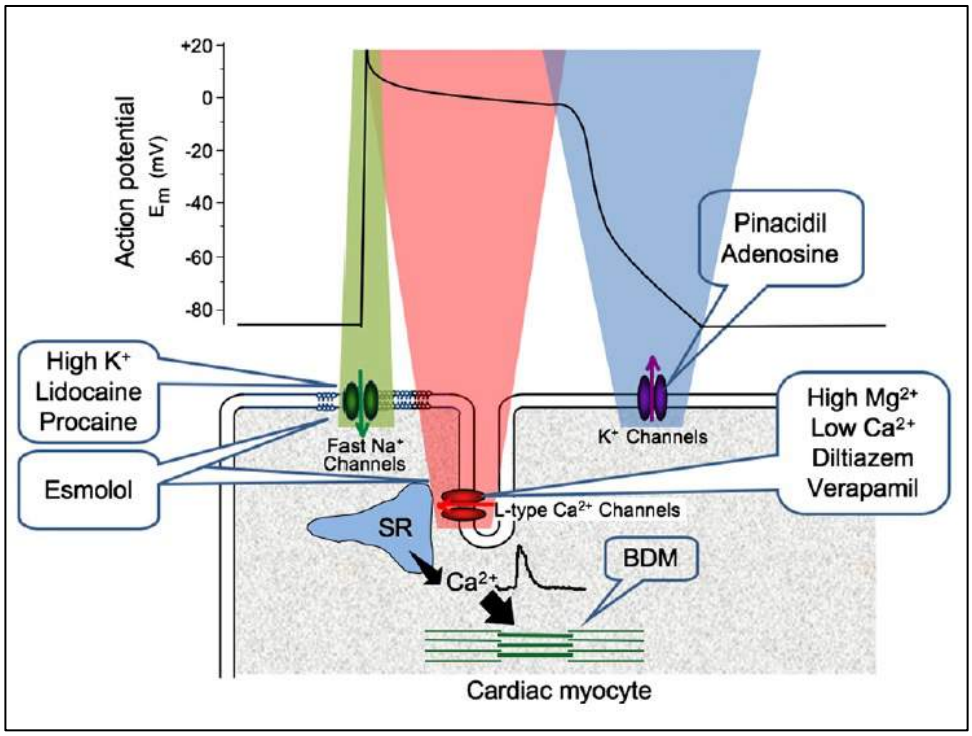

Figure 4.1: The cellular targets for cardioplegic arrest and their influence on the action potential with examples of pharmacological agents.

4.4 Development of acute human model of cardiac ischemia

Cardiac surgery and ECC offer the unique opportunity to have a human model of cardiac ischemia/reperfusion. As in the in-vitro model we observed that NEU3 expression was significantly increase after ischemia, we developed the following model during cardiac

surgery procedure, in order to ascertain if the same variation of NEU3 expression levels occur also in human cardiomyocytes during ischemia. At single venous cannulation, a Satinsky Clamp was applied to the right appendage and the tip of the appendage was harvested, and divided into two samples (***Figure 4.2***).

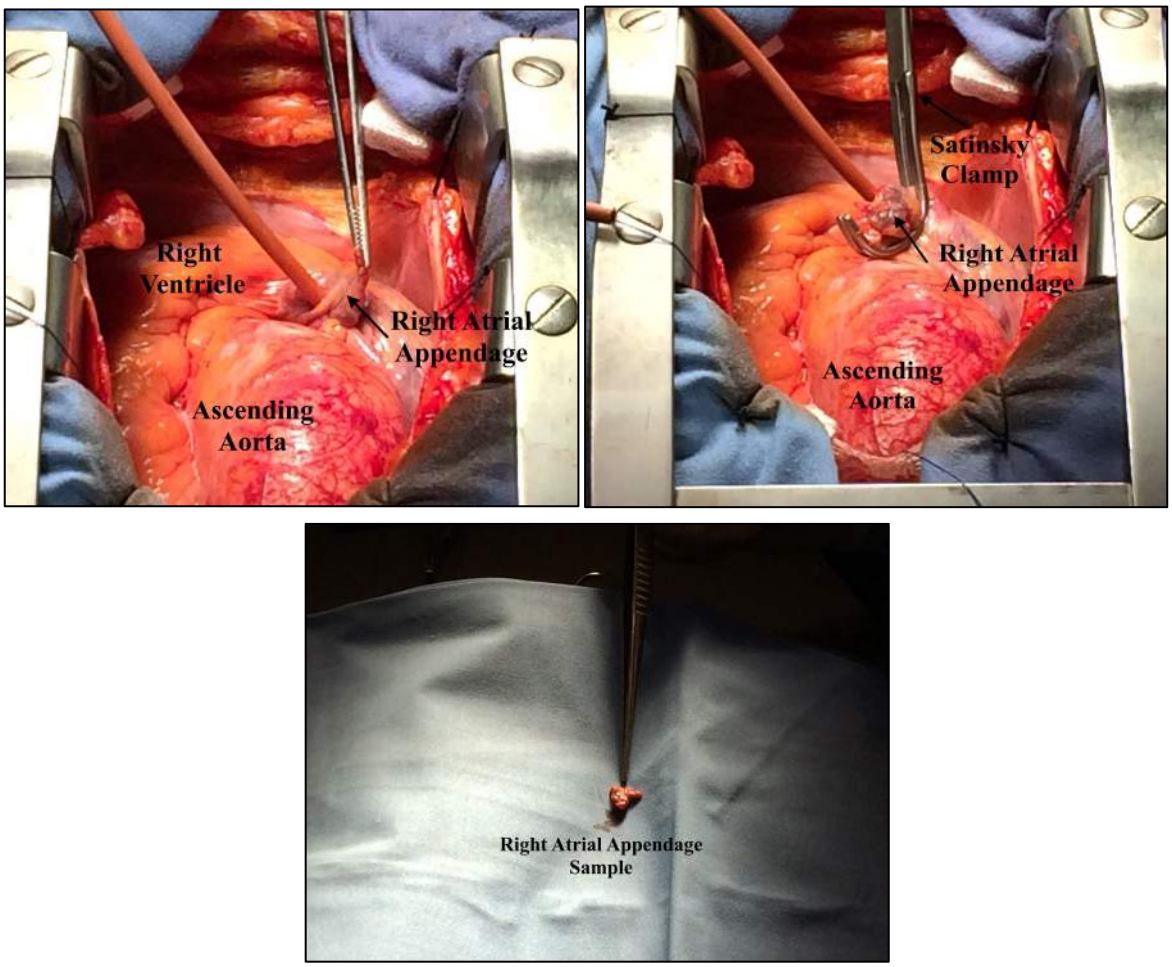

Figure 4.2: Right atrial appendage harvesting in the Operating Room during Cardiac Surgery Procedure.

The first sample constituted the pre-ischemic control and was used to analyze gene and protein expression at baseline. Just before aortic cross-clamping remove (so at the end of the cardiac ischemic time) another sample was harvested from the tip of the right appendage, just near to the venous cannula, and was used to analyze gene and protein expression after ischemia. Aortic cross-clamp time as well as ECC time were collected for further analysis. The second appendage sample collected at the moment of venous cannulation was incubated

in hypoxic condition for the same time of aortic cross-clamp (ischemic time in vivo). This allowed us to rule out any confounding effect due to myocardial protection induced by cardioplegia and systemic cooling performed routinely during surgery.

4.5 Materials and Methods

Sample Collection

Right atrial appendage biopsies were collected during cardiac surgery and ECC. At single venous cannulation, a Satinsky Clamp was applied to the right appendage and the tip of the appendage was harvested, and divided into two samples. The first sample was washed with PBS and freezed immediately in liquid nitrogen. It represented the pre-ischemic control, named “Pre”, and was used to analyze gene and protein expression at baseline. The second sample was incubated in PBS in hypoxic conditions (1% O_2) for the same time of aortic cross-clamp and was names as “Hypoxia”.

Just before aortic cross-clamping remove, at the end of the cardiac ischemic time, another sample of the right appendage was harvested, washed with PBS and freezed in liquid nitrogen. It was named “Post” and used to analyze gene and protein expression after ischemia. At the same time the sample incubated in hypoxic conditions was freezed in liquid nitrogen. Later on, the three samples collected were processed for mRNA isolation.

mRNA isolation from cardiac tissue samples

Regarding mRNA extraction, tissue samples were incubated with 1 ml of Trizol-LS reagent (Invitrogen, Carlsbad, CA, USA) and homogenized using the Tissue homogenizer Lyser® (Qiagen). Each sample was processed with 2 cycles of 10 minutes each at 25 oscillations/second, kept in ice for 30 minutes and finally centrifuged at 12000 rcf for 5 minutes at 4°C. After centrifugation, the supernatant of each sample was transferred in a

new tube and total mRNA was extracted from Trizol-LS following the manufacture's protocol.

mRNA purification and retro-transcription in cDNA

To eliminate possible genomic DNA contaminations in the extracted mRNA, the samples were processed according to the "RNA Cleanup" protocol of RNeasy Mini Kit® (QUIAGEN), supplied by the company.

mRNA quantity and purity were assessed by reading absorbance at 260 nm wavelength with a spectrophotometer Nanodrop (EuroClone). We considered suitable the samples with the following ratio:

- A260/A280 greater than 1,9 that means no contamination by proteins
- A260/A230 greater than 1,9 that means no contamination by carbs or phenol, which could affect retro-transcription efficacy.

All the study samples satisfied both the aforementioned conditions.

After isolation and purification, 1 μg of RNA was reverse-transcribed to cDNA using the iScript cDNA Synthesis Kit (Bio-Rad Laboratories) according to the manufacturer's instruction. Briefly, for every sample the reaction mix was prepared as follow:

Reaction Mix	4 μL
Reverse transcriptase	1 μL
RNA	μL equivalent to 1 μg
H_2O	μL to fill the volume
Final Volume	20 μL

The samples were reverse transcribed in a thermocycler using the following protocol:

5 minutes at 25°C; 30 minutes at 42°C; 5 minutes at 85°C and resting at 4°C

Gene expression analysis by Real Time PCR

The quantitative expression of the genes of interest was assessed by Real Time PCR.

Initially, the specific primers to evaluate the expression of the genes of interest have been designed with the "Primer3" software and then checked with the "Blastn" program to control their correct annealing with the identified target genes.

For the analysis the following primers have been used:

PRIMER	MELTING T (°C)	SEQUENCE
S14	57	Fw- GTGTGACTGGTGGGATGAAGG Rev- TTGATGTGTAGGGCGGTGATAC
NEU3	57	Fw- TGGTCATCCCTGCGTATACC Rev- TCACCTCTGCCACTTCACAT
HIF-1α	57	Fw- TTTTTCAAGCAGTAGGAATTGGA Rev- GTGATGTAGTAGCTGCATGATCG

The single Real-Time PCR reactions were performed in a 96 well plate, mixing in a final volume of 20 μL the following reagents:

- cDNA; 10 ng
- Primers mix; 0,2 μM
- 1X Power SYBR® Green PCR master mix (Thermo Fisher Scientific) containing: Sybr Green, Taq polymerase (0.6 U), $MgCl_2$ (3 mM), Buffer (Tris/HCl 20 mM, KCl 50 mM, pH 8.4), dNTPs (200 μM).

The PCR reaction was performed under the following conditions:

- Initial denaturation: 95°C for 2 minutes (1 cycle)
- Denaturation: 95°C for 30 seconds
- Annealing: 57°C for 30 seconds
- Elongation, fluorescence detection: 72°C for 30 seconds
- Final Elongation: 72°C for 2 minutes

The three steps (denaturation, annealing and elongation) were repeated for 40 cycles. At the end of the reaction, the Melting curve is obtained in order to rule out the presence of nonspecific products. Relative quantification of target genes was performed in triplicate and was calculated by the equation $2^{-\Delta\Delta Ct}$.

Statistical analysis

Data were expressed as a percentage for nominal variables and mean with standard deviations for continuous variables using GraphPad Prism 6 (GraphPad Software Inc, California, USA). Statistical differences were determined by Unpaired T-test (* $p<0,05$; ** $p<0,01$; *** $p<0,001$).

4.6 Results

In this experimental model we enrolled 6 adult patients submitted to cardiac surgical procedure in the Cardiac Surgery Unit at IRCCS Policlinico San Donato. Inclusion criteria were age range between 18-80 years old, and the ability to sign an informed consent to the study protocol. The study was approved by the local ethical committee. All the patient clinical, surgical and follow-up data were collected and progressively inserted in an electronic database.

Mean age was 72±8 years, and 4 patients were female. Regarding cardiac risk factor, hypertension, dyslipidemia and diabetes mellitus were present in 5 patients (83%), 4 patients (67%) and 2 patients (33%) respectively. Three patients (50%) were operated of CABG, 2 patients (33%) underwent aortic valve replacement (AVR) and one patient (17%) was operated for ascending aortic aneurysm. All patients underwent surgical correction via median sternotomy with ECC. CABG was performed with left internal mammary on the left anterior descending coronary artery and great saphenous vein sequentially on the other branches. AVR was performed with bioprosthesis in both patients. Myocardial protection was achieved in every patients with antegrade crystalloid cardioplegia, topical cooling and systemic cooling (32 °C). Mean aortic cross-clamp time was 79±35 minutes. We observed no 30-days mortality.

NEU3 and HIF-1α expression levels were not significantly different in samples harvested before and after aortic cross-clamping. The same lack of increase in NEU3 and HIF-1α expression was observed in the sample harvested before aortic clamping and incubated in hypoxic condition for the same time of in-vivo aortic cross-clamp. VEGF expression showed a trend towards an increase between pre-clamping and post-ischemia levels, even if this trend failed to reach statistical significance (***Figure 4.3***).

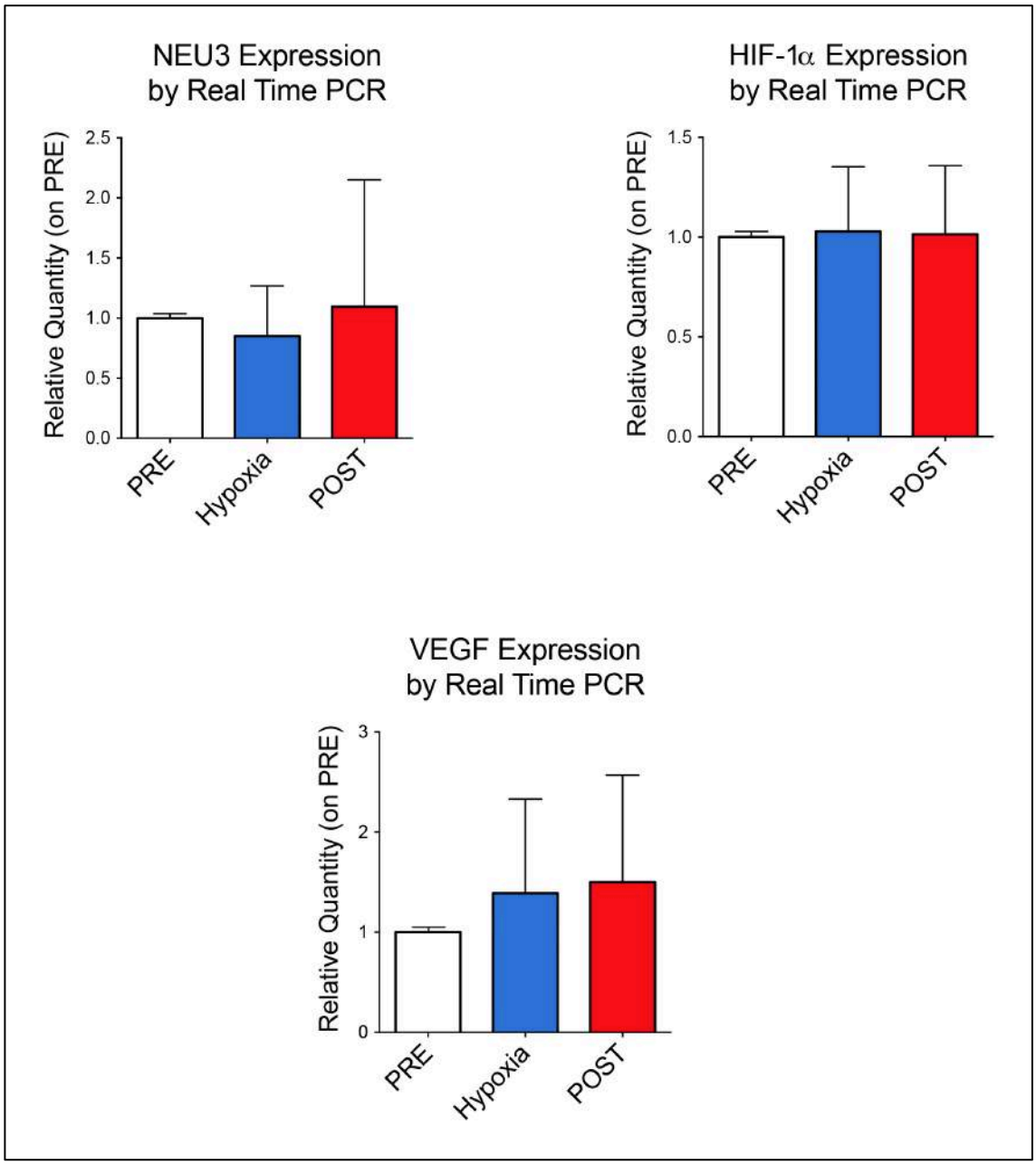

***Figure 4.3*:** NEU3, HIF-1α and VEGF mRNA expression analysis by Real Time PCR of auricles samples harvested before aortic clamping (PRE), incubated in hypoxic conditions (Hypoxia) or harvested after ischemia (POST).

4.7 Discussion

Several studies have found increased levels of HIF-1α messenger RNA (mRNA) in hypoxic cultured cells and in organs (the retina and lung) of animals exposed to short- or long-term hypoxia[96]. On the opposite very few studies reported data on HIF-1α expression in human model of cardiac ischemia. Lee and coworkers[97] examine specimens of 37 human heart tissue affected by various degrees of ischemic insult and correlate the physiologic and pathological state of the heart with the temporal and spatial expression of HIF-1α and VEGF. In this study the authors detected increased steady-state levels of HIF-1α mRNA during the early period (the first 24 hours) after acute myocardial infarction or during acute myocardial ischemia. This accumulation of mRNA was limited to the region of affected myocardium. No HIF-1α transcripts were detectable by PCR analysis in specimens of non-ischemic or non-infarcted tissue (***Figure 4.4***).

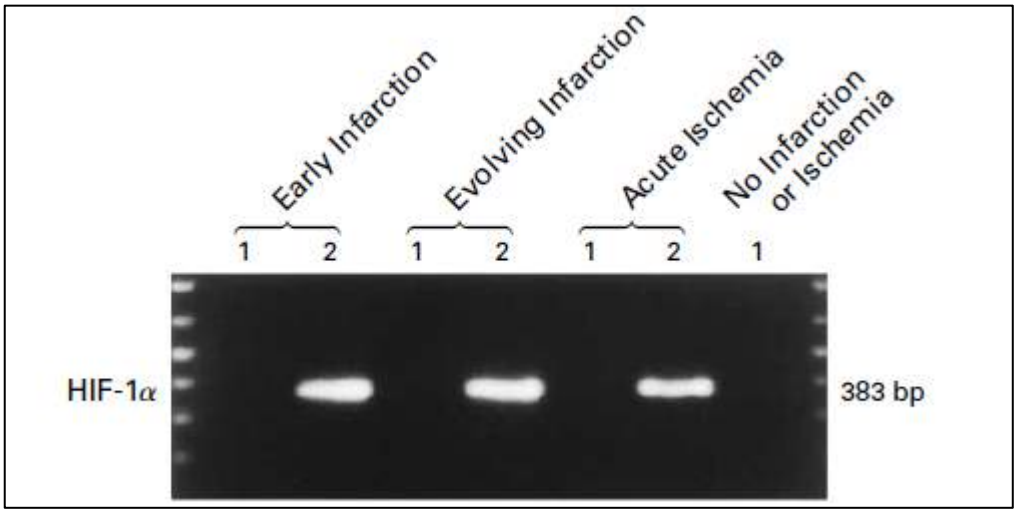

Figure 4.4: Results of Analysis of Ventricular-Biopsy Specimens by the Polymerase Chain Reaction. In specimens in the early-infarction group, the onset of infarction was less than 24 hours before surgery; in those in the evolving-infarction group, the onset of infarction was 24 to 120 hours before surgery; and in those in the ischemia group, the onset of ischemia was less than 48 hours before surgery. In each pair, 1 denotes the specimens taken from an area of normal ventricular tissue, and 2 the specimens taken from an area of ischemic or infarcted ventricular tissue. The lengths of the transcripts detected are shown on the right.

These results suggest that HIF-1α is an early molecular marker of myocardial ischemia or infarction. The production of this protein and its effects appear to be limited to the heart, since it was not detected in the peripheral blood of patients.

Our results are partially consistent with these observations. Indeed, even a short ischemic time was sufficient to determine an increase in NEU3 and HIF-1α expression in cardiac sample harvested before venous cannulation and incubated in hypoxic conditions. On the contrary, in the complete in-vivo model, no significant activation of NEU3 and HIF-1α was evident in cardiac sample harvested before and after aortic cross-clamping. It is interesting to note that incubation time in hypoxic condition was set to be equivalent to in vivo ischemic time (aortic cross-clamping time). In our opinion there are several possible explanations to the lack of NEU3 and HIF-1α increased expression in the cardiac surgery model. First of all, despite in the in-vitro setting even a short ischemic period is enough to induce HIF-1α increased expression, it is possible that in the in-vivo setting the mean aortic cross-clamp time was too short to elucidate the same response.

Secondly, and most important in our opinion, the technique of myocardial protection, especially cardioplegic arrest and hypothermia, by protecting the myocardium from the ischemic injury could have limited NEU3 and HIF-1α expression in our samples. Indeed, it is well known that hypothermia protects myocardium from oxidative injury during ischemic stress and reperfusion[98]. In the isolated, perfused rabbit heart model, Ning and colleagues[99] demonstrated that hypothermia at 30 °C preserves cardiac structural integrity and function for several hours after ischemic insult by the following mechanisms: 1) hypothermia preserves cardiac function by preventing rapid interstitial collagen fragmentation and loss of connective tissue framework due to direct reduction in matrix metalloproteinase 9 activity; 2) the hearts exposed to hypothermia both before and during ischemia demonstrated full preservation of oxidative capacity, as indexed by MVO_2 after 3 h of reperfusion. A hypothermia induced reduction in metabolic demand during ischemia is confirmed by

decreased lactate production; 3) hypothermia alters signaling for apoptosis as very little or no p53 expression was observed in 30°C-treated hearts. The similar lack of expression of p53 after hypothermic adaptation in the ischemia hearts suggests that modification of this pathway represents at least one mode for the hypothermic therapeutic effect. 4) 30 °C hypothermia was able to counteract the effects of severe hypoxia on HIF-1α expression by enhancing synthesis of HIF-1α protein through transcriptional regulation and by the inhibition of protein degradation. Indeed severe hypoxia without hypothermia determines a reduction of HIF-1α expression, while the application of hypothermia was able to maintain the value of HIF-1α protein to the level of non-ischemic control (***Figure 4.5***).

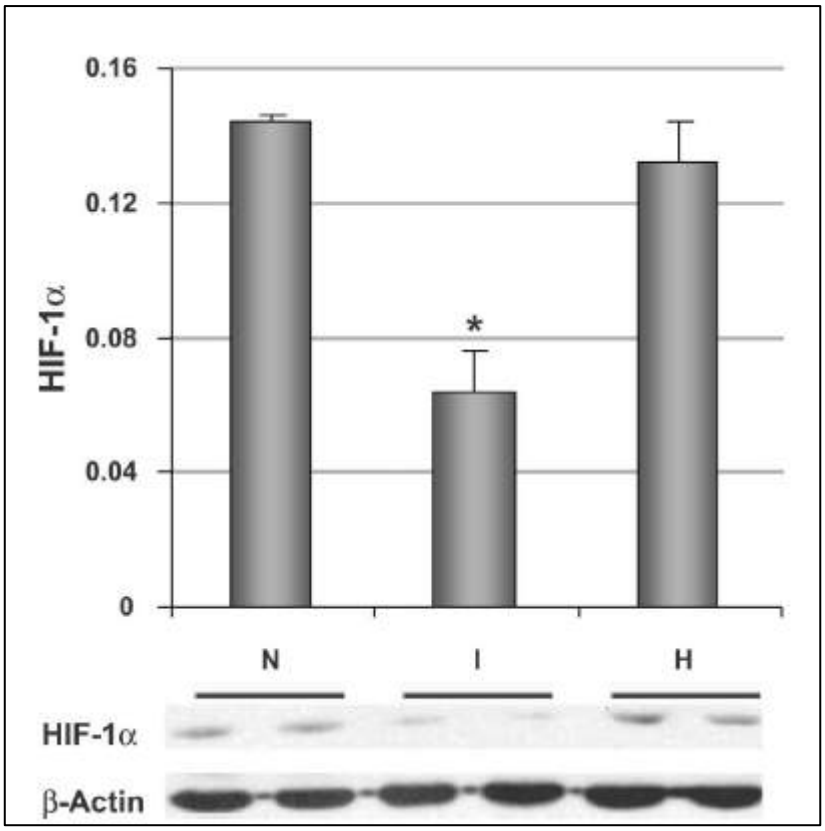

Figure 4.5: RT-PCR results for mRNAs and proteins of hypoxia-inducible factor 1α (HIF-1α). Hypothermia increases HIF-1α ($P<0.05$). Protein content is shown relative to β-actin for representative.

Cardioplegia-induced cardiac arrest is a mainstay of cardiac surgery because attenuates myocardial injury and hastened recovery of cardiac function after aortic cross-clamping.

While it is well known that cardioplegia significantly affect myocardial metabolism, oxidative status and cytokines pattern[100], no or little is described regarding cardioplegia effects on HIF-1α expression. Ryou and colleagues[101] in a pig model of ECC and cardiac arrest analyzed the effects of conventional cardioplegia and pyruvate-enriched cardioplegia on myocardial expression of HIF-1α and erythropoietin. They showed that after 60 minutes of ischemia, myocardial HIF-1α mRNA content was similar between cardioplegia groups and non-ischemic controls. Furthermore, while standard cardioplegia didn't affect myocardial HIF-1α protein content compared to control group, HIF-1α protein content was 60-70% greater in the pyruvate cardioplegia group compared to the other two groups (***Figure 4.6***).

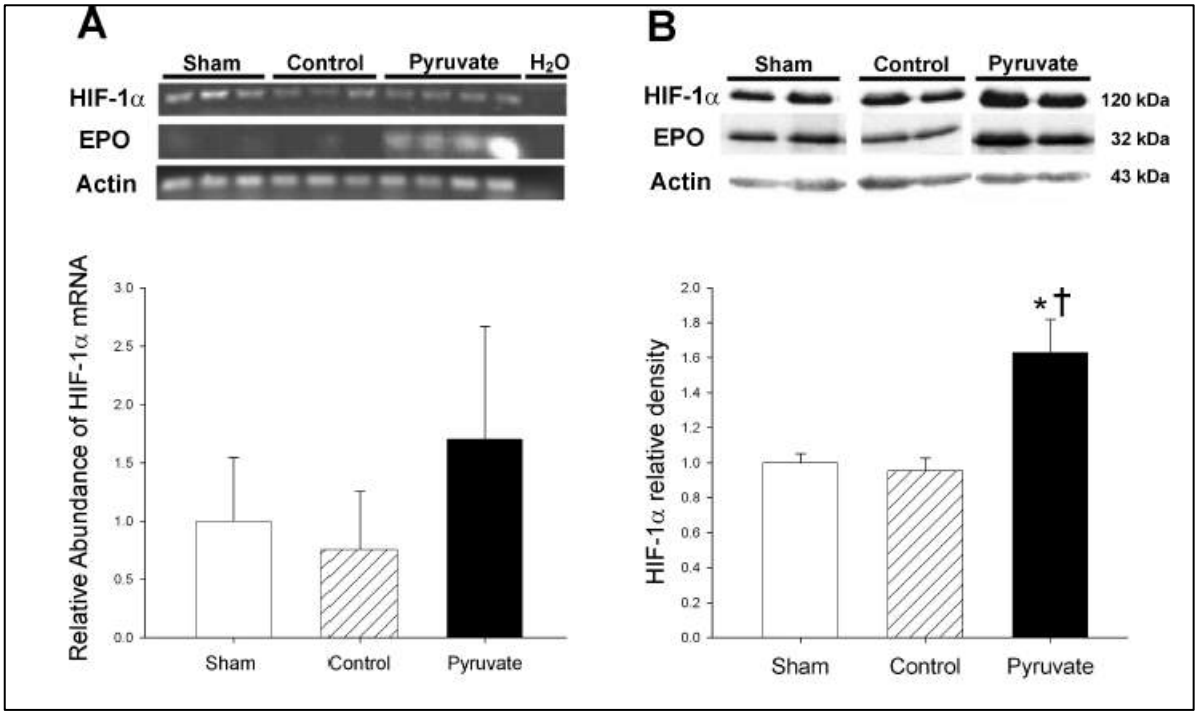

Figure 4.6: HIF-1α mRNA expression and protein contents in left ventricular myocardium. Messenger RNA (A) and protein (B) were measured in myocardium sampled 4 h after CPB with control (hatched bars) or pyruvate-fortified (solid bars) cardioplegia, or at the corresponding sham time point (open bars).

Thus 60-min exposure to pyruvate-fortified cardioplegia during CPB augmented myocardial HIF-1α content 4 h later, without a significant increase in the corresponding mRNA. These results suggest that pyruvate augments HIF-1α content by suppressing degradation, not increasing expression of HIF-1α. We previously described that Fe2+, O2-, and α-ketoglutarate-dependent hydroxylation of two proline residues, catalyzed by prolyl hydroxylase, targets HIF-1α for proteosomal degradation. Pyruvate can interfere with this mechanism by competing with α-ketoglutarate for access to prolyl hydroxylase's catalytic core[102].

In conclusion, the results of our in-vivo model of acute cardiac ischemia were partially conflicting. Indeed, as in the human cardiac samples cultured in the hypoxic incubator we were able to demonstrate an increase in HIF-1α and NEU3 gene expression, in cardiac samples from the same patients, submitted to aortic cross-clamping model of in-vivo ischemia we failed to demonstrate the same behavior of HIF-1α and NEU3 gene expression. This phenomenon was probably due, in our opinion, to the protective role of hypothermia and cardioplegia on human heart submitted to ischemic insult. Unfortunately, no cardiac surgery procedure is nowadays performed without these strategies of myocardial protection. We believe that our series of experiments could be useful to better elucidate the cardio-protective effect of cardioplegia and hypothermia at cellular level, and it will be the object of future investigation. Unfortunately, at the moment, this is the major limitation of our model designed to evaluate HIF-1α and NEU3 expression in human in-vivo cardiac ischemia.

To overcome these limitation, in the final part of my PhD program we sought to evaluate HIF-1α and NEU3 expression in a human in-vivo model of chronic cardiac hypoxia, studying patients affected by cyanotic cardiac defects submitted to surgical correction.

CHAPTER 5: Chronic Human Model of Cardiac Hypoxia

5.1 Congenital Heart Defects

Congenital heart disease (CHD) is the most common congenital anomaly, occurring in almost 1% of live births. Among birth defects, CHD is the leading cause of infant mortality.

Etiology

Environmental and genetic factors contribute to the development of CHD. Common environmental factors include maternal illness (eg, diabetes, rubella, systemic lupus erythematosus) or maternal intake of teratogenic agents (eg, lithium, isotretinoin, anticonvulsants). Paternal age may also be a risk factor.

Certain numerical chromosomal abnormalities, such as trisomy 21, trisomy 18, trisomy 13, and monosomy X (Turner syndrome), are strongly associated with CHD. However, these abnormalities account for only about 5% of patients with CHD. Many other cases involve microscopic deletions on chromosomes or single-gene mutations. Often, the microscopic deletions and mutations cause congenital syndromes affecting multiple organs in addition to the heart. Examples include DiGeorge syndrome (microdeletion in 22q11.2) and Williams-Beuren syndrome (microdeletion in 7p11.23). Single-gene defects that cause syndromes associated with CHD include mutations in fibrillin-1 (Marfan syndrome), TXB5 (Holt-Oram syndrome), and possibly PTPN11 (Noonan syndrome). Single-gene defects can also cause isolated (ie, nonsyndromic) congenital heart defects.

The recurrence risk of CHD in a family varies depending on the cause. Risk is negligible in de novo mutations, 2 to 5% in nonsyndromic multifactorial CHD, and 50% when an autosomal dominant mutation is the cause. It is important to identify genetic factors because more patients with CHD are surviving into adulthood and potentially starting families.

Pathophysiology

Congenital heart anomalies are classified as

1. Cyanotic
2. Acyanotic (left-to-right shunts or obstructive lesions)

The physiologic consequences of congenital heart anomalies vary greatly, ranging from an asymptomatic heart murmur or abnormal pulses to severe cyanosis, congestive heart failure (HF), or circulatory collapse.

*Classification of Congenital Heart Anomalies**

Cyanotic	
	Tetralogy of Fallot Transposition of the great arteries Tricuspid atresia Pulmonary atresia Persistent truncus arteriosus Total anomalous pulmonary venous return
Acyanotic	
Left-to-right shunt	Ventricular septal defect Atrial septal defect Patent ductus arteriosus Atrioventricular septal defect
Obstructive	Pulmonic stenosis Aortic stenosis Aortic coarctation Hypoplastic left heart syndrome (often also manifests with cyanosis, which may be mild)
*In decreasing order of frequency.	

Left-to-right shunts

Oxygenated blood from the left heart (left atrium or left ventricle) or the aorta shunts to the right heart (right atrium or right ventricle) or the pulmonary artery through an opening or communication between the 2 sides. Immediately after birth, pulmonary vascular resistance is high and flow through this communication may be minimal or bidirectional. Within the first 24 to 48 h of life, however, the pulmonary vascular resistance progressively falls, at

which point blood will increasingly flow from left to right. The additional blood flow to the right side increases pulmonary blood flow and pulmonary artery pressure to a varying degree. The greater the increase, the more severe the symptoms; a small left-to-right shunt typically does not cause symptoms or signs.

High-pressure shunts (those at the ventricular or great artery level) become apparent several days to a few weeks after birth; low-pressure shunts (atrial septal defects) become apparent considerably later. If untreated, elevated pulmonary blood flow and pulmonary artery pressure may lead to pulmonary vascular disease and eventually Eisenmenger syndrome. Large left-to-right shunts (eg, large ventricular septal defect [VSD], patent ductus arteriosus [PDA]) cause excess pulmonary blood flow and volume overload, which may lead to signs of HF and during infancy often result in failure to thrive. A large left-to-right shunt also decreases lung compliance, leading to frequent lower respiratory tract infections.

Obstructive lesions

Blood flow is obstructed, causing a pressure gradient across the obstruction. The resulting pressure overload proximal to the obstruction may cause ventricular hypertrophy and HF. The most obvious manifestation is a heart murmur, which results from turbulent flow through the obstructed (stenotic) point. Examples are congenital aortic stenosis, which accounts for 3 to 6% of congenital heart anomalies, and congenital pulmonary stenosis, which accounts for 8 to 12%.

Cyanotic heart anomalies

Varying amounts of deoxygenated venous blood are shunted to the left heart (right-to-left shunt), reducing systemic arterial O_2 saturation. If deoxygenated hemoglobin is greater than 5 g/dL, cyanosis results. Detection of cyanosis may be delayed in infants with dark pigmentation. Complications of persistent cyanosis include polycythemia, clubbing,

thromboembolism (including stroke), bleeding disorders, brain abscess, and hyperuricemia. Hypercyanotic spells can occur in infants with unrepaired tetralogy of Fallot. Depending on the anomaly, pulmonary blood flow may be increased (often resulting in HF in addition to cyanosis), normal, or reduced, resulting in cyanosis of variable severity. Heart murmurs are variably audible and are not specific.

Heart failure

Some congenital heart anomalies (eg, bicuspid aortic valve, mild aortic stenosis) do not significantly alter hemodynamics. Other anomalies cause pressure or volume overload, sometimes causing HF. HF occurs when cardiac output is insufficient to meet the body's metabolic needs or when the heart cannot adequately handle venous return, causing pulmonary congestion (in left ventricular failure), edema primarily in dependent tissues and abdominal viscera (in right ventricular failure), or both. HF in infants and children has many causes other than congenital heart anomalies.

Symptoms and Signs

Manifestations of CHDs are varied but commonly include

- Murmurs
- Cyanosis
- HF

Other physical examination abnormalities may include circulatory shock, poor perfusion, abnormal 2nd heart sound (S 2 —single or widely split), systolic click, gallop, or irregular rhythm. Most left-to-right shunts and obstructive lesions cause systolic murmurs. Systolic murmurs and thrills are most prominent at the surface closest to their point of origin, making location diagnostically helpful. Increased flow across the pulmonary or aortic valve causes a midsystolic crescendo-decrescendo (ejection systolic) murmur. Regurgitant flow through an atrioventricular valve or flow across a VSD causes a holosystolic (pansystolic)

murmur, often obscuring heart sounds as its intensity increases. PDA causes a continuous murmur that is uninterrupted by the S 2 because blood flows through the ductus during systole and diastole. This murmur is 2-toned, having a different sound during systole (when driven by higher pressure) than during diastole.

Central cyanosis is characterized by bluish discoloration of the lips and tongue and/or nail beds; it implies a low O 2 level (usually O 2 saturation < 90%). Perioral cyanosis and acrocyanosis (cyanosis of the hands and feet) without lip or nail bed cyanosis is caused by peripheral vasoconstriction rather than hypoxemia and is a common, normal finding in neonates. Older children with longstanding cyanosis often develop clubbing of the nail beds.

In infants, symptoms or signs of HF include:

- Tachycardia
- Tachypnea
- Dyspnea with feeding
- Diaphoresis, especially with feeding
- Restlessness, irritability
- Hepatomegaly

Dyspnea with feeding causes inadequate intake and poor growth, which may be worsened by increased metabolic demands in HF and frequent respiratory tract infections. In contrast to adults and older children, most infants do not have distended neck veins and dependent edema; however, they occasionally have edema in the periorbital area. Findings in older children with HF are similar to those in adult.

5.2 Material and Methods

Tissue biopsies

Right atrial appendage biopsies were obtained from the point of atrial cannulation at the beginning of extracorporeal circulation. The tissue specimens weighed about 100 mg and were collected in cold phosphate buffer solution (PBS) at pH 7.4, kept in ice and processed within minutes after collection.

mRNA isolation from cardiac tissue samples

Regarding mRNA extraction, tissue samples were rapidly retrieved from saline solution and incubated with 1 ml of Trizol-LS reagent (Invitrogen, Carlsbad, CA, USA). Biopsies were homogenized using the Tissue homogenizer Lyser® (Qiagen). Each sample was processed with 2 cycles of 10 minutes each at 25 oscillations/second, kept in ice for 30 minutes and finally centrifuged at 12000 rcf for 5 minutes at 4°C. After centrifugation, the supernatant of each sample was transferred in a new tube and total mRNA was extracted from Trizol-LS following the manufacture's protocol.

mRNA purification and retro-transcription in cDNA

To eliminate possible genomic DNA contaminations in the extracted mRNA, the samples were processed according to the "RNA Cleanup" protocol of RNeasy Mini Kit® (QUIAGEN), supplied by the company. mRNA quantity and purity were assessed by reading absorbance at 260 nm wavelength with a spectrophotometer Nanodrop (EuroClone). We considered suitable the samples with the following ratio:

- A260/A280 greater than 1,9 that means no contamination by proteins
- A260/A230 greater than 1,9 that means no contamination by carbs or phenol, which could affect retro-transcription efficacy.

All the study samples satisfied both the aforementioned conditions.

After isolation and purification, 1 µg of RNA was reverse-transcribed to cDNA using the iScript cDNA Synthesis Kit (Bio-Rad Laboratories) according to the manufacturer's instruction. Briefly, for every sample the reaction mix was prepared as follow:

Reaction Mix	4 µL
Reverse transcriptase	1 µL
RNA	µL equivalent to 1 µg
H_2O	µL to fill the volume
Final Volume	20 µL

The samples were reverse transcribed in a thermocycler using the following protocol:

5 minutes at 25°C; 30 minutes at 42°C; 5 minutes at 85°C and resting at 4°C

Gene expression analysis by Real Time PCR

The quantitative expression of the genes of interest was assessed by Real Time PCR.

Initially, the specific primers to evaluate the expression of the genes of interest have been designed with the "Primer3" software and then checked with the "Blastn" program to control their correct annealing with the identified target genes.

For the analysis the following primers have been used:

PRIMER	**MELTING T (°C)**	**SEQUENCE**
S14	57	Fw- GTGTGACTGGTGGGATGAAGG Rev- TTGATGTGTAGGGCGGTGATAC
NEU3	57	Fw- TGGTCATCCCTGCGTATACC Rev- TCACCTCTGCCACTTCACAT
SP1	57	Fw- ATCATCACAAGCCAGTTCCA Rev- AGATGTCTGGTTTTGCTGGA
SP3	57	Fw- AGTGGGCAGTATGTTCTTCC Rev- TTTGAACCTGCTGACCATCT
HIF-1α	57	Fw- TTTTTCAAGCAGTAGGAATTGGA Rev- GTGATGTAGTAGCTGCATGATCG
PHD2	57	Fw- TGGGAGTTGCTGTTGAAGTCG Rev- CGTGCCGCCTGGAGAAAC
GLUT1	57	Fw- GGTTGTGCCATACTCATGACC Rev- CAGATAGGACATCCAGGGTAGC
ALDO-A	57	Fw- TTGCCAGTATGTGACCGAGAA Rev- GCCTTCCAGGTGATGTGGT
GAPDH	57	Fw- ACGGATTTGGTCGTATTGG Rev- CATGGGTGGAATCATATTGG
PDK1	57	Fw- ACCAGGACAGCCAATACAAG Rev- CCTCGGTCACTCATCTTCAC
VEGF	57	Fw- TGCCCGCTGCTGTCTAAT Rev- CCTCGGTCACTCATCTTCAC

The single Real-Time PCR reactions were performed in a 96 well plate, mixing in a final volume of 20 μL the following reagents:

- cDNA; 10 ng
- Primers mix; 0,2 μM
- 1X Power SYBR® Green PCR master mix (Thermo Fisher Scientific) containing: Sybr Green, Taq polymerase (0.6 U), $MgCl_2$ (3 mM), Buffer (Tris/HCl 20 mM, KCl 50 mM, pH 8.4), dNTPs (200 μM).

The PCR reaction was performed under the following conditions:

- Initial denaturation: 95°C for 2 minutes (1 cycle)
- Denaturation: 95°C for 30 seconds
- Annealing: 57°C for 30 seconds
- Elongation, fluorescence detection: 72°C for 30 seconds
- Final Elongation: 72°C for 2 minutes

The three steps (denaturation, annealing and elongation) were repeated for 40 cycles. At the end of the reaction, the Melting curve is obtained in order to rule out the presence of nonspecific products. Relative quantification of target genes was performed in triplicate and was calculated by the equation $2^{-\Delta\Delta Ct}$.

Total proteins extraction from Trizol-LS samples

Proteins from the phenol/chloroform layer obtained during the RNA extraction with Trizol-LS, were extracted by the following protocol. Initially, 1,2 mL of cold methanol were added to the phenol/chloroform layer and vortexed. The samples were left for 10 minutes at 30°C and, after an incubation on ice for 5 minutes, were centrifuged at 12000 rcf for 10 minutes at 4°C to sediment the proteins. The protein pellets were washed with 1 mL of cold methanol and centrifuged again at 12000 rcf for 10 minutes at 4°C. After centrifugation, the proteins

were resuspended in 0,5 mL of cold methanol and sonicated for 4 cycles of 5 seconds each in ice using burst sonication to generate a fine protein powder. Samples were then centrifuged for 1 minute at 2000 rcf and methanol was left to evaporate. Proteins were resuspended with 200 mL of a 0.25% Rapigest® solution in 50 mM ammonium bicarbonate and solubilized by alternate cycles of vortex and heat at 60°C. The obtained proteins were stored at -80 °C until used for Western Blot experiments.

Membrane and citosol proteins separation

To obtain membrane and cytosolic protein fractions, the fragments of auricles were incubated with PBS containing 1% protease and phosphatase inhibitors (Sigma-Aldrich) and homogenized using the Tissue homogenizer Lyser® (Qiagen). Each sample was processed with 4-5 cycles of 10 minutes each at 25 oscillations/second and the total tissue suspensions were lysed by sonication and then centrifuged at 800 rcf for 10 minutes to eliminate debris, unbroken cells and nuclear components. The obtained supernatants were subsequently centrifuged at 200000 rcf at 4°C for 20 min on a TL100 Ultracentrifuge (Beckman) to obtain soluble and particulate fractions. The particulate fraction contains the plasmatic membranes, the lysosomal membranes and the endoplasmic reticulum, while the supernatant contains the cytosol. Both the fractions were used for NEU3 expression analysis by Western Blot.

Proteins expression analysis by Western Blot

Proteins concentrations were measured by the Pierce™ BCA Protein Assay Kit (Thermo Fisher Scientific) following the manufacturer's protocol. 30 μg of proteins were denatured by boiling for 5 minutes in sample buffer (62,5 mM Tris-HCl pH 6.8, 2% SDS (w/v), 10% glycerol (v/v), 5% 2-mercaptoethanol (w/v), 0,01% bromophenol blue (w/v)) and separated on a 10% polyacrylamide gel in denaturing conditions.

A discontinuous gel has been prepared composed by the stacking and the running gels.

Stacking Gel Composition

- Deionized water
- Tris-HCl 1.5 M, pH 6.8
- SDS 0.1% w/v
- Acrylamide 4%
- APS 10% w/v
- TEMED

10% Running Gel composition

- Deionized water
- Tris-HCl 1.5 M, pH 8.8
- SDS 0.1% w/v
- Acrylamide 10-12%
- APS 10% w/v
- TEMED

Proteins were subsequently transferred onto nitrocellulose membranes by electroblotting using 100 Volt for 2 hours. Then, the membranes were incubated overnight in Tris-buffered saline (TBS: 10 mM Tris-HCl, pH 7.4, 150 mM NaCl), 0.1% (v/v) Tween 20 (TBS-Tween) containing 5% (w/v) dried milk or 5% (w/v) bovine serum albumin (BSA; Sigma) for the blocking buffer. Blots were incubated with a primary antibody in the appropriate blocking solution for 3 hours at room temperature.

The primary antibodies used for the analysis were the following:

PRIMARY ANTIBODY	DILUTION	MANUFACTURER
Calnexin	1:10000	Epitomics ®
NEU3	1:700	Abcam ®
HIF-1α	1:1000	Novus Biologicals ®

PHD2	1:1000	Novus Biologicals®
EGFR	1:1000	Cell Signaling ®
p-EGFR	1:1000	Cell Signaling ®
ERK	1:1000	Cell Signaling ®
p-ERK	1:1000	Cell Signaling ®
p38 MAPK	1:1000	Cell Signaling ®
p-p38 MAPK	1:1000	Cell Signaling ®
p70S6K	1:1000	Cell Signaling ®
p-p70S6K	1:1000	Cell Signaling ®
GAPDH	1:5000	Millipore ®

The membranes were washed four times for 10 minutes with TBS-Tween and then incubated with the appropriate secondary antibody horseradish peroxidase (HRP) conjugated for 1 hour at room temperature. After four washes in TBS-Tween, the protein bands were detected using an ECL detection kit (Thermo Fisher Scientific) as described by the manufacturer.

Statistical analysis

Data were expressed as a percentage for nominal variables and mean with standard deviations for continuous variables using GraphPad Prism 6 (GraphPad Software Inc, California, USA). Statistical differences were determined by Unpaired T-test (* $p<0,05$; ** $p<0,01$; *** $p<0,001$). Linear regression was performed on Delta Ct values of gene expression analysis of cyanotic patients to investigate trend and correlation using GraphPad Prism 6 (GraphPad Software Inc, California, USA).

5.3 Results

Clinical Data and comparison among the two study Groups

The study have enrolled 35 patients (17 cyanotic - Group A and 18 controls - Group B) submitted to elective cardiac surgery for cyanogen and non-cyanogen heart defects. Inclusion and exclusion criteria are herein reported. Enrollment began after the local Ethical Committee approved the study protocol. Every single patient included in the study was identified univocally by an alphanumeric code. All the patient clinical, surgical and follow-up data were collected and progressively inserted in an electronic database.

Inclusion Criteria:

- Male or Female patients aged 2 months – 18 years
- Patients affected by cyanogen or non-cyanogen heart defect
- Patients listed for surgical correction of heart defect
- Patients (or parents) must read and sign the informed consent to surgery.

The two study groups included patients affected by different cardiac defects, as reported in

Table 5.1

Cyanotic Patients			**Non-Cyanotic Patients**	
Tetrology of Fallot (TOF)	6		Atrial Septal Defect (ASD)	9
Doble-outlet Right Ventricle (DORV)	3		Ventricular Septal Defect (VSD)	6
Great Arteries Transposition (TGA)	4		Supra-aortic Stenosis	1
Truncus Arteriosus	2		AtrioVentricular Septal Defect	2
Pulmonary Atresia + DIV + MAPCAS	1			
Congenitally corrected TGA	1			
Total Number of pts	**17**		**Total Number of pts**	**18**

Regarding the preoperative characteristics, the two groups resulted not significantly different for what concern mean age (41±19 vs 49±30 months in Group A and B respectively), gender, renal function, serum glucose and platelet count.

On the opposite mean arterial saturation resulted significantly lower in cyanogen patients (74% vs 99% in Group A and B respectively; p=0.01), while mean hemoglobin level (15±3 mg/dl vs 12±1 mg/dl in Group A and B respectively) and mean hematocrit (45±9 vs 34±3% in Group A and B respectively) were significantly higher in cyanotic group.

Evaluation of genic expression, protein expression and activity of NEU3 sialidases

Right appendage samples in cyanotic and not cyanotic (Controls) patients were isolated and processed for mRNA and protein extraction, as described in the Materials and Methods section. This procedure allowed us to evaluate for the protocol genes mRNA levels, by means of Real Time PCR, and protein expression, by means of Western Blot.

The analysis of NEU3 expression by Real-Time PCR was performed on 17 cyanotic samples and on 18 controls. The results showed that in cyanotic group, NEU3 mRNA level was 1.28 greater compared to controls ($p < 0.05$; ***Figure 5.1 A***). Furthermore, as we demonstrated in the in-vitro model that the transcription factors SP1 and SP3 regulate NEU3 gene transcription under hypoxic stress, we found that SP1/SP3 expression was significantly higher in cyanotic group (***Figure 5.1 B and C***). Finally, as NEU3 sialidase is linked to plasma membrane, we evaluated the differences in NEU3 expression in cellular membranes or in cytosol among the two study groups. As expected, NEU3 membrane expression was significantly higher in cyanotic group, while no differences between the two groups were observed regarding cytosol NEU3 expression (***Figure 5.1 D and E***)

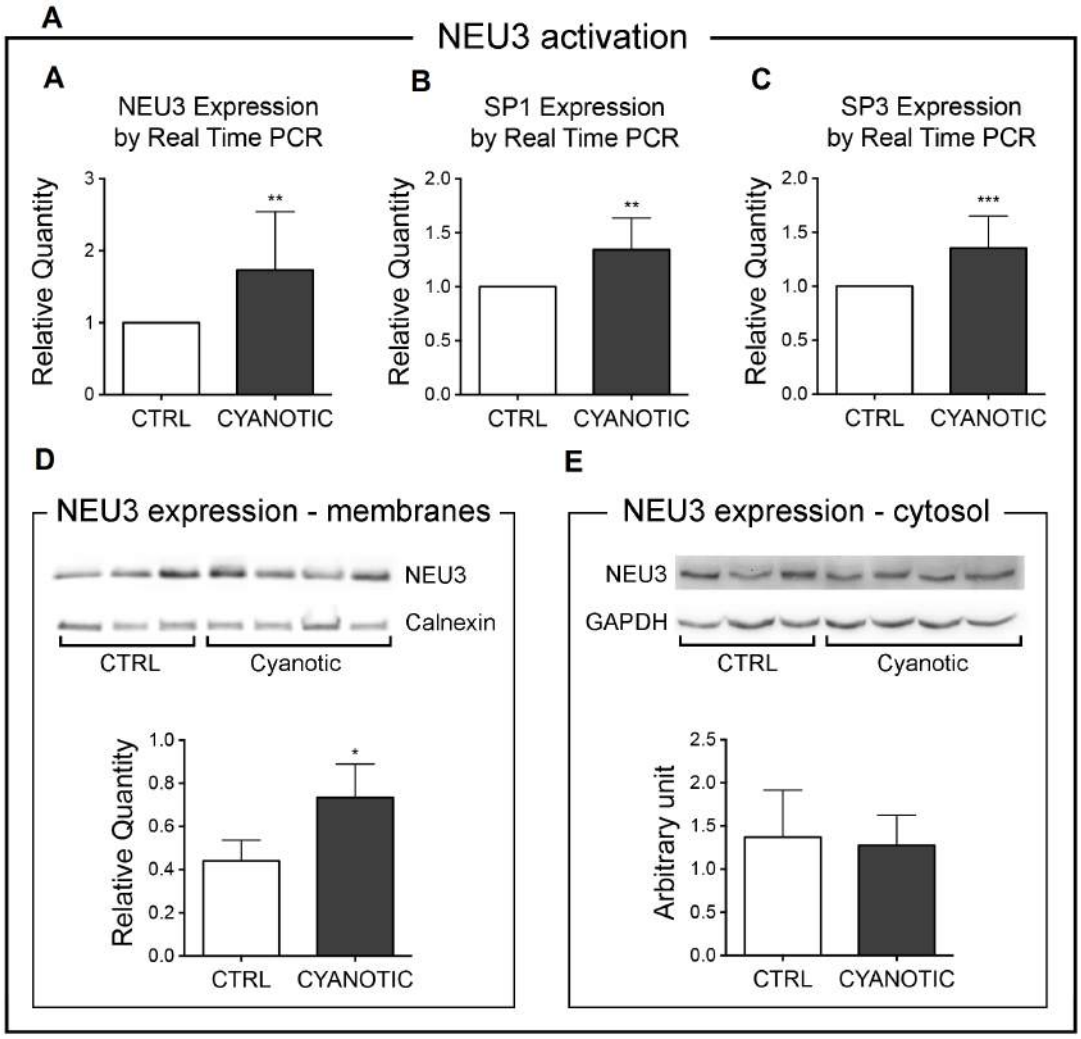

Figure 5.1: A) NEU3 mRNA expression in both study groups. B-C) SP1 and SP3 mRNA expression in both study groups. D-E) NEU3 mRNA expression in membranes and cytosol. Cyanotic are depicted as gray bar, controls are the white bar. All data assessed by means of Real-Time PCR. *, **, *** all p level < 0.05

Evaluation of activation of epidermal growth factor receptor (EGFR) and of its downstream signaling pathways

As assessed in our in-vitro model, NEU3 activity results in a direct activation of EGFR and its anti-apoptotic and proliferative downstream pathways. In both the study groups, we studied both EGFR expression and its activation by phosphorylation. In cyanotic group both EGFR expression (6.34 folds higher as compared to controls; p=.05) and EGFR activation (4.26 folds higher than controls; p=.05) resulted significantly greater compared to controls

(***Figure 5.2-A***). We further evaluated the expression of the proteins involved in the EGFR downstream signaling pathways. The analysis by Western Blotting showed an activation of ERK and AKT pathways in cyanotic compared to controls. Particularly, cyanotic patients showed both increased levels of proteins involved in cellular proliferation ERK and p38 MAPK (8 and 3.5 folds greater than controls, respectively) and an increase in key proteins for cellular survival like p70S6K (2.18 folds greater than controls). The same results were observed in the phosphorylated isoform of the same proteins, which resulted significantly more expressed in cyanotic compared to controls (***Figure 5.2 B-D***)

Evaluation of gene and protein expression of hypoxia inducible factor (HIF) and of its transcriptional targets

We further evaluated Hypoxia Inducible Factor 1α (HIF-1α) expression by Real Time PCR and Western Blot in cyanotic and in control groups. We observed that in patients with chronic hypoxia there is an increase of HIF-1α gene expression of 1.3 folds as compared to controls (p=.05). This fact is also confirmed by a moderate increase in protein expression (***Figure 5.3***).

Furthermore we evaluated the expression of some HIF target genes in order to verify the activation of the signaling pathway in response to the hypoxia. Particularly, the gene expression of the Vascular Endothelial Growth Factor (VEGF), a key angiogenetic factor, as assessed by Real Time PCR resulted 1.16 greater in cyanotic compared to controls, even if the expression of the corresponding protein, as assessed by Western Blot, was not significantly different among the two study groups (***Figure 5.4***)

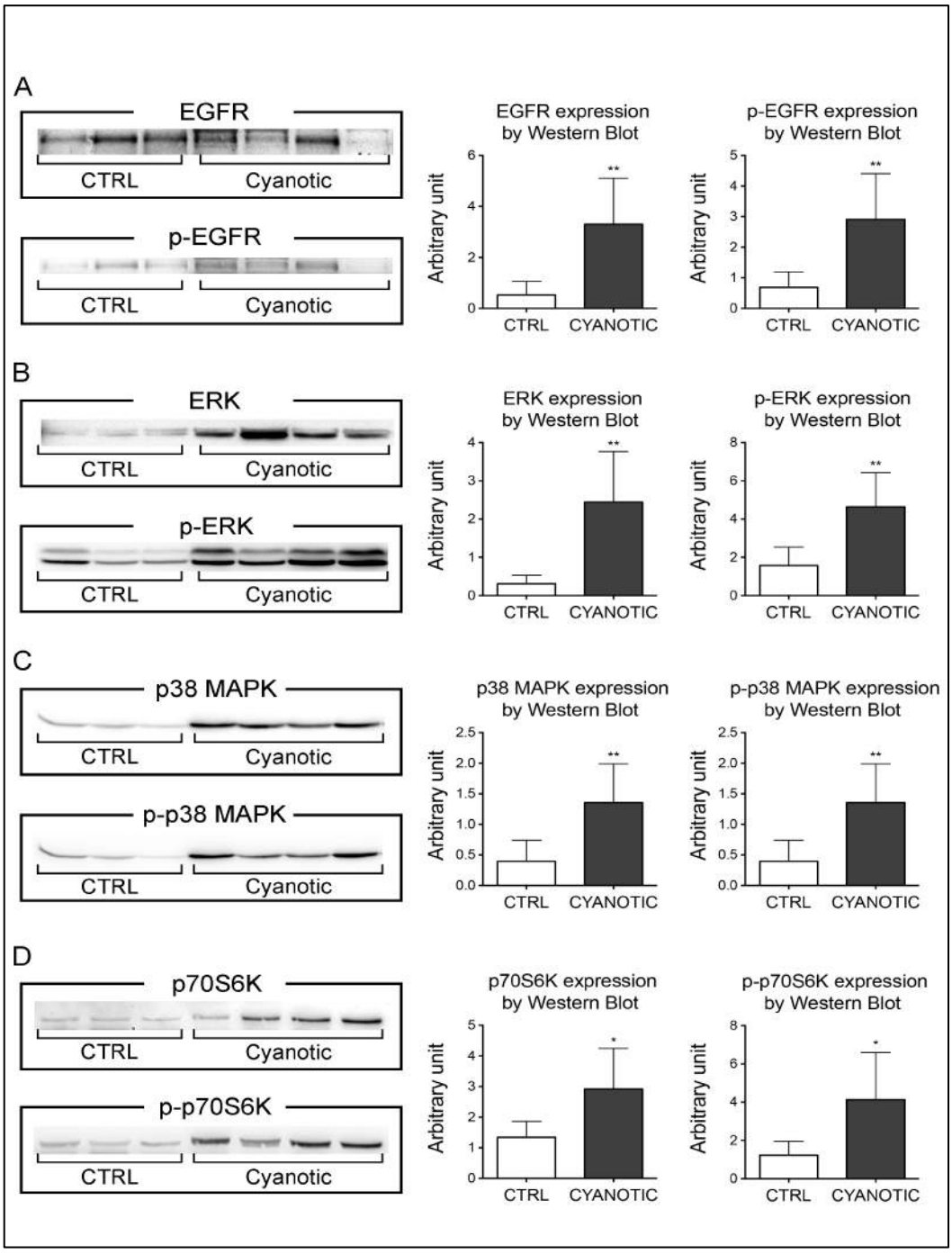

Figure 5.2: Levels of protein expression and of their phosphorylated form in Western Blot of A) EGFR, p-EGFR; B) ERK, p-ERK; C) p38,p-p38; and D) p70S6K and p- p70S6K. Cyanotic are depicted as gray bar, controls are the white bar.

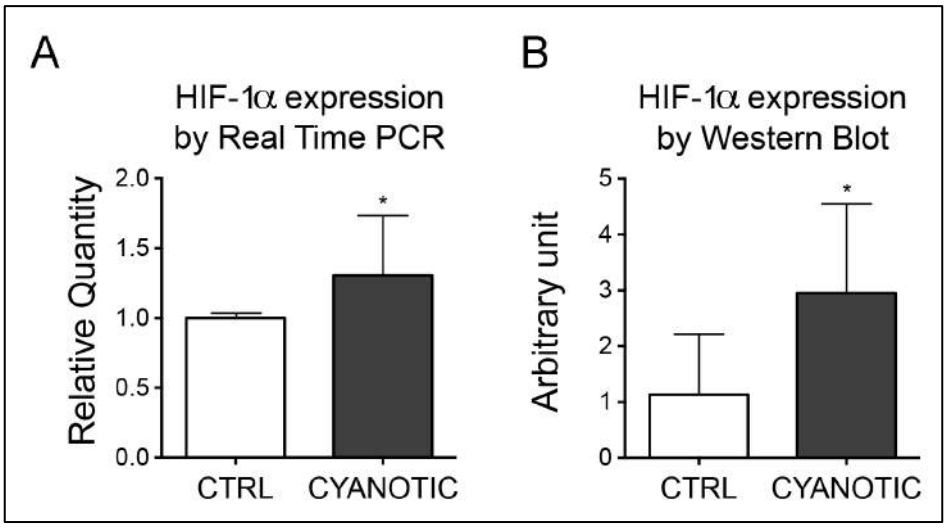

Figure 5.3: Gene and protein expression levels of HIF-1α assessed by Real Time PCR and Western Blot. Cyanotic are depicted as gray bar, controls are the white bar

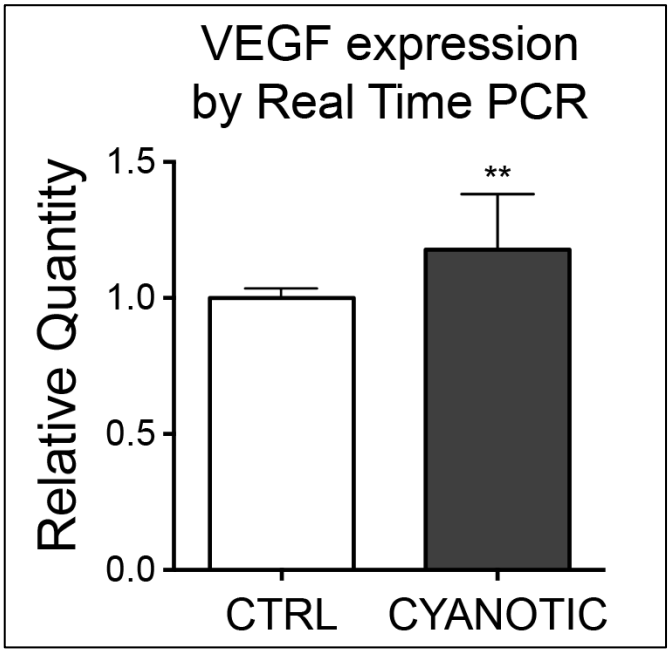

Figure 5.4: Gene expression levels of VEGF assessed by Real Time PCR. Cyanotic are depicted as gray bar, controls are the white bar

We further examined some genes, downstream HIF-1α signaling pathway, involved in the regulation of glycolytic metabolism. Data showed that the gene expression of glyceraldehyde-3-phosphate dehydrogenase (GAPDH), of the glucose transporter GLUT1

and of the aldolase was 1.127, 2.22 and 1.59 greater in cyanotic as compared to controls, respectively (p=.05) (***Figure 5.5 A,B,D***). Furthermore, we found a metabolic switch toward a glycolysis in cardiac cells of cyanotic patients as compared to controls. This was confirmed by a 1.26-fold increase in gene expression of pyruvate dehydrogenase kinase (PDK1) in cyanotic compared to controls (***Figure 5.5 C***). PDK1inhibits the transformation from pyruvate to Acetil-CoA, thus inhibiting mitochondrial function, oxygen consumption and energy production, which can only be obtained from the glycolytic pathway.

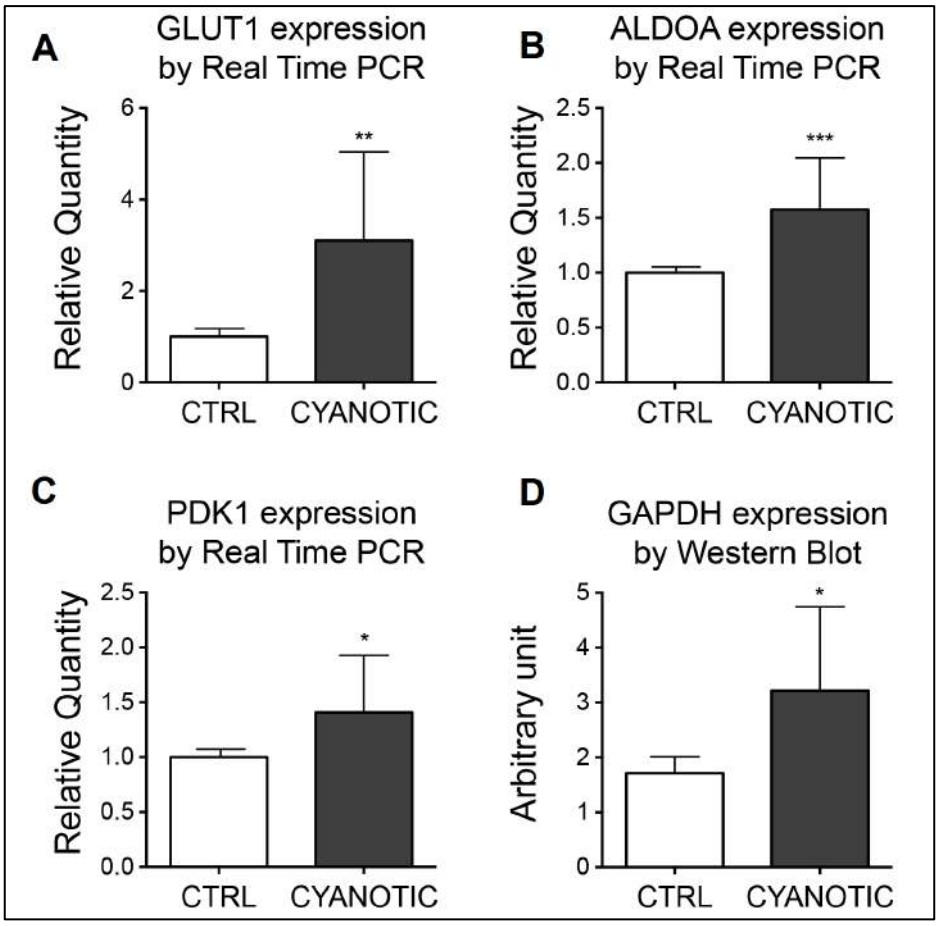

Figure 5.5: Gene expression levels of GLUT1, Aldolase, PDK1 and GAPDH, assesses by Real Time PCR. Cyanotic are depicted as gray bar, controls are the white bar

As a target of HIF-1α we further evaluated the prolyl hydroxylases PHD2 because, in hypoxic condition, its expression is regulated by HIF-1α itself through a mechanism of negative feedback. As shown in ***Figure 5.6***, the level of mRNA was not significantly

different between the two groups, while the protein level as assessed by Western Blot was 2.5 greater in cyanotic patients compared to controls.

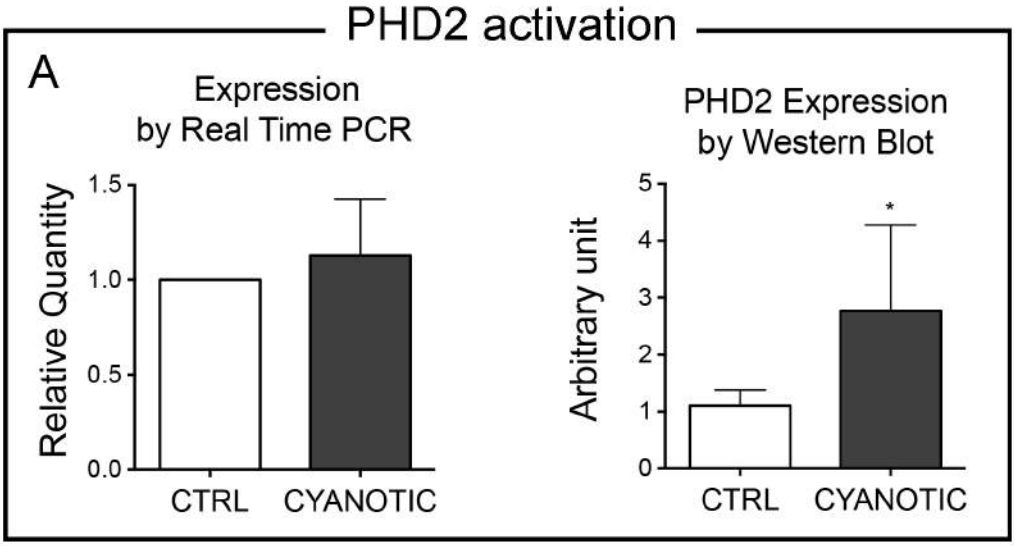

Figure 5.6: Gene and Protein expression levels of PHD2 assessed by Real Time PCR and Western Blot. Cyanotic are depicted as gray bar, controls are the white bar. *, p=<0.05

Finally we observed a strong correlation between NEU3 and HIF-1α expression levels in both groups, which was significantly stronger and steeper among the cyanotic group (R^2=0.49; p= 0.02; ***Figure 5.7***)

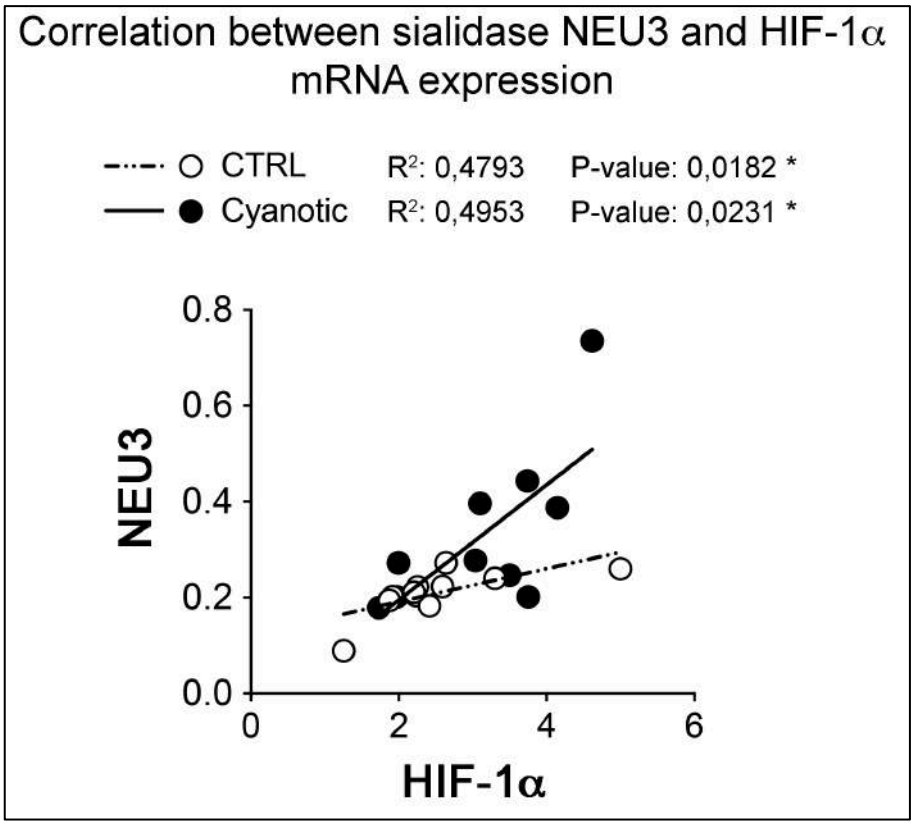

Figure 5.7: Correlation between sialidase NEU3 and HIF-1α mRNA expression. Cyanotic are black circles, controls are white circles.

5.4 Discussion

The present research project was developed analyzing samples of human cardiac right appendage, harvested during surgery on patients with low arterial saturation (SaO2<90% - Cyanotic Group) compared to patients with normal saturation (Controls). The results showed a significant increase in NEU3 expression and activity in patients affected by chronic hypoxia. Furthermore a significant increase of EGFR was observed, supporting the hypothesis that this signaling pathway is upregulated by the sialidase NEU3. Indeed we observed an increase in expression of genes downstream of EGFR, both related to cellular proliferation (ERK and p38) and to apoptosis resistance (AKT and p70S6K). Finally we observed a significant activation of HIF-1α and of its downstream genes.

To our knowledge, there are no published studies on NEU3 sialidase expression in human in-vivo model of chronic hypoxia. Furthermore, there are very few papers in literature reporting on HIF-1α activation in the same model. Quing and colleagues[103] reported data on HIF-1α and VEGF expression in cardiac samples from 7 cyanotic and 7 control patients submitted to surgical correction of congenital cardiac defects. The authors demonstrated that HIF-1α expression and activity are significantly elevated in the myocardium of infants with cyanotic congenital heart disease compared to those with acyanotic CHD, and that this response directly correlates with the degree of hypoxemia (***Figure 5.8***).

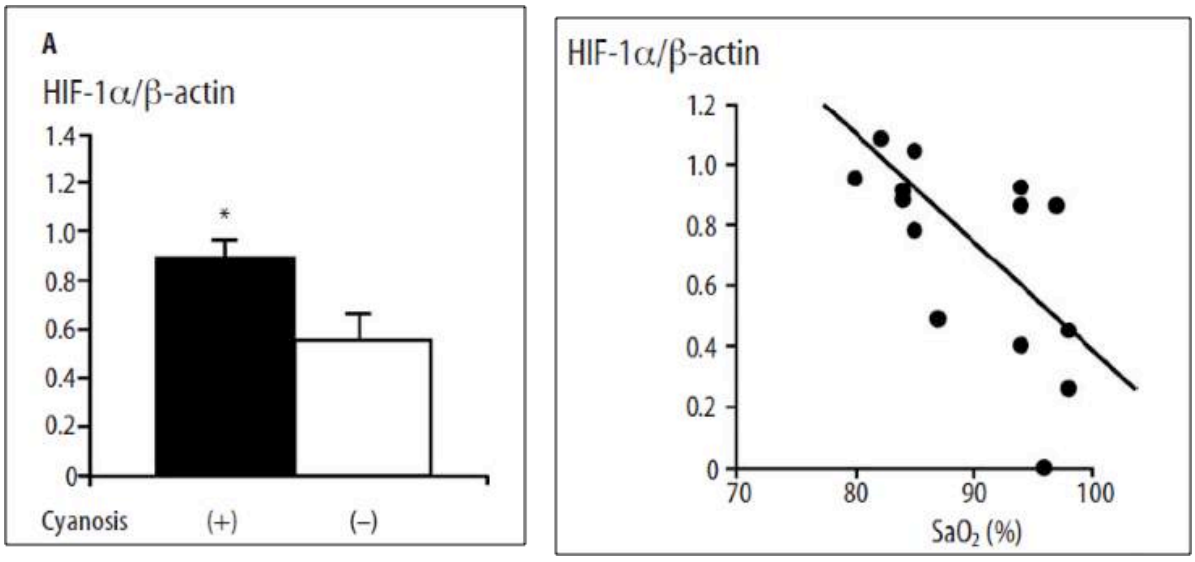

Figure 5.8: A) Levels of hypoxia-inducible factor-1α (HIF-1α) were measured by Western blotting in the right ventricular myocardium of infants with congenital cardiac defects using an antibody against human HIF-1α. β-actin levels served as loading controls. (+): samples derived from infants with cyanosis (solid bar, n=7); [-] samples derived from patients without cyanosis (open bar, n=7). Results are expressed as the mean value±SEM. * $p<0.05$ between groups. B) HIF-1α protein levels correlate with the degree of hypoxemia. The ratio HIF-1α/ β-actin was related to the preoperative transcutaneous arterial oxygen saturation (SaO2) (n=14). Spearman correlation coefficient: -0.74 ($p<0.005$).

Furthermore they showed increased intra-myocardial levels of VEGF in cyanotic compared to acyanotic patients, indicating that reduced oxygen availability is the critical element promoting VEGF expression in infants with congenital heart disease. These findings are supported by previous studies showing higher serum levels of VEGF in children with cyanotic cardiac defects as compared to others with acyanotic defects[104]. The importance of myocardial upregulation of VEGF is highlighted by an elegant study by Giordano et al.[105] where cardiomyocyte-specific deletion of VEGF-A resulted in fewer coronary microvessels, thinned ventricular walls, and depressed basal contractile function, but had also systemic consequences confirming the important role of cardiomyocytes in VEGF secretion. Since VEGF is the major factor promoting angiogenesis and neovascularization and can contribute

to myocardial remodeling, enhanced levels of VEGF may contribute to the abnormal vessel formation (i.e., aortopulmonary collateral arteries) and myocardial remodeling in infants with cyanotic congenital heart defects.

As we demonstrated that NEU3 activity results in a direct activation of EGFR and its anti-apoptotic and proliferative downstream pathways, in the present study cyanotic patients showed both increased levels of proteins involved in cellular proliferation ERK and p38 MAPK as an increase in key proteins for cellular survival like p70S6K and AKT. These results are consistent with those reported by Kietzmann and coworkers[106], who demonstrated that activation of p38 MAP kinase was significantly enhanced in the myocardium of infants with cyanotic congenital heart disease compared to those with acyanotic defects. They showed that an over-expression of the upstream kinases of p38 MAP kinase, MKK3 and MKK6, but not of ERK1/2, induced HIF-1α protein levels and activated the HIF pathway in hypoxia, suggesting that activation of p38 MAP kinase may contribute to enhanced levels of HIF-1α in infants with cyanotic congenital heart disease.

It has been shown in the literature that HIF-1α reaches its maximum expression level after four hours of hypoxia, while during more extensive hypoxic periods, and ultimately in chronic hypoxia, HIF-1α levels progressively decrease[107]. Indeed, through a negative feedback mechanism, HIF-1α stimulates the transcription and the expression of prolyl hydroxylases (PHDs), aiming to limit an excessive concentration of HIF-1α itself. This reduction of HIF-1α level prepares the cell to better resist to an eventual re-oxygenation, thus limiting the ischemia/reperfusion injury. This is consistent with the data emerging from the present study, which showed a significant increase in PHD2 levels in hypoxic patients compared to controls. This process of autoregulation of HIF-1α expression by means of activation of its degradative proteins has been highlighted in an elegant study by Reddy and colleagues[108], and is extremely important to understand the mechanisms of right ventricular

response to chronic hypoxia in congenital heart defects. The authors reported on 23 patients affected exclusively by Tetralogy of Fallot (TOF) and showed that the right ventricle in TOF failed to mount an adaptive response to hypoxia. Increasing hypoxia was associated with downregulation instead of upregulation of angiogenic and metabolic genes. Furthermore, they showed an upregulation of procollagen type 1 α1 gene expression, which is one of the major forms of collagen in endomyocardial tissue. Endomyocardial fibrosis has been described in TOF after late repair and it has been postulated that this may cause a restrictive RV physiology, which adversely impacts the early postoperative course. However, it must be note that TOF is a pathology in which sub-pulmonary stenosis determines an important RV hypertrophy, that consequently triggers endomyocardial fibrosis resulting in RV impaired response to cyanotic defect.

Another important aspect of cellular adaptation to hypoxia is the metabolic switch between oxidative and glycolytic metabolism, the so-called “Pasteur effect”. The Pasteur effect, which describes the increased conversion of glucose to lactate in hypoxic cells, has been considered a critical cellular metabolic adaptation to hypoxia for over a century. Under normal oxygen tensions, cells catabolize glucose to pyruvate via glycolytic enzymes. Pyruvate is then taken up by the mitochondria for further catabolism through the tricarboxylic acid (TCA) or Krebs cycle, which transfers electrons to the respiratory chain. Electron transport through this chain results in ATP production and terminates in the donation of electrons to oxygen. In low oxygen tension, in which there is a paucity of oxygen as an electron acceptor, hypoxic cells are surmised to undergo anaerobic glycolysis as a default mode. Increased glycolytic flux requires transcriptional activation of genes encoding glucose transporters and glycolytic enzymes that is mediated by HIF-1α[109]. Hypoxic activation of HIF-1α promotes ATP production through increased anaerobic glycolysis, which partially compensates for hypoxic cellular energy demands. According to these observation, in the present study we found that the glycolytic enzymes Glucose

transporter Glut1, the Aldolase and the GAPDH were significantly enhanced in the cyanotic group which in turn demonstrates that the myocardium of patients affected by cyanogen cardiac defects is metabolic adapted to chronic hypoxia.

Increased ATP production via the glycolytic pathway, however, may not be sufficient for hypoxic adaptation since hypoxia paradoxically causes oxidative stress from uncontrolled mitochondrial generation of reactive oxygen species (ROS) that may pose a barrier for cell survival. The hypoxia inducible pyruvate dehydrogenase kinase 1 (PDK1) is critical for the attenuation of mitochondrial ROS production, maintenance of ATP levels, and adaptation to hypoxia. PDK1 phosphorylates the pyruvate dehydrogenase (PDH) E1α subunit and inactivates the PDH enzyme complex that converts pyruvate to acetyl-coenzyme A, thereby inhibiting pyruvate metabolism via the Krebs cycle. Because the TCA cycle is coupled to electron transport, regulation of the PDH complex by PDK1 is critical for the attenuation of mitochondrial respiration and ROS production. Recently Kim and coworkers[110] demonstrated that the gene encoding PDK1 is a direct target of HIF-1α, and that overexpression of PDK1 in hypoxic HIF-1α knock-out cells was able to protect the cell itself against apoptosis, limiting the production of ROS. According to these authors HIF-1α plays three critical roles in the hypoxia-induced metabolic switch from oxidative to glycolytic metabolism. HIF-1α induces expression of: (1) upstream glucose transporters and glycolytic enzymes to increase flux from glucose to pyruvate; (2) PDK1 to block the conversion of pyruvate to acetyl CoA; and (3) lactate dehydrogenase A to convert pyruvate to lactate (***Figure 5.9***).

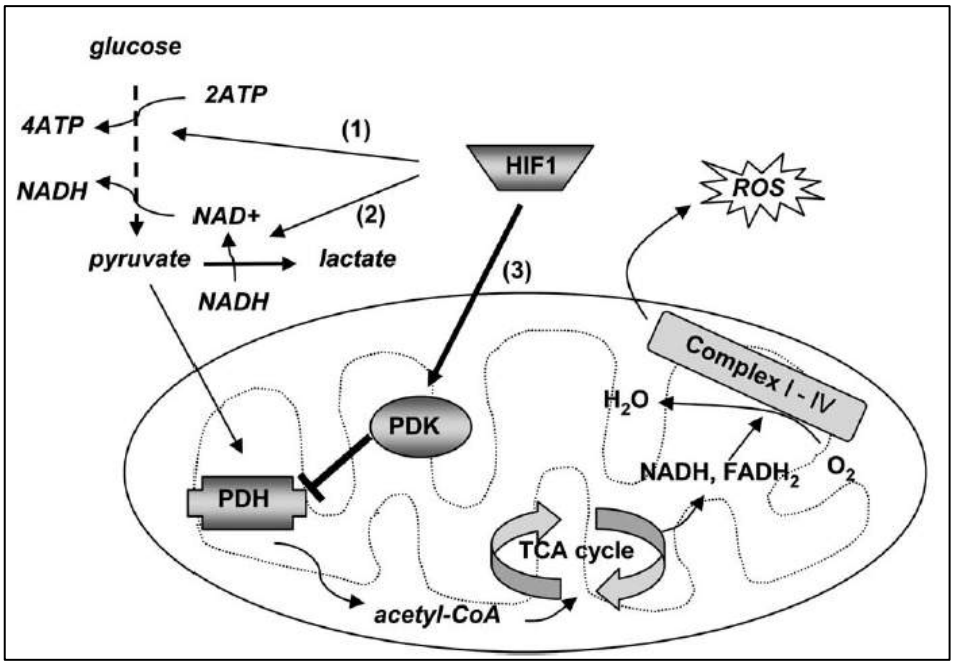

Figure 5.9: Coordinate regulation of hypoxia-induced metabolic switches by HIF-1α. In hypoxic cells, HIF-1α stimulates increased glycolytic flux to pyruvate (1) and its reduction to lactate (2). In addition, HIF-1α-induced PDK1 activity inhibits PDH (3), resulting in decreased flux through the TCA cycle. HIF-1α mediates these effects through transcriptional activation of genes encoding glucose transporters and glycolytic enzymes (1), lactate dehydrogenase A (2), and PDK1 (3).

Our results are consistent with these observations, as we found that PDK1 expression is significantly greater in cyanotic patients compared to controls. Furthermore, the PDK1 enzyme is activated by the protein PI3K which is downstream the EGFR pathway. As we demonstrated that NEU3-induced EGFR expression is enhanced in cyanotic group, it is reasonable to conclude that in chronic ischemic myocardium NEU3 sialidase contributes to cellular metabolic adaptation

In conclusion, the present study showed that NEU-3 sialidase is activated in human cardiac cells that are chronically hypoxic. These results support the hypothesis of a physiological role of NEU-3 in mediating cellular response to hypoxic stress. It’s interesting to underline that NEU-3 activation is mediated by ganglioside GM3 on cellular membrane. Indeed, an

increase in NEU-3 level determines a reduction of GM3, which is a well know inhibitor of EGF receptor. Thus NEU-3 activation ultimately lead to EGF receptor activation. On these premises, to mimic the effects of NEU-3 activation, it could be possible to inhibit GM3 synthesis, in example by the selective inhibition of the sialyl-transferase involved in the last passage of its synthesis. In this direction, our laboratory is performing some experiments with small chemical molecules, designed for blocking selectively the GM3 synthesis with the aim of activating the endogenous response to hypoxic stress.

CHAPTER 6: Conclusions

The hypoxic condition determines several functional consequences that ultimately lead to cellular death and irreversible damage to cardiac myocytes. Under hypoxic condition, cells activate several protective pathways; among them, HIF-1α plays a key role in controlling cellular response to hypoxia at molecular level. However, HIF-1α regulatory mechanisms are extremely complex. On these premises the present work was based on the hypothesis that NEU3 sialidase, a glycolytic enzyme ubiquitously expressed over the plasmatic membrane, can have a regulatory activity on HIF-1α expression in hypoxic/ischemic cardiac myocytes.

The experiments performed in this in-vitro model allowed us to draw the following conclusions:

1) Endogenous NEU3 sialidase expression and activity are up-regulated in murine skeletal muscle cells (C2C12) upon oxygen starvation, leading to a signaling cascade resulting in the activation of HIF-1α.
2) Moreover, induced overexpression of NEU3 significantly increases HIF-1α expression and cell resistance to hypoxic stress, whereas NEU3 silencing causes the opposite effects and renders myoblasts more susceptible to apoptosis.
3) The hypoxia-driven activation of NEU3 sialidase can activate the EGFR pro-survival signaling pathway by controlling the content of ganglioside GM3. Furthermore, we demonstrated that NEU3 overexpression causes a reduction of ganglioside GM3, which is known to block EGFR autophosphorylation.

Then resulted were extended from skeletal muscle to cardiac myocytes, particularly aiming to ascertain the role of NEU3 in activating the human cardiomyocyte response to hypoxia. Particularly, we evaluated if NEU3 activation occurred in human cardiomyocytes using two different models:

- A model of acute cardiac ischemia achieved during aortic cross-clamp time and extracorporeal circulation in adult patient submitted to cardiac surgical procedures.
- A model of chronic hypoxia in neonates and young patients operated for cyanogen congenital cardiac defects.

In the acute model of cardiac ischemia, we harvested a sample of right atrial appendage just before and after aortic cross-clamping, during routine adult cardiac surgery procedure. After initiating the extracorporeal circulation, the application of aortic clamp excludes the aortic root (and the coronary arteries) from systemic perfusion. This step is mandatory for cardiac surgeons in order to operate on a bloodless, empty field, but it's also a unique opportunity to have an in-vivo model of human cardiac ischemia.

However, no significant activation of NEU3 and HIF-1α was evident in cardiac sample harvested before and after aortic cross-clamping. In our opinion there are several possible explanations for the lack of NEU3 and HIF-1α increased expression in the cardiac surgery model. First of all, it is possible that in the in-vivo setting the mean aortic cross-clamp time was too short (mean time = 79 minutes) to elucidate the same response that we observed in the in vitro model, where the cells were incubated under hypoxic conditions for at least 12 hours. This fact suggests the hypothesis that NEU3 activation in ischemic condition is a relatively slow response and that its transcriptional pathways ultimately leading to HIF-1α activation requires a sufficient time of hypoxia to induce cell adaptive mechanisms.

Secondly, and most important in our opinion, the technique of myocardial protection, especially cardioplegic arrest and hypothermia, by protecting the myocardium from the ischemic injury could have limited NEU3 and HIF-1α expression in our samples. Unfortunately, no cardiac surgery procedure is nowadays performed without these strategies of myocardial protection. We believe that our series of experiments could be useful to better elucidate the cardio-protective effect of cardioplegia and hypothermia at cellular level, and it will be the object of future investigation. Unfortunately, at the moment, this is the major

limitation of our model designed to evaluate HIF-1α and NEU3 expression in human in-vivo cardiac ischemia.

To overcome these limitation, in the final part of my PhD program we evaluated HIF-1α and NEU3 expression in a human in-vivo model of chronic cardiac hypoxia, studying patients affected by cyanotic cardiac defects submitted to surgical correction. In this model we harvested the tip of the right appendage at the moment of venous cannulation (with the same technique we validated in the acute model) and we compared the levels of NEU3, HIF-1α and their downstream pathways expression to those of patients operated for non-cyanogen cardiac defects (controls). Patients with cyanogen cardiac defects live since their birth with a mean arterial oxygen saturation of nearly 70%, compared to patients affected by non-cyanogen defects who have normal saturation levels. So cyanogen patients are exposed to chronic hypoxia till the moment of surgical correction, which occurs at least some months after the birth, depending on the different pathologies.

In this model of chronic hypoxia we observed a significant increase in NEU3 expression and activity in cyanotic patients. Furthermore a significant increase of EGFR was observed, supporting the hypothesis that this signaling pathway is upregulated by the sialidase NEU3. Indeed we observed an increase in expression of genes downstream of EGFR, both related to cellular proliferation (ERK and p38) and to apoptosis resistance (AKT and p70S6K). Finally we observed a significant activation of HIF-1α and of its downstream genes.

Another important aspect of cellular adaptation to hypoxia is the metabolic switch between oxidative and glycolytic metabolism, the so-called “Pasteur effect”. Increased glycolytic flux requires transcriptional activation of genes encoding glucose transporters and glycolytic enzymes that is mediated by HIF-1α. Hypoxic activation of HIF-1α promotes ATP production through increased anaerobic glycolysis, which partially compensates for hypoxic cellular energy demands. According to these observation, in the present study we found that the glycolytic enzymes Glucose transporter Glut1, the Aldolase and the GAPDH were

significantly enhanced in the cyanotic group which in turn demonstrates that the myocardium of patients affected by cyanogen cardiac defects is metabolic adapted to chronic hypoxia.

In conclusion, the results of this PhD project support the hypothesis of a physiological role of NEU3 in mediating cellular response to hypoxic stress. It is interesting to underline that NEU3 activation is mediated by ganglioside GM3 on cellular membrane. Indeed, an increase in NEU3 level determines a reduction of GM3, which is a well know inhibitor of EGF receptor. Thus NEU3 activation ultimately lead to EGF receptor activation. On these premises, to mimic the effects of NEU3 activation, it could be possible to inhibit GM3 synthesis, in example by the selective inhibition of the sialyltransferase involved in the last passage of its synthesis. In this direction, our laboratory is performing some experiments with small chemical molecules, designed for blocking selectively the GM3 synthesis with the aim of activating the endogenous response to hypoxic stress.

References

1) Braunwald E. Shattuck lecture–cardiovascular medicine at the turn of the millennium: triumphs, concerns, and opportunities. N Engl J Med. 1997;337:1360–1369.

2) Jessup M, Abraham WT, Casey DE, Feldman AM, Francis GS, Ganiats TG, Konstam MA, Mancini DM, Rahko PS, Silver MA, Stevenson LW, Yancy CW. 2009 focused update: ACCF/AHA Guidelines for the Diagnosis and Management of Heart Failure in Adults: a report of the American College of Cardiology Foundation/American Heart Association Task Force on Practice Guidelines: developed in collaboration with the International Society for Heart and Lung Transplantation. Circulation. 2009;119:1977–2016.

3) McKee PA, Castelli WP, McNamara PM, Kannel WB. The natural history of congestive heart failure: the Framingham study. N Engl J Med. 1971;285:1441–1446.

4) Carlson KJ, Lee DC, Goroll AH, Leahy M, Johnson RA. An analysis of physicians' reasons for prescribing long-term digitalis therapy in outpatients. J Chronic Dis. 1985;38:733–739.

5) Eriksson H, Caidahl K, Larsson B, Ohlson LO, Welin L, Wilhelmsen L, Svärdsudd K. Cardiac and pulmonary causes of dyspnoea–validation of a scoring test for clinical-epidemiological use: the Study of Men Born in 1913. Eur Heart J. 1987;8:1007–1014.

6) Swedberg K, Cleland J, Dargie H, et al; Task Force for the Diagnosis and Treatment of Chronic Heart Failure of the European Society of Cardiology. Guidelines for the diagnosis and treatment of chronic heart failure: executive summary (update 2005): The Task Force for the Diagnosis and Treatment of Chronic Heart Failure of the European Society of Cardiology. Eur Heart J. 2005;26:1115–1140.

7) Croft JB, Giles WH, Pollard RA, Casper ML, Anda RF, Livengood JR. National trends in the initial hospitalization for heart failure. J Am Geriatr Soc. 1997;45:270–275.

8) McCullough PA, Philbin EF, Spertus JA, Kaatz S, Sandberg KR, Weaver WD; Resource Utilization Among Congestive Heart Failure (REACH) Study. Confirmation of a heart

failure epidemic: findings from the Resource Utilization Among Congestive Heart Failure (REACH) study. J Am Coll Cardiol. 2002;39:60–69.

9) Levy D, Kenchaiah S, Larson MG, Benjamin EJ, Kupka MJ, Ho KK, Murabito JM, Vasan RS. Long-term trends in the incidence of and survival with heart failure. N Engl J Med. 2002;347:1397–1402.

10) Roger VL, Weston SA, Redfield MM, Hellermann-Homan JP, Killian J, Yawn BP, Jacobsen SJ. Trends in heart failure incidence and survival in a community-based population. JAMA. 2004;292:344–350.

11) Barker WH, Mullooly JP, Getchell W. Changing incidence and survival for heart failure in a well-defined older population, 1970-1974 and 1990-1994. Circulation. 2006;113:799–805.

12) Bleumink GS, Knetsch AM, Sturkenboom MC, Straus SM, Hofman A, Deckers JW, Witteman JC, Stricker BH. Quantifying the heart failure epidemic: prevalence, incidence rate, lifetime risk and prognosis of heart failure The Rotterdam Study. Eur Heart J. 2004;25:1614–1619.

13) Mosterd A, Cost B, Hoes AW, de Bruijne MC, Deckers JW, Hofman A, Grobbee DE. The prognosis of heart failure in the general population: The Rotterdam Study. Eur Heart J. 2001;22:1318–1327.

14) Chugh SS, Reinier K, Teodorescu C, Evanado A, Kehr E, Al Samara M, Mariani R, Gunson K, Jui J. Epidemiology of sudden cardiac death: clinical and research implications. Prog Cardiovasc Dis. 2008;51:213–228.

15) Curtis LH, Whellan DJ, Hammill BG, Hernandez AF, Anstrom KJ, Shea AM, Schulman KA. Incidence and prevalence of heart failure in elderly persons, 1994-2003. Arch Intern Med. 2008;168:418–424.

16) Yeung DF, Boom NK, Guo H, Lee DS, Schultz SE, Tu JV. Trends in the incidence and outcomes of heart failure in Ontario, Canada: 1997 to 2007. CMAJ. 2012;184:E765–E773.

17) Jhund PS, Macintyre K, Simpson CR, Lewsey JD, Stewart S, Redpath A, Chalmers JW, Capewell S, McMurray JJ. Long-term trends in first hospitalization for heart failure and subsequent survival between 1986 and 2003: a population study of 5.1 million people. Circulation. 2009;119:515–523.

18) Henkel DM, Redfield MM, Weston SA, Gerber Y, Roger VL. Death in heart failure: a community perspective. Circ Heart Fail. 2008;1:91–97.

19) Roger VL, Go AS, Lloyd-Jones DM, et al. Heart disease and stroke statistics--2012 update: A report from the American Heart Association. Circulation. 2012;125:e2–e220.

20) Dharmarajan K, Hsieh AF, Lin Z, Bueno H, Ross JS, Horwitz LI, Barreto-Filho JA, Kim N, Bernheim SM, Suter LG, Drye EE, Krumholz HM. Diagnoses and timing of 30-day readmissions after hospitalization for heart failure, acute myocardial infarction, or pneumonia. JAMA. 2013;309:355–363.

21) Heidenreich PA, Sahay A, Kapoor JR, Pham MX, Massie B. Divergent trends in survival and readmission following a hospitalization for heart failure in the Veterans Affairs health care system 2002 to 2006. J Am Coll Cardiol. 2010;56:362–368.

22) Fang J, Mensah GA, Croft JB, Keenan NL. Heart failure-related hospitalization in the U.S., 1979 to 2004. J Am Coll Cardiol. 2008;52:428–434.

23) Dunlay SM, Redfield MM, Weston SA, Therneau TM, Hall Long K, Shah ND, Roger VL. Hospitalizations after heart failure diagnosis a community perspective. J Am Coll Cardiol. 2009;54:1695–1702.

24) Blecker S, Paul M, Taksler G, Ogedegbe G, Katz S. Heart failure– associated hospitalizations in the United States. J Am Coll Cardiol. 2013;61:1259–1267.

25) Roger VL. The changing landscape of heart failure hospitalizations. J Am Coll Cardiol. 2013;61:1268–1270.

26) Mehra MR, Kobashigawa J, Starling R, Russell S, Uber PA, Parameshwar J, Mohacsi P, Augustine S, Aaronson K, Barr M. Listing criteria for heart transplantation: International Society for Heart and Lung Transplantation guidelines for the care of cardiac transplant candidates—2006. J Heart Lung Transplant 2006;25:1024–1042.

27) Slaughter MS, Rogers JG, Milano CA, Russell SD, Conte JV, Feldman D, Sun B, Tatooles AJ, Delgado RM 3rd, Long JW, Wozniak TC, Ghumman W, Farrar DJ, Frazier OH. Advanced heart failure treated with continuous-flow left ventricular assist device. N Engl J Med 2009; 361:2241–2251.

28) Konstam MA, Kramer DG, Patel AR, Maron MS, Udelson JE. Left ventricular remodeling in heart failure: current concepts in clinical significance and assessment. JACC Cardiovasc Imaging 2011;4:98–108.

29) Pfeffer MA, Braunwald E. Ventricular remodeling after myocardial infarction. Experimental observations and clinical implications. Circulation 1990; 81:1161–72.

30) Di Donato M, Sabatier M, Toso A, Barletta G, Baroni M, Dor V et al. Regional myocardial performance of non-ischaemic zones remote from anterior wall left ventricular aneurysm. Effects of aneurysmectomy. Eur Heart J 1995;16:1285–92.

31) Menicanti L, Castelvecchio S, Ranucci M, Frigiola A, Santambrogio C, de Vincentiis C, et al. Surgical therapy for ischemic heart failure: single-center experience with surgical anterior ventricular restoration. J Thorac Cardiovasc Surg 2007;134:433–41.

32) Castelvecchio S, Menicanti L, Di Donato M. Surgical ventricular restoration to reverse left ventricular remodeling. Curr Cardiol Rev 2010;6:15–23.

33) Wijns W, Kolh P, Danchin N, Di Mario C, Falk V, Folliguet T et al. Guidelines on myocardial revascularization: The Task Force on Myocardial Revascularization of the

European Society of Cardiology (ESC) and the European Association for Cardio-Thoracic Surgery (EACTS). Eur Heart J 2010;31:2501–55.

34) Karantalis V, Hare JM. Use of mesenchymal stem cells for therapy of cardiac disease. Circ Res. 2015 Apr 10;116(8):1413-30.

35) Semenza, G. L., and Wang, G. L. (1992) A nuclear factor induced by hypoxia via de novo protein synthesis binds to the human erythropoietin gene enhancer at a site required for transcriptional activation. Molecular and cellular biology 12, 5447-5454

36) Wang, G. L., and Semenza, G. L. (1995) Purification and characterization of hypoxia-inducible factor 1. J Biol Chem 270, 1230-1237

37) Li H, Ko HP, Whitlock JP. Induction of phosphoglycerate kinase 1 gene expression by hypoxia. Roles of Arnt and HIF1alpha. J Biol Chem 1996; 271: 21262–7.

38) Jaakkola P, Mole DR, Tian YM, Wilson MI, Gielbert J, Gaskell SJ, et al. Targeting of HIF-alpha to the von Hippel-Lindau ubiquitylation complex by O2-regulated prolyl hydroxylation. Science 2001; 292: 468–72.

39) Jeong JW, Bae MK, Ahn MY, Kim SH, Sohn TK, Bae MH, et al. Regulation and destabilization of HIF-1alpha by ARD1-mediated acetylation. Cell 2002; 111: 709–20.

40) Tanimoto K, Makino Y, Pereira T, Poellinger L. Mechanism of regulation of the hypoxia-inducible factor-1 alpha by the von Hippel-Lindau tumor suppressor protein. EMBO J 2000; 19: 4298–309.

41) Lando D, Peet DJ, Gorman JJ, Whelan DA, Whitelaw ML, Bruick RK. FIH-1 is an asparaginyl hydroxylase enzyme that regulates the transcriptional activity of hypoxia-inducible factor. Genes Dev 2002;16: 1466–71.

42) Salceda S, Caro J. Hypoxia-inducible factor 1alpha (HIF-1alpha) protein is rapidly degraded by the ubiquitin-proteasome system under normoxic conditions. Its stabilization by hypoxia depends on redox-induced changes. J Biol Chem 1997; 272: 22642–7.

43) Cockman ME, Masson N, Mole DR, Jaakkola P, Chang GW, Clifford SC, et al. Hypoxia inducible factor-alpha binding and ubiquitylation by the von Hippel-Lindau tumor suppressor protein. J Biol Chem 2000; 275: 25733–41.

44) Ema M, Taya S, Yokotani N, Sogawa K, Matsuda Y, Fujii-Kuriyama Y. A novel bHLH-PAS factor with close sequence similarity to hypoxia inducible factor 1alpha regulates the VEGF expression and is potentially involved in lung and vascular development. Proc Natl Acad Sci USA 1997; 94: 4273–8.

45) Weidemann, A., and Johnson, R. S. (2008) Biology of HIF-1alpha. Cell death and differentiation 15, 621-627

46) Harris AL. Hypoxia—a key regulatory factor in tumour growth. Nat Rev Cancer 2002; 2:38-47.

47) Riley T, Sontag E, Chen P, Levine A. Transcriptional control of human p53-regulated genes.

Nat Rev Mol Cell Biol 2008; 9:402-12.

48) Schmid T, Zhou J, Kohl R, Brune B. p300 relieves p53-evoked transcriptional repression of hypoxia-inducible factor-1 (HIF-1). Biochem J 2004; 380:289-95.

49) Frontini, M., and Proietti-De-Santis, L. (2009) Cockayne syndrome B protein (CSB): linking p53, HIF-1 and p300 to robustness, lifespan, cancer and cell fate decisions. Cell cycle 8, 693-696

50) Manalo DJ, Rowan A, Lavoie T, Natarajan L, Kelly BD, Ye SQ, et al. Transcriptional regulation of vascular endothelial cell responses to hypoxia by HIF-1. Blood 2005; 105: 659–69.

51) Semenza GL, Shimoda LA, Prabhakar NR. Regulation of gene expression by HIF-1. Novartis Found Symp 2006; 272: 2–8.

52)Yuan Y, Hilliard G, Ferguson T, Millhorn DE. Cobalt inhibits the interaction between hypoxia-inducible factor-alpha and von Hippel-Lindau protein by direct binding to hypoxia-inducible factor-alpha. J Biol Chem 2003; 278: 15911–6.

53) Page EL, Robitaille GA, Pouyssegur J, Richard DE. Induction of hypoxia-inducible factor-1alpha by transcriptional and translational mechanisms. J Biol Chem 2002; 277: 48403–9.

54) Cai Z, Manalo DJ, Wei G, Rodriguez ER, Fox-Talbot K, Lu H, et al. Hearts from rodents exposed to intermittent hypoxia or erythropoietin are protected against ischemia-reperfusion injury. Circulation 2003; 108: 79–85.

55) Xi L, Serebrovskaya TV. Intermittent hypoxia: from molecular mechanisms to clinical applications. New York: Nova Science Publishers; 2009. p 1–615.

56) Ding HL, Zhu HF, Dong JW, Zhu WZ, Yang WW, Yang HT, et al. Inducible nitric oxide synthase contributes to intermittent hypoxia against ischemia/reperfusion injury. Acta Pharmacol Sin 2005; 26: 315–22.

57) Belaidi E, Beguin PC, Levy P, Ribuot C, Godin-Ribuot D. Prevention of HIF-1 activation and iNOS gene targeting by low-dose cadmium results in loss of myocardial hypoxic preconditioning in the rat. Am J Physiol Heart Circ Physiol 2008; 294: H901–H908.

58) Wasserfuhr D, Cetin SM, Yang J, Freitag P, Frede S, Jakob H, et al. Protection of the right ventricle from ischemia and reperfusion by preceding hypoxia. Naunyn Schmiedebergs Arch Pharmacol 2008; 378: 27–32.

59) Shohet RV, Garcia JA. Keeping the engine primed: HIF factors as key regulators of cardiac metabolism and angiogenesis during ischemia. J Mol Med 2007; 85: 1309–15.

60) Date T, Mochizuki S, Belanger AJ, Yamakawa M, Luo Z, Vincent KA, et al. Expression of constitutively stable hybrid hypoxia-inducible factor-1alpha protects cultured rat

cardiomyocytes against simulated ischemia-reperfusion injury. Am J Physiol Cell Physiol 2005; 288: C314–20.

61) Martin C, Yu AY, Jiang BH, Davis L, Kimberly D, Hohimer AR, et al. Cardiac hypertrophy in chronically anemic fetal sheep: Increased vascularization is associated with increased myocardial expression of vascular endothelial growth factor and hypoxia-inducible factor 1. Am J Obstet Gynecol 1998; 178: 527–34.

62) Xi L, Taher M, Yin C, Salloum F, Kukreja RC. Cobalt chloride induces delayed cardiac preconditioning in mice through selective activation of HIF-1alpha and AP-1 and iNOS signaling. Am J Physiol Heart Circ Physiol 2004; 287: H2369–75.

63) Kerendi F, Kirshbom PM, Halkos ME, Wang NP, Kin H, Jiang R, et al. Thoracic Surgery Directors Association Award. Cobalt chloride pretreatment attenuates myocardial apoptosis after hypothermic circulatory arrest. Ann Thorac Surg 2006; 81: 2055–62.

64) Ivan M, Haberberger T, Gervasi DC, Michelson KS, Gunzler V, Kondo K, et al. Biochemical purification and pharmacological inhibition of a mammalian prolyl hydroxylase acting on hypoxia-inducible factor. Proc Natl Acad Sci USA 2002; 99: 13459–64.

65) Ockaili R, Natarajan R, Salloum F, Fisher BJ, Jones D, Fowler AA III, et al. HIF-1 activation attenuates postischemic myocardial injury: role for heme oxygenase-1 in modulating microvascular chemokine generation. Am J Physiol Heart Circ Physiol 2005; 289: H542–8.

66) Luciano JA, Tan T, Zhang Q, Huang E, Scholz P, Weiss HR. Hypoxia inducible factor-1 improves the actions of nitric oxide and natriuretic peptides after simulated ischemia-reperfusion. Cell Physiol Biochem 2008; 21: 421–8.

67) Bao W, Qin P, Needle S, Erickson-Miller CL, Duffy KJ, Ariazi JL, et al. Chronic inhibition of hypoxia-inducible factor (hif) prolyl 4-hydroxylase improves ventricular

performance, remodeling and vascularity following myocardial infarction in the rat. J Cardiovasc Pharmacol 2010. doi: 10.1097/FJC.0b013e3181e2bfef

68) E. Monti, A. Preti, B. Venerando, G. Borsani, Recent development in mammalian sialidase molecular biology, Neurochem. Res. 27 (2002) 649–
663.

69) K.E. Achyuthan, A.M. Achyuthan, Comparative enzymology, biochemistry and pathophysiology of human exo-a-sialidases (neuraminidases), Comp. Biochem. Physiol. B:9 Biochem. Mol. Biol. 129 (2001) 29–64.

70) E. Bonten, S.A. Van der, M. Fornerod, G. Grosveld, A. d'Azzo, Characterization of human lysosomal, neuraminidase defines the molecular basis of the metabolic storage disorder sialidosis, Genes Dev. 10 (1996) 3156–3169.

71) E. Monti, A. Preti, E. Rossi, A. Ballabio, G. Borsani, Cloning and characterization of NEU2, a human gene homologous to rodent soluble sialidases, Genomics 57 (1999) 137–143.

72) E. Monti, M.T. Bassi, N. Papini, M. Riboni, M. Manzoni, B. Venerando, G. Croci, A. Preti, A. Ballabio, G. Tettamanti, G. Borsani, Identification and expression of NEU3, a novel human sialidase associated to the plasma membrane, Biochem. J. 349 (2000) 343–351.

73) E. Monti, M.T. Bassi, R. Bresciani, S. Civini, G.L. Croci, N. Papini, M. Riboni, G. Zanchetti, A. Ballabio, A. Preti, G. Tettamanti, B. Venerando, G. Borsani, Molecular cloning and characterization of NEU4, the fourth member of the human sialidase gene family, Genomics 83 (2004) 445–453.

74) V. Seyrantepe, K. Landry, S. Trudel, J.A. Hassan, C.R. Morales, A.V. Pshezhetsky, Neu4, a novel human lysosomal lumen sialidase, confers normal phenotype to sialidosis and galactosialidosis cells, J. Biol. Chem. 279 (2004) 37021–37029.

75) V. Seyrantepe, H. Poupetova, R. Froissart, M.T. Zabot, I. Maire, A.V. Pshezhetsky, Molecular pathology of NEU1 gene in sialidosis, Hum. Mutat. 22 (2003) 343–352.

76) K. Gee, M. Kozlowski, A. Kumar, Tumor necrosis factor-alpha induces functionally active hyaluronan-adhesive CD44 by activating sialidase through p38 mitogen-activated protein kinase in lipopolysaccharide-stimulated human monocytic cells, Biol. Chem. 278 (2003) 37275–37287.

77) K. Sato, T. Miyagi, Involvement of an endogenous sialidase in skeletal muscle cell differentiation, Biochem. Biophys. Res. Commun. 221 (1996) 826–830.

78) K.T. Ha, Y.C. Lee, S.H. Cho, J.K. Kim, C.H. Kim, Molecular characterization of membrane type and ganglioside-specific sialidase (Neu3) expressed in E. coli, Mol. Cells 17 (2004) 267–273.

79) Anastasia, L., Papini, N., Colazzo, F., Palazzolo, G., Tringali, C., Dileo, L., Piccoli, M., Conforti, E., Sitzia, C., Monti, E., Sampaolesi, M., Tettamanti, G., and Venerando, B. (2008) NEU3 sialidase strictly modulates GM3 levels in skeletal myoblasts C2C12 thus favoring their differentiation and protecting them from apoptosis. J. Biol. Chem. 283, 36265–36271

80) S. Proshin, K. Yamaguchi, T.Wada, T. Miyagi, Modulation of neuritogenesis by ganglioside-specific sialidase (Neu3) in human neuroblastoma NB-1 cells, Neurochem. Res. 27 (2002) 841–846.

81) Rodriguez, J. A., Piddini, E., Hasegawa, T., Miyagi, T., and Dotti, C. G. (2001) Plasma membrane ganglioside sialidase regulates axonal growth and regeneration in hippocampal neurons in culture. J. Neurosci. 21, 8387–8395

82) K. Yamaguchi, K. Hata, K. Koseki, K. Shiozaki, H. Akita, T. Wada, S. Moriya, T. Miyagi, Evidence for mitochondrial localization of a novel human sialidase (NEU4), Biochem. J. 390 (2005) 85–93.

83) Miyagi, T., and Yamaguchi, K. (2012) Mammalian sialidases: physiological and pathological roles in cellular functions. Glycobiology 22, 880–896

84) Miyagi, T., Wada, T., Yamaguchi, K., Hata, K., and Shiozaki, K. (2008) Plasma membrane-associated sialidase as a crucial regulator of transmembrane signalling. J. Biochem. 144, 279–285.

85) Keith, B., Johnson, R. S., and Simon, M. C. (2012) HIF1 and HIF2: sibling rivalry in hypoxic tumour growth and progression. Nat. Rev. Cancer 12, 9–22

86) Yamaguchi, K., Koseki, K., Shiozaki, M., Shimada, Y., Wada, T., and Miyagi, T. (2010) Regulation of plasma membrane-associated sialidase NEU3 gene by Sp1/Sp3 transcription factors. Biochem. J. 430, 107–117

87) Cummins, E. P., and Taylor, C. T. (2005) Hypoxia-responsive transcription factors. Pflugers Arch. 450, 363–371

88) Galletti PM: Cardiopulmonary bypass. A historical perspective. Artif Org 1993; 17: 675

89) Katz, A. M., & Tada, M. (1972). The “stone heart”: A challenge to the biochemist. Am J Cardiol 29(4), 578−580.

90) Melrose, D. G., Dreyer, B., Bentall, H. H., & Baker, J. B. (1955). Elective cardiac arrest.
Lancet 269(6879), 21−22.

91) Bretschneider, H. J. (1964). Survival time and recuperative time of the heart in normothermia and hypothermia. Verh Dtsch Ges Kreislaufforsch 30, 11−34.

92) Hearse, D. J., Stewart, D. A., & Braimbridge, M. V. (1976). Cellular protection during myocardial ischemia: The development and characterization of a procedure for the induction of reversible ischemic arrest. Circulation 54(2), 193−202.

93) Braimbridge, M. V., Chayen, J., Bitensky, L., Hearse, D. J., Jynge, P., & Cankovic Darracott, S. (1977). Cold cardioplegia or continuous coronary perfusion? Report on preliminary clinical experience as assessed cytochemically. J Thorac Cardiovasc Surg 74(6), 900−906.

94) Buckberg, G. D., Allen, B. S., & Beyersdorf, F. (1993). Blood cardioplegic strategies during adult cardiac operations. In H. M. Piper, & C. J. Preusse (Eds.), Ischemia–reperfusion in cardiac surgery (pp. 181−227). AA Dordrecht: Kluwer Academic Publishers.

95) Buckberg, G. D., Brazier, J. R., Nelson, R. L., Goldstein, S. M., McConnell, D. H., & Cooper, N. (1977). Studies of the effects of hypothermia on regional myocardial blood flow and metabolism during cardiopulmonary bypass. I. The adequately perfused beating, fibrillating, and arrested heart. J Thorac Cardiovasc Surg 73(1), 87−94.

96) Ozaki H, Yu AY, Della N, et al. Hypoxia inducible factor-1a is increased in ischemic retina: temporal and spatial correlation with VEGF expression. Invest Ophthalmol Vis Sci 1999;40:182-9.

97) Lee SH, Wolf PL, Escudero R, Deutsch R, Jamieson SW, Thistlethwaite PA.Early expression of angiogenesis factors in acute myocardial ischemia and infarction. N Engl J Med. 2000 Mar 2;342(9):626-33.

98) Ning XH, Chen SH, Xu CS, Hyyti OM, Qian K, Krueger JJ, Portman MA. Hypothermia preserves myocardial function and mitochondrial protein gene expression during hypoxia. Am J Physiol Heart Circ Physiol 285: H212–H219, 2003.

99) Ning XH, Chi EY, Buroker NE, Chen SH, Xu CS, Tien YT, Hyyti OM, Ge M, Portman MA.Moderate hypothermia (30 degrees C) maintains myocardial integrity and modifies response of cell survival proteins after reperfusion. Am J Physiol Heart Circ Physiol. 2007 Oct;293(4):H2119-28.

100) Gay WA, Ebert PA. Functional, metabolic, and morphologic effects of potassium induced cardioplegia. Surgery 1973;4: 284‑290.

101) Ryou MG, Flaherty DC, Hoxha B, Sun J, Gurji H, Rodriguez S, Bell G, Olivencia-Yurvati AH, Mallet RT. Pyruvate-fortified cardioplegia evokes myocardial erythropoietin signaling in swine undergoing cardiopulmonary bypass. Am J Physiol Heart Circ Physiol. 2009 Nov;297(5):H1914-22

102) Lu H, Dalgard CL, Mohyeldin A, McFate T, Tait AS, Verma A. Reversible inactivation of HIF-1 prolyl hydroxylases allows cell metabolism to control basal HIF-1. J Biol Chem 280: 41928–41939, 2005.

103) Qing M1, Görlach A, Schumacher K, Wöltje M, Vazquez-Jimenez JF, Hess J, Seghaye MC. The hypoxia-inducible factor HIF-1 promotes intramyocardial expression of VEGF in infants with congenital cardiac defects. Basic Res Cardiol. 2007 May;102(3):224-32. Epub 2007 Feb 2.

104) Starnes SL, Duncan BW, Kneebone JM, Rosenthal GL, Jones TK, Grifka RG, Cecchin F, Owens DJ, Fearneyhough C, Lupinetti FM (2000) Vascular endothelial growth factor and basic fibroblast growth factor in children with cyanotic congenital heart disease. J Thorac Cardiovasc Surg 119:534‑539

105) Giordano FJ, Gerber HP, Williams SP, VanBruggen N, Bunting S, Ruiz-Lozano P, Gu Y, Nath AK, Huang Y, Hickey R, Dalton N, Peterson KL,Ross J, Jr., Chien KR,Ferrara N (2001) A cardiac myocyte vascular endothelial growth factor paracrine pathway is required to maintain cardiac function. Proc Natl Acad Sci U S A 98:5780‑5785

106) Kietzmann T, Jungermann K,Gorlach A (2003) Regulation of the hypoxia-dependent plasminogen activator inhibitor 1 expression by MAP kinases. Thromb Haemost 89:666‑673

107) Wiesener, M. S., Turley, H., Allen, W. E., Willam, C., Eckardt, K. U., Talks, K. L., Wood, S. M., Gatter, K. C., Harris, A. L., Pugh, C. W., Ratcliffe, P. J., and Maxwell, P. H. (1998) Induction of endothelial PAS domain protein-1 by hypoxia: characterization and comparison with hypoxia-inducible factor-1alpha. Blood 92, 2260-2268

108) Reddy S, Osorio JC, Duque AM, Kaufman BD, Phillips AB, Chen JM, Quaegebeur J, Mosca RS, Mital S.Failure of right ventricular adaptation in children with tetralogy of Fallot. Circulation. 2006 Jul 4;114(1 Suppl):I37-42

109) Seagroves, T.N., Ryan, H.E., Lu, H., Wouters, B.G., Knapp, M., Thibault, P., Laderoute, K., and Johnson, R.S. (2001). Transcription factor HIF-1 is a necessary mediator of the pasteur effect in mammalian cells. Mol. Cell. Biol. 21, 3436–3444.

110) Kim, J. W., Tchernyshyov, I., Semenza, G. L., and Dang, C. V. (2006) HIF-1-mediated expression of pyruvate dehydrogenase kinase: a metabolic switch required for cellular adaptation to hypoxia. Cell metabolism 3, 177-185